

SHAKING TABLE TEST OF SIMPLE STRUCTURE PHYSICAL MODEL

Structural Analysis

Final Report

Michal Hajduk

SHAKING TABLE TEST OF SIMPLE STRUCTURE PHYSICAL MODEL

Structural Analysis

Final Design

Author: Michal Hajduk
Project: Graduation Thesis
Study programme: Civil Engineering
Study year/semester: 2019-2020, Semester 2
University: HZ University of Applied Sciences
Supervisor: Giuliana Scuderi
Place & Date: Ferrara, 1st June 2020
Version: 1.0



UNIVERSITÀ
DEGLI STUDI
DI FERRARA
- EX LABORE FRUCTUS -



UNIVERSITY
OF APPLIED SCIENCES

Colophon

Student Information

Student name: Michal Hajduk
Student number: 00073938
E-mail: hajd0001@hz.nl

University Information

University: HZ University of Applied Sciences
Department: Civil Engineering
University Supervisor: Giuliana Scuderi
Supervisor e-mail: g.scuderi@hz.nl

Graduation Location

University: University of Ferrara
In-university supervisors: Alessandra Aprile
Fabio Minghini
Supervisor e-mail: alessandra.aprile@unife.it
fabio.minghini@unife.it

ABSTRACT

This thesis analyses the behaviour of the design of a physical model of a cable-stayed bridge during a dynamic analysis. To obtain the dynamic response of the design of a physical model, I had to create various designs and compared them to select a final one. I utilized the selected design for a shaking table test. My results demonstrated the natural frequency of a physical model as the main objectives of a dynamic analysis. Results also revealed the mass and stiffness of a physical model. However, the physical model stiffness was possible to determine after having known the natural frequency. This study emphasizes the requirement to consider the impact of the physical model composition on the dynamic response.

ACKNOWLEDGEMENTS

This bachelor thesis was accomplished on behalf of the contribution of several parties I would like to acknowledge everybody who guided me during this period.

First of all, I wish to express my deepest gratitude to my university supervisor, Giuliana Scuderi, who helped me to obtain this thesis, for the suggestions on the research improvements and endless support. Without her persistent encourage, the goal of this study would not have been achieved.

Secondly, special thanks to Alessandra Aprile and Fabio Minghini, the professors from the University of Ferrara who introduced me to the dynamics of structures and made this thesis possible. Their guidance helped me in all the time of research and experiments of this thesis.

Thirdly, I would like to recognize the invaluable assistance that my parents provided during this period, for their constant support and great inspiration.

A handwritten signature in black ink, appearing to read "Michele Maggi". The signature is fluid and cursive, with a long horizontal stroke extending to the right.

Ferrara, June 2020

TABLE OF CONTENTS

ABSTRACT	IV
ACKNOWLEDGEMENTS	V
TABLE OF CONTENTS.....	VI
LIST OF FIGURES	VIII
LIST OF TABLES	XII
LIST OF ABBREVIATIONS	XIV
1 Introduction.....	15
1.1 Background	15
1.2 Research Overview	15
1.2.1 Case Study.....	15
1.2.2 Problem Statement.....	16
1.2.3 Objective	17
1.2.4 Research Question	17
1.2.5 Research Scope	18
2 Theoretical Framework	19
2.1 The cable-stayed bridge type.....	19
2.1.1 Arrangement of the stay cables.....	19
2.1.2 Positions of the cables along the deck.....	22
2.1.3 Tower Type	25
2.1.4 Deck Type.....	25
2.1.5 Cable Type.....	27
2.2 Physical Model.....	28
2.2.1 Mola Kit application to realize physical model in simple structure analysis	31
2.2.2 Schedule of requirements for the design of a scaled model for a cable-stayed bridge.	34
2.3 Structural Analysis	42
2.2.3 Seismic Analysis	46
2.2.4 Static vs Dynamic Analysis	50
2.3.3 Preliminary Test	53
2.3.4 Fast Fourier Transformation in MATLAB.....	54
2.3.5 Shaking Table Test.....	55
3 Methodology	59

3.1	Construction of a physical model.....	59
3.1.1	Materials used.....	62
3.2	Preselection Test of Acceleration Response	65
3.3	Transforming Acceleration using Fast Fourier Transform.....	69
3.4	Multi-criteria analysis for selecting the design of a physical model	73
3.5	Shaking Table Test	74
4	Results.....	82
4.1	Introduction	82
4.2	Results of Preliminary Test.....	82
4.3	Selected Design Model.....	89
4.4	Shaking Table Test Results	90
4.4.1	Natural Frequency of Selected Design.....	90
4.4.2	Stiffness of Selected Design	94
5	Discussion & Conclusion	95
5.2	Limitations of Results.....	96
5.3	Results Complication.....	96
5.4	Implication of Results.....	97
5.5	Recommendations	97
6	Bibliography.....	99

LIST OF FIGURES

Figure 1-1 Mola Structural Model Example1	16
Figure 1-2 Mola Structural Model Example2	16
Figure 1-3 Mola Structural Model Example3	16
Figure 1-4 Research Procedure.....	18
Figure 2-1 Typical cable-stayed bridge and its forces.....	19
Figure 2-2 Pasco-Kennewick Bridge, Washington, USA.....	20
Figure 2-3 Øresund Bridge, Malmo & Copenhagen, Sweden & Denmark	21
Figure 2-4 Normandy Bridge, Le Havre-Honfleur, France	21
Figure 2-5 Abdoun Bridge, Amman, Jordan.....	22
Figure 2-6 Space positions of cables a) Two vertical planes system b) Two inclined planes system c) Single plane system	22
Figure 2-7 Jingyue Yangtze River Bridge, Hunan, China	23
Figure 2-8 Kanchanaphisek bridge, Samut Prakan, Thailand.....	24
Figure 2-9 Tsurumi Tsubasa Bridge, Yokohama, Japan.....	24
Figure 2-10 Types of towers	25
Figure 2-11 Steel deck and composite deck; (A) steel section for middle span, (B) composite section for side span	26
Figure 2-12 Types of ribs a) torsionally weak/open type b) torsionally stiff/box type	26
Figure 2-13 The cable types for cable-stayed bridges. a) Locked coil cable. b) Spiral strand cable. c) Parallel wire strand.....	27
Figure 2-14 The front view of model.	29
Figure 2-15 The front view of the ProtironFigure 2-16 The fully assembled model of Protiron	30
Figure 2-17 Compression on a Mola model.....	31
Figure 2-18 Bending on a Mola model.....	31
Figure 2-19 The shaking table test of the 2-story frame with Side Bracing	32
Figure 2-20 The shaking table test of the 2-story frame with Rigid Connectors.....	32
Figure 2-21 The front view of the 1 st Model Design	37
Figure 2-22 The top view of the 1 st Model Design.....	37
Figure 2-23 The side view of the 1 st Model Design.....	37
Figure 2-24 The front view of the 2 nd Model Design	39
Figure 2-25 The top view of the 2 nd Model Design.....	39
Figure 2-26 The side view of the 2 nd Model Design.....	39
Figure 2-27 The front view of the 3 rd Model Design.....	41
Figure 2-28 The top view of the 3 rd Model Design	41

Figure 2-29 The side view of the 3 rd Model Design	41
Figure 2-30 Various Degree of Freedom.....	47
Figure 2-31 Stress-Strain Curve.....	47
Figure 2-32 Simple Harmonic Load	48
Figure 2-33 Random load	48
Figure 2-34 Damped Free Vibration	49
Figure 2-35 Lateral shear forces along two orthogonal axes	50
Figure 2-36 Acceleration Response of healthy Mola Model of a truss bridge	
Acceleration Response of damaged Mola Model of a truss bridge	54
Figure 2-37	
Figure 2-38 The acceleration amplitude expressed against time.....	55
Figure 2-39 The acceleration amplitude presented against the frequency called the Fourier Spectrum	55
Figure 2-40 E-Defense shaking table	56
Figure 2-41 The plan and elevation view of a shaking table	57
Figure 2-42 Acceleration record from a shaking table test	58
Figure 3-1 The ground and ground connections.	59
Figure 3-2 The bar 6, diagonal D6x6 and rigid connection 90° attached to the ground connection.	60
Figure 3-3 The first part of the deck	60
Figure 3-4 The first part of the deck attached to the bottom part of the tower	61
Figure 3-5 The rigid connections attached to the joint between the tower and deck	61
Figure 3-6 The second part of the deck	62
Figure 3-7 The finished physical model	62
Figure 3-8 The ground plate.....	63
Figure 3-9 The ground connection.....	63
Figure 3-10 The bar 6	63
Figure 3-11 The diagonals D6x6 and D6x12.....	64
Figure 3-12 The rigid connection 90°	64
Figure 3-13 The connection	64
Figure 3-14 The plate 6x6	64
Figure 3-15 The plate 6x12	64
Figure 3-16 MATLAB mobile menu interface.....	65
Figure 3-17 Sensors Tab in MATLAB mobile	65
Figure 3-18 MATLAB mobile, “Stream to” tab.....	66
Figure 3-19 MATLAB mobile, “Sample rate” tab	66
Figure 3-20 MATLAB mobile Acceleration sensor activation	66
Figure 3-21 MATLAB mobile recording start	66
Figure 3-22 MATLAB mobile “STOP” button.....	67

Figure 3-23 MATLAB mobile entering log name	67
Figure 3-24 MATLAB Drive & its folder	67
Figure 3-25 MATLAB Drive from computer interface	68
Figure 3-26 Opened folder of “MobileSensorData” with the logged acceleration recordings	68
Figure 3-27 MATLAB code for plotting the acceleration in X-axis into the time domain.....	70
Figure 3-28 MATLAB code for plotting the acceleration in Y-axis into the time domain.....	71
Figure 3-29 MATLAB code of FFT for the X-axis.....	72
Figure 3-30 The “Run” button in MATLAB Editor tab	72
Figure 3-31 MATLAB code of FFT for the Y-axis.....	73
Figure 3-32 The table platform with the attached bolt nuts.....	77
Figure 3-33 The emergency bottom, gear knob and frequency knob.....	77
Figure 3-34 The shaking table with the 3 rd Design of a physical model	78
Figure 3-35 Testing the 3 rd Design of the physical model in transversal direction; the bridge tower with the bracing	79
Figure 3-36 Testing the 3 rd Design of the physical model in transversal direction; the bridge tower with the rigid connection 90°	79
Figure 3-37 The 3 rd Design of the physical model on the shaking table.....	79
Figure 3-38 Collapse of the 3 rd Design of the physical model during testing.....	80
Figure 3-39 Testing the 3 rd Design of the physical model with the centric load	80
Figure 3-40 Testing the 3 rd Design of the physical model with the eccentric load	80
Figure 4-1 Acceleration signal of the 1 st model design in X-axis	82
Figure 4-2 Acceleration signal of the 1 st model design of the physical model in Y-ax	83
Figure 4-3 Acceleration signal of the 2 nd model design in X-axis.....	83
Figure 4-4 Acceleration signal of the 2 nd model design in Y-axis.....	84
Figure 4-5 Acceleration signal of the 3 rd model design in X-axis.....	84
Figure 4-6 Acceleration signal of the 3 rd model design in Y-axis	85
Figure 4-7 Fast Fourier Transform of the 1 st model design in X-axis.....	85
Figure 4-8 Fast Fourier Transform of the 1 st model design in Y-axis.....	86
Figure 4-9 Fast Fourier Transform of the 2 nd model design in X-axis.....	86
Figure 4-10 Fast Fourier Transform of the 2 nd model design in Y-axis	87
Figure 4-11 Fast Fourier Transform of the 3 rd model design in X-axis	87
Figure 4-12 Fast Fourier Transform of the 3 rd model design in Y-axis.....	88
Figure 4-13 The physical model (3 rd Design) with bracing and its natural frequency in the transversal direction on a shaking table test.....	91
Figure 4-14 The physical model (3 rd Design) without bracing and its natural frequency in the transversal direction on a shaking table test.....	91

Figure 4-15 The physical model (3rd Design) and its natural frequency in the longitudinal direction on a shaking table test.....92

Figure 4-16 The physical model (3rd Design) with a centric load and its natural frequency in the longitudinal direction on a shaking table test92

Figure 4-17 The physical model (3rd Design) with an eccentric load and its natural frequency in the longitudinal direction on a shaking table test93

LIST OF TABLES

Table 2-1 The classification of a cable-stayed bridge	19
Table 2-2 Types of main girder	27
Table 2-3 The scale factors of the Similitude Law (Candeias, Costa, & Coelho, 2004).....	29
Table 2-4 The scaling factors for the Protiron model	30
Table 2-5 Advantages and Disadvantages of 1 st Model Design.....	38
Table 2-6 Advantages and Disadvantages of 2 nd Model Design.....	40
Table 2-7 Advantages and Disadvantages of 3 rd Model Design	42
Table 2-8 Classification of loads.....	44
Table 2-9 Eurocode Standards	44
Table 3-1 The weight of criteria for the design selection	74
Table 4-1 The final design selection.....	89
Table 4-2 The final design selection including values.....	90
Table 4-3 Comparison of Natural Frequencies	94
Table 4-4 The stiffness values for all the tested design modifications.....	94

LIST OF EQUATIONS

Equation 2-1 The Undamped Natural Frequency Equation	49
Equation 2-2 Equation of Motion for Single Degree of Freedom.....	52
Equation 2-3 Equation of Motion for Non-linear System.....	52
Equation 3-1 Stiffness vs Frequency and Mass Equation	81

LIST OF ABBREVIATIONS

DOF	degree-of-freedom
SDOF	single degree-of-freedom
MDOF	multi degree-of-freedom
FFT	fast Fourier transform

1 Introduction

1.1 Background

The graduation internship has been accomplished at the Department of Civil Engineering of the University of Ferrara in Italy. The department provided the opportunity to students who want to become skilled in traditional civil engineering areas.

The department of Civil Engineering provides high quality in research and education. The research quality has been highly ranked across Italy. It provides a range of researches specializing in Hydraulic Construction, Environmental Engineering and Structural Engineering.

The thesis discussed in this report was supervised by Professor Alessandra Aprile and Professor Fabio Minghini, specialized in seismic engineering and structural rehabilitation.

Professor Aprile suggested topic investigates the dynamic response of a simple structure. A simple structure has a simplified design including fundamental components avoiding unnecessary complexity (BREEAM, 2016). The dynamic response was obtained by conducting an acceleration response test of the structure and transform the acquired data in MATLAB. The test results were validated by a shaking table test. It was necessary to use a physical model, which was made of Structural Mola Kit 1&2, to test on a shaking table. The simple structure had a form of a cable-stayed bridge due to two reasons. Firstly, cable supported bridges perform better under seismic circumstances comparing to other types of bridges (Chen & Duan, 2014). Secondly, the Structural Mola Kit 1&2 do not have needed elements to construct a different type of a model, such as a suspension bridge (Mola Model, 2020).

1.2 Research Overview

1.2.1 Case Study

As mentioned, the dynamic response of simple structures can be obtained by conducting an acceleration response test of the structure and processing the obtained data using MATLAB

According to the technical specification, the shaking table used at the University of Ferrara laboratory allows to test structures with a maximum base size of 35x35 cm² and maximum weight 5 kg.

This means that to test a simple structure on the shaking table, it is necessary to use a physical model. A physical model is a reproduction of a physical system including the acting dominant forces in correct proportion to the actual physical system (Hughes, 1993).

There are many methods to build a physical model, but this research focuses only upon the use of Structural Mola Kit 1&2. The Structural Mola Kit 1&2 is a set of modular parts that connects through magnetism. It allows to build an interactive physical model that simulates the structural behaviour (Mola Model, 2020). Exemplary physical models constructed of Mola Kits are presented in Figures 1-1, 1-2 & 1-3.

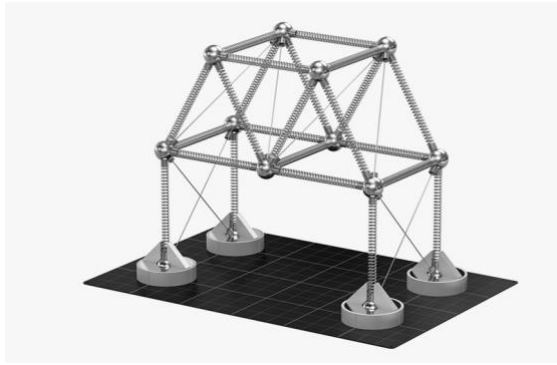


Figure 1-1 Mola Structural Model
Example1

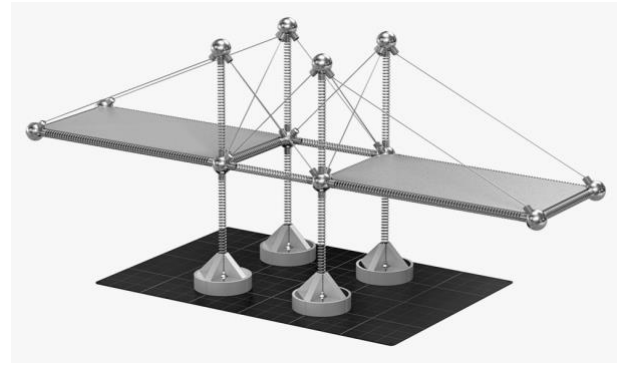


Figure 1-2 Mola Structural Model
Example2

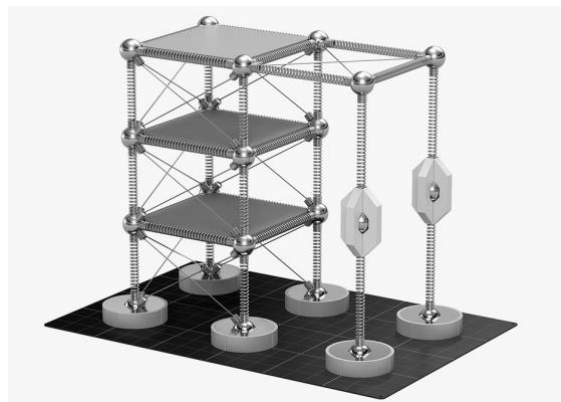


Figure 1-3 Mola Structural Model Example3

Concerning simple structures, the Structural Mola Kit 1&2 contains pieces that allow to build models for cable-supported bridges (Mola Model, 2020). Cable supported bridges perform better under seismic circumstances comparing other types of bridges such as truss or arch bridges (Chen & Duan, 2014), and they are therefore a suitable simple structure for this research.

Using a physical model entails many challenges, among which the scaling of the model and its parameters. The difficulty is to conduct scaling precisely both in terms of structural scheme and in terms of applied loads, only then the results can be reliable. The more precisely model parameters are scaled, the higher validity of result can be achieved (Dihoru, Crewe, Dietz, & Taylor, 2010).

1.2.2 Problem Statement

The physical model must be realized according to the technical specification of the available shaking table: maximum base size of 35x35 cm², maximum allowed weight 5 kg, and maximum vibration frequency 4,8 Hz.

The Mola Kit 1&2 allows easily to verify the requirements in terms of weight, however the challenge is in the vibration frequency of a physical model that cannot be greater than the vibration frequency of a shaking table. To verify that this condition is met, it is necessary to

know the vibration modes of the physical model. As defined by Young (2014), a vibration mode is “A characteristic manner in which vibration occurs. In a freely vibrating system, oscillation is restricted to certain characteristic patterns of motion at certain characteristic frequencies; these motions are called normal modes of vibration.” Collins (2019) says that “Frequency indicates the number of times an object oscillates, or vibrates, per unit of time and is often expressed in either cycles per second (referred to as Hertz, Hz)”.

There are two methods to obtain the vibration modes of a physical model. The first is to perform an acceleration response test on the physical model and to transport the recorded data in a software, such as MATLAB. In MATLAB, it is possible to vectorise the data against the time of a test, and conduct the Fast Fourier Transformation (FFT). The result of the FFT will provide the vibration mode and vibration frequency. Such approach allows to obtain the research objectives without knowing the stiffness of Mola pieces, since Mola system was designed for qualitative analysis while, this research is focused on quantitative analysis (Smith, Qualitative Analysis, 2020). The second method involves the use of a shaking table test, which assesses the dynamic performance of a physical model by simulating ground motions. The ground motions effect on structures may be different due to the input parameters such as vibration frequency and system degree-of-freedom (Stikeleather, 1976). A correct set of input parameters must be selected in order to ensure a vibration frequency according to the specification of the shaking table.

1.2.3 Objective

Broadly speaking, this research investigates the application of physical models to the analysis of the dynamic behaviour of simple structures.

The objective of this research is to determine the design of a physical model of a cable-stayed bridge by using the Mola Structural Kit 1&2. Due to the specification of the shaking table, the vibration modes and vibration frequency of this model must be below 4,8 Hz. The stiffness and mass of a physical model must be determined to provide full insight into the dynamic response.

1.2.4 Research Question

The research question bases on the objectives and states as:

What is the best design for a physical model of a cable-stayed bridge by using Mola Structural Kit 1&2 whose vibrations mode and vibration frequency are below 4,8 Hz?

To provide more insightful area of knowledge. The sub-research questions are below to gather more information helping to answer the main question.

- What are design criteria to structure the physical model?
- What are the functional and technical requirements of the physical model?
- What are alternative designs for a cable-stayed bridge using Mola Structural Kit pieces?

- What will be the linear and elastic dynamic response of the physical model during a shaking table test?
- What is the stiffness and mass of the selected physical model?

1.2.5 Research Scope

Some assumptions are made at the beginning of this research:

- The model is designed as the Single Degree-of-Freedom System in X-axis and SDOF in Y-axis, because a SDOF system is the simplest way to describe a vibrating system. In a SDOF system, model parameters such as mass or elastic properties are treated as a single physical element (Clough & Penzien, 1995). Furthermore, the model will not be investigated as Multi Degree-of-Freedom System. A MODF system does not have one state, but a finite number of natural vibration modes. Such approach overcomplicates as a system can vibrate in any of these modes or a combination of them. Moreover, each vibration mode has its own vibration frequency (Rotordynamics Laboratory, 2019). In this research, only one vibration modes and vibration frequency is needed. The vibration mode and vibration frequency of the whole system, not of its elements.
- The stability and rigidity of a model will be assessed.
- The deck torsion and pylon stiffness will be considered during evaluation of the physical model.
- Creation of the detailed design of the bridge elements such as a deck, pylon and stays will be kept out of the scope. Only the overall design is considered due to the structure of Mola pieces which work as a complete element.
- The non-linear analysis is not a part of this research, and the inelastic dynamic response will not be investigated. This assumption is valid because the vibration frequency of a shaking table will not generate a loading exceeding the Yield Strength (Engineers Edge , 2020).

Figure 1-4 presents the research procedure included the order of activities in this study.

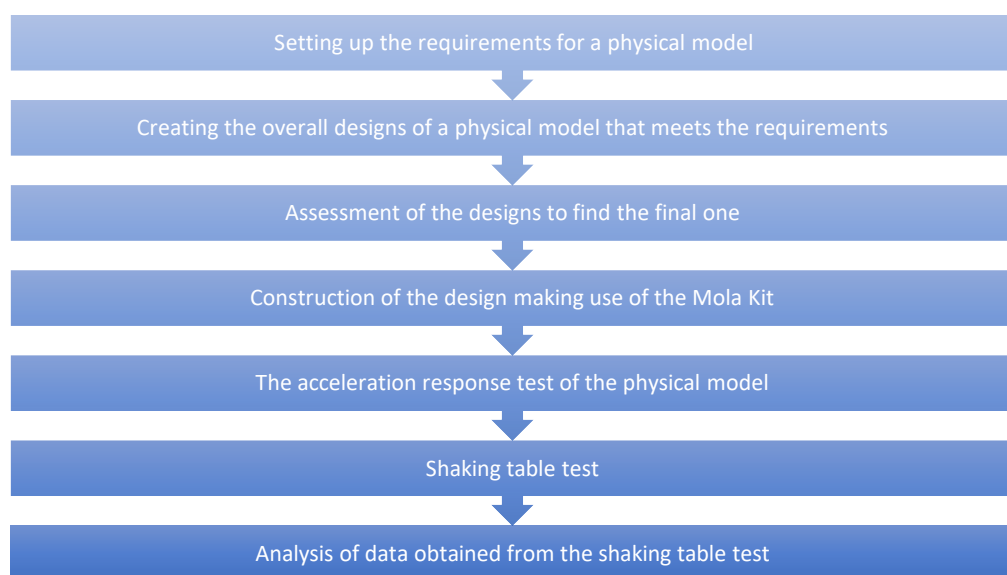


Figure 1-4 Research Procedure

2 Theoretical Framework

2.1 The cable-stayed bridge type

As mentioned in the introduction, this thesis focuses on the design of a physical model for a cable-stayed bridge.

In general, the structural design of a cable-stayed bridge must include a deck, stays and towers (figure 2-1). The cables support the bridge deck while working as elastic supports. The bridge deck, which is in flexure compression, transfers the loads to the stays. The tower is a compressed component by the forces from the cables, which are in tension, the compression forces move from the tower to the foundation (Lin & Yoda, 2017).

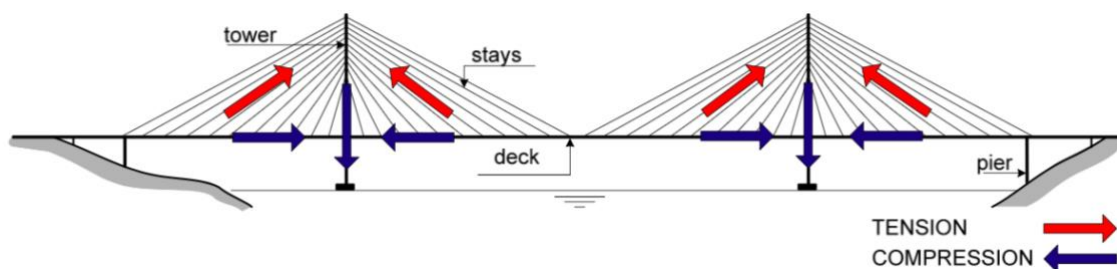


Figure 2-1 Typical cable-stayed bridge and its forces

2.1.1 Arrangement of the stay cables

There are four main classes of a cable-stayed bridge based on the arrangement of the cables, how they run from the tower to the deck. The basic bridge classes are shown in the rows of Figure 6. However, the number of cables may vary based on the structural requirements. Therefore, the system is further classified based on the number of cables, as shown in table 2-2. From the single cable, to the double, triple, multiple or variable (Troitsky, 1998) The point in which a stay is fixed to a deck is called a point of attachment. The number of stays defines the number of points of attachment.

STAY SYSTEM	SINGLE	DOUBLE	TRIPLE	MULTIPLE	VARIABLE
	1	2	3	4	5
1 BUNDLE OR CONVERGING OR RADIAL					
2 HARP OR PARALLEL					
3 FAN					
4 STAR					

Table 2-1 The classification of a cable-stayed bridge

The crucial aspects to be considered during choosing the bridge class are (Anwar, 2016):

- The horizontal distance from the tower to a point of attachment
- The height of a point of attachment above bridge level
- The stretched length of a cable
- The angle between a cable and the tower

In the following paragraphs the four classes are presented in further details.

1. Radial System

This system is characterized by cables running from the top of the tower (figure 2-2). The main advantage of this system is in the structural optimization: because of the maximum inclination between the cables and the deck, each cable carries the maximum component of the dead and live load forces. By optimizing the performance and layout of the cables, smallest amount of steel is needed. Contemporarily also the axial loads in the deck are at a minimum (Troitsky, 1998).

On the other hand, a greater number of cables is very densely dislocated at the top of the tower, which experiences also concentrated compressive forces. Therefore, more attention must be placed at the detailing of the tower, due to its complexity (ESDEP, 2011).



Figure 2-2 Pasco-Kennewick Bridge, Washington, USA

2. Parallel System

The parallel system integrates dislocating the cables along different heights of the tower and placing them parallel to each other (figure 2-3). This solution is highly esthetical, although it causes bending moments in the tower. The support of the lower cables must be investigated under the ability to being fixed at the tower leg. This cable arrangement provides a great stiffness for the main span. The material usage is higher than for the radial system. Additionally, a higher tower is structurally preferred to increase the stiffness and decrease the cable deflection (Troitsky, 1998).



Figure 2-3 Øresund Bridge, Malmo & Copenhagen, Sweden & Denmark

3. Fan System

The fan system is a modified version of the parallel system and the difference may be seen by the cable arrangement, that concentrates closer to the tower top (figure 2-4). Such method requires smaller quantities of steel. The forces acting on cables are deciding, what kind of ropes can be used, single or double. The connection between the cables and the tower remains fixed (Troitsky, 1998); (ESDEP, 2011).



Figure 2-4 Normandy Bridge, Le Havre-Honfleur, France

4. Star System

The star system focuses on the aesthetics of the cable arrangement (figure 2-5). The idea of the star system is unconventional, as it contradicts the idea of distributing the cables along the tower and the main girder. This system is characterized by smaller structural resistance comparing to the rest of the systems (ESDEP, 2011).



Figure 2-5 Abdoun Bridge, Amman, Jordan

2.1.2 Positions of the cables along the deck

The positioning the cables along the deck may be classified by three main kinds (Troitsky, 1988), the three main types are presented in Figure 2-6:

- Double-plane vertical system (a);
- Double-plane inclined system (b);
- Single-plane system (c);

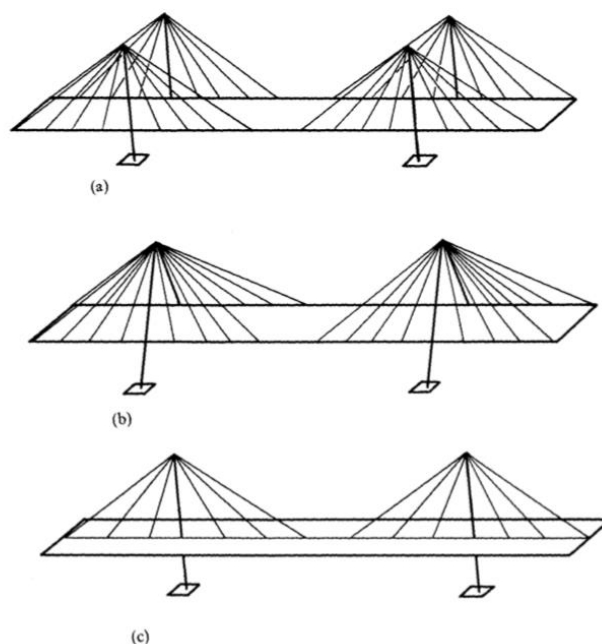


Figure 2-6 Space positions of cables a) Two vertical planes system b) Two inclined planes system c) Single plane system

1. Double-plane vertical system

This system integrates two vertical towers which offer anchorage to the cables, which may be attached outside the deck or along the main girder (figure 2-7). One advantage of the system is that the vertical towers do not interfere with the deck, leaving out all obstruction of cables and towers. An important disadvantage is the transverse distance of the cable anchorage from the web to the main deck, which must be supported by considerable cantilevers transferring the shear and bending moment into the deck. Moreover, the height of the piers of the tower must be increased, so this system cannot be used as part of the road. Thus, the deck width has to be increased to contain all the elements.



Figure 2-7 Jingyue Yangtze River Bridge, Hunan, China

2. Double-plane inclined system

This system involves the same approach as the previous system, although the towers are inclined and connected at the top (figure 2-8). Its application may be found in very long spans, in which the towers must be high enough to require lateral stiffness, which is provided by the second tower connected at the top. Connecting all the cables at the top improves the resistance against the wind oscillations as it prevents the torsional movement of the deck. There is, however, a disadvantage due to the presence of the cables and the tower around the deck. In the wind, it may cause an instability it is common that the points of attachment may be damaged due to the oscillation of the stays.



Figure 2-8 Kanchanaphisek bridge, Samut Prakan, Thailand

3. Single-plane system

A completely different system is made of only one vertical plane of stay cables located along the middle of the main girder of the deck (figure 2-9). The cables are attached in a form of a single vertical strip. This system must be used in combination with a hollow box main girder, which offers substantial torsional rigidity to maintain the change of cross-section deformation due to eccentric live load within allowable limits. The single plane system divides the deck into two parts with a separation line. This separation is an economically and aesthetically tolerable solution due to its advantage of relatively small piers.



Figure 2-9 Tsurumi Tsubasa Bridge, Yokohama, Japan

2.1.3 Tower Type

The towers are determined based on the bridge design, and they can be inclined or perpendicular to the deck. In turn, the inclination of the tower affects its positioning on the bridge deck due to the structural requirements. Also, the design specifies the type of a frame namely, a single column passing through the centre or a pair of columns on both sides of the bridge deck. Various tower types are presented in Figure 2-10.

The materials used for constructing towers are usually concrete and steel (Chen & Duan, 2014)



Figure 2-10 Types of towers

A different name of a bridge tower is a pylon. The most decisive aspect during designing phase of pylon is the axial force that comes from the support of the cable system (Gimsing, 1983).

In the past, portal pylons were the most common type of pylons used to obtain stiffness against the wind load that is transferred by the cables to the towers. After more investigation of the forces acting on the pylon in the cable-stayed bridges, it was discovered that the horizontal cable forces were relatively small (Giavoni, 2017). Therefore, more bridges were built with freely standing tower legs. When the tower legs are inclined, the stabilizing restrain force is granted by the inclined cables to the top of the tower. The single or twin tower without cross-member remains stable in the lateral direction, only if the cable anchorage level is positioned above the level of the tower base (Bruneau, 1992). If the wind force causes displacement at the top tower, there is an increase in the cables length and in increasing tension as a restoring force. The restraining effect of the cables fixed restricts the longitudinal moment of the tower. The single-pylon and single plane system requires the tower to be fixed to the box. Moreover, the box must be reinforced, but strong bearing must be provided. In such set-up, the supports can resist the horizontal forces that are caused by the friction forces in the bearings (Chena, Aub, Thamb, & Leeb, 2000).

2.1.4 Deck Type

A bridge deck in cable-stayed bridges consists of concrete, steel or composite. However, its composition depends on the bridge span. The mid-span needs to be lighter to minimize the displacement, thus it is constructed of steel or composite. While the side spans need heavier components and concrete is its main element. This approach is applied to reduce the downward deflection in midspan, and eliminates the upward deflection in side spans (Lin & Yoda, 2017). The recommended sections for middle and side spans of a cable-stayed bridge (figure 2-11), the steel section for the midspan decreases the deck self-weight.

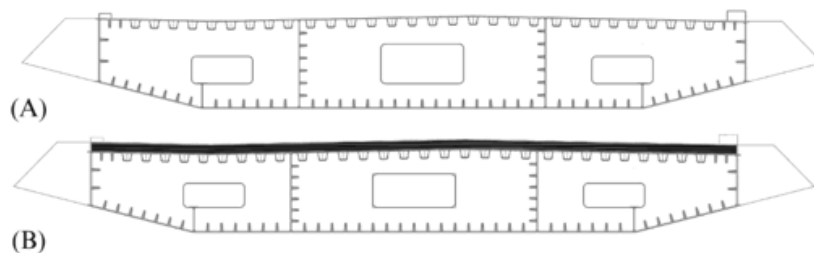


Figure 2-11 Steel deck and composite deck; (A) steel section for middle span, (B) composite section for side span

Majority of the cable-stayed bridges is built with orthotropic decks which specification is defined by the type of the ribs (figure 2-12). The differences in the deck may be found in the cross-sections of the longitudinal ribs and the spacing of the cross-girders (Troitsky, 1988).

The orthotropic deck performs as the top part of the main girders.

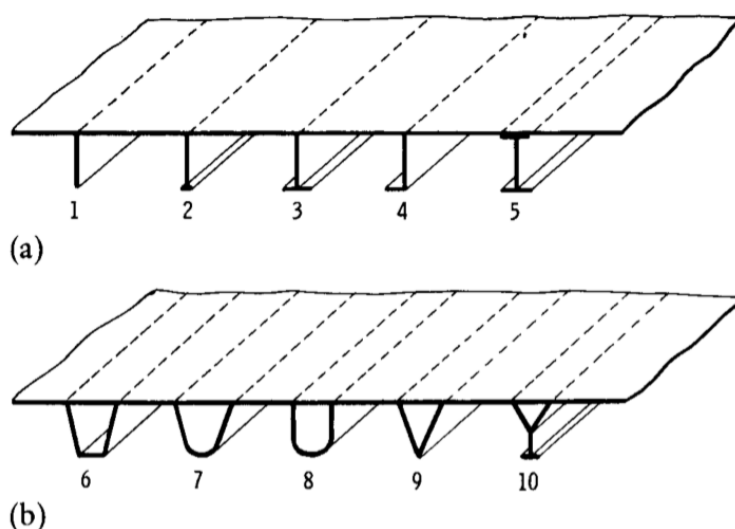


Figure 2-12 Types of ribs a) torsionally weak/open type b) torsionally stiff/box type

The main solid girders can be divided into two kind, shown in table 2-2 (Troitsky, 1988):

- **Plate I-girders** which are equipped with a built-up bottom flange that is made of several cover plates. Such approach ensures that the inertia of the section fits the moment. That method does not require excessive amount of steel to be constructed, achieving the minimal steel weight.
- **Box girders** are characterized by maintaining minimal plate thickness of the span to prevent local buckling. On the contrary, the inertia does not need such thickness as it is provided. Their main advantage is the fabrication simplicity comparing to the plate I-girder. Importantly, a standard section with the plate thickness can be produced in series what impacts on the reduction of fabrication costs.

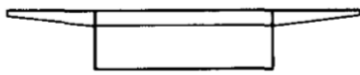
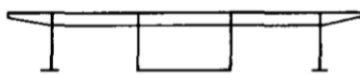
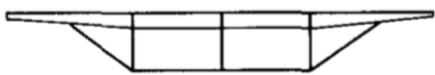
Types of main girder		
Arrangement	Deck cross - sections	
1	Twin I girder	
2	Single rectangular box girder	
3	Central box girder and side single web girders	
4	Single twin cellular box girder and sloping struts	

Table 2-2 Types of main girder

2.1.5 Cable Type

The cables used for the cable-stayed bridges may be different under numerous aspects. Mainly, they may comprise of multi-strand cable made up of cold drawn wires or single strand cable (mono-strand cable) consisting of parallel wires (figure 2-13). The diameters are usually in the range from 40 mm to 125 mm.

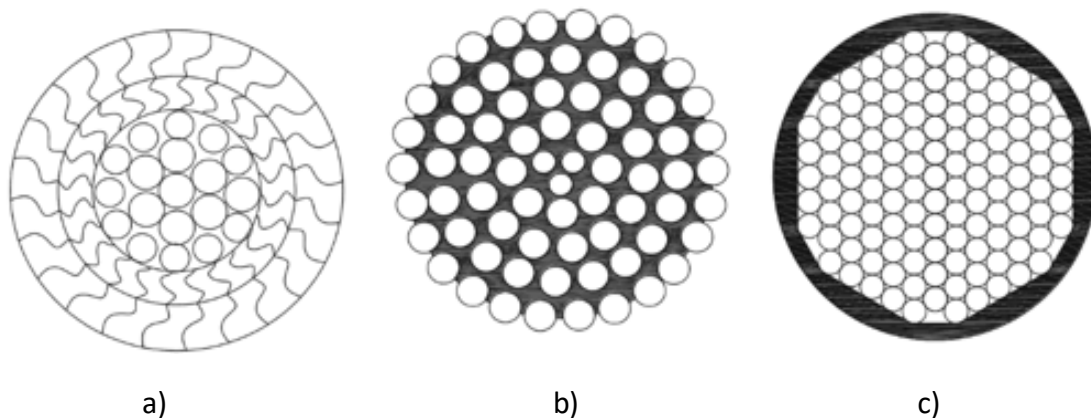


Figure 2-13 The cable types for cable-stayed bridges. a) Locked coil cable. b) Spiral strand cable. c) Parallel wire strand

The key tensile element of the cable is made of high tensile pre-stressed steel and standardized structural steel for anchorages. The cables must be covered with a protection against corrosion as it creates the main concern: as protective measures zinc and other corrosion protective coating substances are applied on the steel components. Moreover, the cables can be covered with high density polyethylene protective cover to increase the resistance against corrosion (Anwar, 2016). The steel wires are also galvanized to avoid corrosion (Lin & Yoda, 2017).

The cables are the indispensable component of a cable-stayed bridge as they carry and transfer the loads. Attaching the cables is achieved due to the anchorage system that stabilizes them between the deck and the tower. The different wiring reaches different tensile strength which differs from 1230 N/mm² for bar bundles to 1770 N/mm² for the prefabricated locked coil.

While the cables are being chosen for the structure, it is crucial to consider such elements as (Anwar, 2016):

- Durability
- Wide size range
- Easiness of Installation
- Unitary Stressing (Strand by Strand)
- Adjustable anchorages for full stay stressing or distressing
- Force checking or monitoring at any time
- Replacement of stay or strand by strand individually
- Ability to damper Installation Longer Fatigue Life (2 million cycles)

2.2 Physical Model

Physical models are usually constructed for experiments and visualization (Price, 1978). Models structure can be modified according to project needs (Design Technology, 2020) but the model design must always be accurately constructed to implement a reliable testing component (Yalin, 1989).

A physical model is a physical reproduction of a structure, including the most influential forces that act on the system in appropriate ratio to the model size (Hughes, 1993). Therefore, the most important characteristic is to determine how to scale the structure geometry and acting forces, for which scaling criteria and similitude law are applied respectively. These two principles are based on geometrical or dynamic similarity between a structure and a physical model. The geometrical similarity focuses on scaling the size of a model maintaining its shape and characteristics, while the dynamic similarity displays the ratio of all acting forces on the model in the system (Balawi, Shahid, & Al Mulla, 2015). The similitude law and scaling criteria must be obtained applying formal mathematical conditions and mathematical representation of the physical properties must be presented to determine these criteria (Yalin, 1971).

Physical modelling is an essential component of shaking table tests, mainly because most shaking tables do not have such dimensions to test the real-size structure. Thus, the structures must be replaced with their scaled physical models. The size of the models may vary in line with the available resources and with the technical requirements of the shaking table used.

For instance, Candeias, Costa and Coelho (2014) conducted a shaking table test of a 1:3 scale model of four store unreinforced masonry building.

The prototype structure used in the research had depth of 9.45 and width of 12.45m², and the geometrical scale of 1:3 was adopted. Thus, the scaled models had 3.15x4.15m². The model was created out of a self-compacting concrete with a composition investigated to

reproduce the behaviour of the prototype masonry walls. This concrete was used to reproduce the most reliable outcome as possible (figure 2-14).

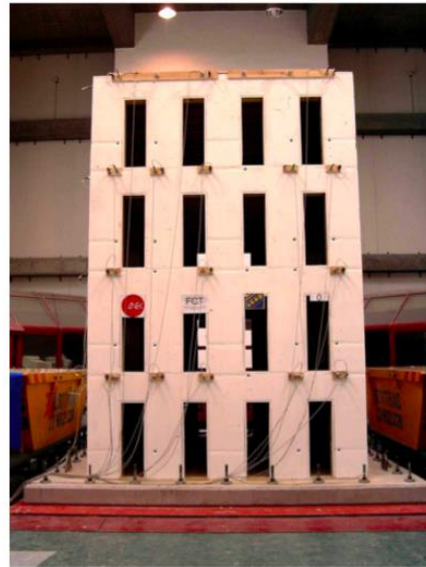


Figure 2-14 The front view of model.

As the geometrical scaling was finished, all phenomena involved in the dynamic test were reduced according to a proportionality. Below Table 2-3 presents all phenomena.

Parameter	Symbol	Scale factor
Length	L	$L_p/L_m=\lambda=3$
Elasticity modulus	E	$E_p/E_m=e=1$
Specific mass	ρ	$\rho_p/\rho_m=\rho=1$
Area	A	$A_p/A_m=\lambda^2=9$
Volume	V	$V_p/V_m=\lambda^3=27$
Mass	m	$m_p/m_m=\lambda^3=27$
Displacement	d	$d_p/d_m=\lambda=3$
Velocity	v	$v_p/v_m=1$
Acceleration	a	$a_p/a_m=\lambda^{-1}=1/3$
Weight	W	$W_p/W_m=\lambda^3=27$
Force	F	$F_p/F_m=\lambda^2=9$
Moment	M	$M_p/M_m=\lambda^3=27$
Stress	σ	$\sigma_p/\sigma_m=1$
Strain	ϵ	$\epsilon_p/\epsilon_m=1$
Time	t	$t_p/t_m=\lambda=3$
Frequency	f	$f_p/f_m=\lambda^{-1}=1/3$

Table 2-3 The scale factors of the Similitude Law (Candeias, Costa, & Coelho, 2004)

The similitude law and scaling criteria are determined from scale ratios between model and prototype. They must be obtained applying formal mathematical conditions. Mathematical representation of the physical properties must be presented to determine these criteria (Yalin, 1971).

Another shaking table test was conducted about the Protiron dry stone masonry structure scaled in 1:4 (Nikolića, Krstevskab, Marovića, & Smoljanovića, 2017), as showed in Figure 2-15 and 2-16.



Figure 2-15 The front view of the Protiron



Figure 2-16 The fully assembled model of Protiron

Being the dimensions of the Protiron 13mx13m (width x height) and the dimension of the shaking table platform 5mx5m, the model was scaled to ca. 3.3mx3.3m.

The physical model was created as a true replica model. The corresponding material for stone was chosen to fulfil the adequate scaling criteria (table 2-4).

Parameter	Required scaling factor	Obtained scaling factor
Length, displacement (L_r)	1/4	1/4
Time (t_r)	$(1/4)^{1/2}$	$(1/4)^{1/2}$
Frequency (f_r)	$(1/4)^{-1/2}$	-
Mass density (ρ_r)	1	1
Inertia force	$(1/4)^3$	$(1/4)^3$
Modulus of elasticity (E_r)	1/4	1/2.6
Strain (ϵ_r)	1	1
Acceleration (a_r)	1	1

Table 2-4 The scaling factors for the Protiron model

Physical models are a successful engineering tool due to their range of benefits. Two main advantages of using physical models can be distinguished (Dalrymple, 1985). Firstly, using the physical models integrates the main equations, which are related to the acting forces, without simplifying assumptions as commonly done in the analytical or numerical models. Secondly, the reduced size eases the data collection at lower costs in comparison to field data collection.

Additionally, observing a physical model during testing presents the immediate qualitative impression of the physical process which in turn boosts the studying focus and diminish the planned testing (Kamphuis, 1991). Finally, a physical model represents an idea in a clear way, narrowing room for any kind of misunderstanding between team members so a group working on a model has more freedom in modifying ideas (Design Technology, 2020).

However, physical models have numerous disadvantages too. For example, scale models need time to be built and people engaged in the physical modelling are required to possess some level of a model-building competence. Furthermore, depending on the model characteristics, prototypes can be expensive. Modifications require access to materials and

some models might not be built of the same material (Design Technology, 2020). Another point of attention is that performing experiments must be realized with the highest precision to obtain reliable results (Hansen i Svendsen, 1985).

The goal of the physical model used in this research is to work as a verification tool for an analytical computation. This model is idealized and simplified to minimize scale effects and to provide a test case that resembles the assumptions included in the numerical computation. Therefore, such type of a physical model might be named as a validation model (Dalrymple, 1989).

2.2.1 Mola Kit application to realize physical model in simple structure analysis

Mola Structural Kit is a set of pieces that allow to create an interactive physical model. Its main feature is that it simulates the structural behaviour. The Mola pieces are a set of modular parts, which can be connected by magnetism. Mola Kit allows to create numerous structural systems that are able to visualize the deformations and movements of structures under loading conditions. It works as a qualitative analysis tool that is used for conceptualization and verification of structures. Working with Mola Kit develops an intuitive knowledge of the structural behaviour.

Mola models make the displacement and deformation visible, because they were designed with certain materials that allow to visualize these phenomena. The Mola Pieces represent tension, compression and bending by applying an external force (figure 2-17 and 2-18).

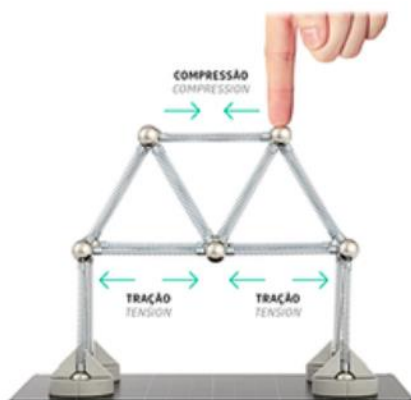


Figure 2-17 Compression on a Mola model



Figure 2-18 Bending on a Mola model

Mola Kit was studied and validated by the research of Gerais (2018), in which more than 40 tests were conducted testing single elements, flat and spatial structures. The results of this research ensured high similarities between models made of Mola Kit and real structural elements. Mola Kit was constructed in this way to represent the behaviour of acting forces on Mola models in the very realistic way.

Mola Models were used in the past for shaking table test (Quanser, 2019) too. In this test, the stability of two-story frame was presented, and a difference in the structure stability between using bracing with Rigid connection 90° and diagonals D6x6 was compared (figure 2-19 and 2-20).

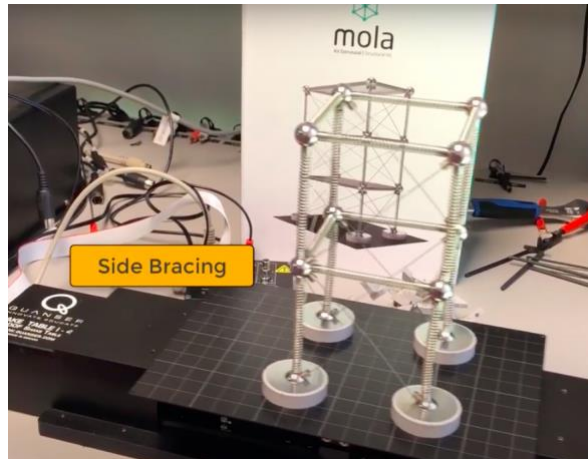


Figure 2-19 The shaking table test of the 2-story frame with Side Bracing

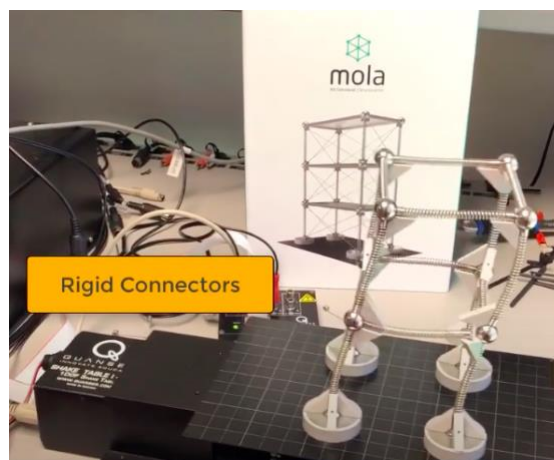


Figure 2-20 The shaking table test of the 2-story frame with Rigid Connectors

The shaking table generated harmonic loading with sinusoidal wave, with the frequency of 3 Hz and displacement of 1cm. The effect was that the rigid connectors did not provide as much stiffness as the side bracing. Thus, the frame with bracing was much stiffer, and maintained its structure in the same form as before the shaking table started working. While, the rigid connectors did not provide that much stiffness, and the vibration even made the beam detached from one joint, as visible in Figure 2-20.

This research considers three designs of a physical model of a cable-stayed bridge realized using the Mola Structural Kit 1&2.

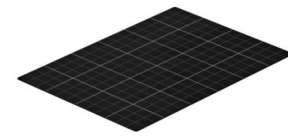
The three models must comply with the available number of pieces in the kits, and must optimize their use.

Following a list of the pieces available within the two kits (Mola Model, 2020):

Element Number	Name of Element	Quantity of Kit 1 & 2	Function	Visual Representation
1.	Connection	12 & 18	It is responsible for the attachment between the elements.	

2.	Rigid connection 90°	48 & 12	It is used to tighten the connection to 90°.	
3.	Continuous connection	0 & 12	It is used to provide the connection between two columns or beams that they work as a single element.	
4.	Continuous connection 90°	0 & 12	It is used to provide the connection between two columns or beams that they work as a single element.	
5.	Ground connection	4 & 6	It represents the foundation of the structure, provides the attachment of the structure to the soil.	
6.	Bar 4	0 & 18	It represents the column or beam.	
7.	Bar 6	24 & 30	It represents the column or beam.	
8.	Bar 12	6 & 0	It represents the column or beam.	
9.	Diagonal D4x6	0 & 24	It represents the slender structure elements such as braces.	
10.	Diagonal D6x6	12 & 9	It represents the slender structure elements such as braces.	
11.	Diagonal D6x12	12 & 0	It represents the slender structure elements such as braces.	
12.	Plate 6x6	0 & 3	It is a rigid element that represents a planar surfaces such as slab.	

- | | | | |
|-----|------------|-------|---|
| 13. | Plate 6x12 | 3 & 0 | It is a rigid element that represents a planar surfaces such as slab. |
| 14. | Ground | 1 & 1 | The base plate represents the soil. |



2.2.2 Schedule of requirements for the design of a scaled model for a cable-stayed bridge

Functional Requirements

Broadly speaking, the design of a physical model for a cable-stayed bridge must fulfil several functions:

- Provide the scheme how a model of a cable-stayed bridge should look like
- It must work for a physical model of a cable-stayed bridge in such way that the model will be stable
- It must provide possibility to test a physical model on a shaking table

The design will integrate the elements of a cable-stayed bridge such as the design of the pylon, arrangement and position of cable stays. The Mola Kit provides a set of modular elements. Thus, the design will cover the overall elements, not a detailed design of a cable-stayed components. The design must provide such structure of the Mola pieces that a physical model will have enough stability. This stability is necessary for shaking table test, a model cannot be attached to any different area than to the shaking platform of a shaking table to obtain reliable results.

Technical Requirements

The model weight cannot be greater than 5 kg, because that is the limit of the shaking table capacity.

The vibration mode and vibration frequency of the model cannot exceed the vibration frequency generated by the shaking table. Therefore, these properties must be below 4,8 Hz.

The distance between the model pylons must be smaller than 35 cm, because the larger span will not fit on the shaking table platform.

The deck stiffness must be continuous, because it keeps a uniform forces distribution along the deck.

The design of a physical model must be verified with reliable standards which ensure its stability. Avoidance of failure can be pursued by conducting structural check that are integrated into the Eurocode standards. The design standards for structures in earthquake-prone areas are the following:

- Eurocode EN 1990 (Basis of structural design)
- Eurocode 1 EN 1991 (Actions on structures)
- Eurocode 8 EN 1998 (Design of structures for earthquake resistance)

The shaking table test must be performed according to the procedure given by the University of Ferrara. The shaking table test procedure must be delivered to utilize the design of a physical model. The approach integrates the maximum usability of the design. Providing an outline of the necessary steps that must be executed affect the results reliability.

2.2.3 Preliminary design of the model variants

The limitation of Mola pieces is due to the fixed length of bars and diagonals is fixed. Model columns and beams use bars; model cable stays are made of diagonals.

The limitation enables to construct only a few types of cable-stayed components. In the next paragraph, the possibility of reproducing each bridge component is described focusing on the limitation of Mola Kits.

Arrangement of the cable stays can be modified as it integrates numerous elements. The radial system can be constructed as the upper part of the tower is made of one bar. Cables are attached to the top of a tower providing stability. Parallel, Fan and Star systems are impossible to reproduce due to the cables positioned parallelly along the tower. Such arrangement needs multiple very short bars that cannot be found in Mola Kits. The length of diagonals, which is also fixed, affects the positioning the cables along the deck. It excludes to reproduce the double-inclined system, as the length of the diagonals is with the bar length that are only positioned vertically. Trying to create the single-plane system, it was presented that the diagonals do not have enough strength to support the whole deck. Choosing the tower type is crucial for the arrangement of the stay cables, as the tower type defines the cable arrangement. The A-type is used for the double-plane inclined system, and the single type integrates the single-plane system. The H-type is used in the double-plane vertical system; hence it may be realized in the designs. The deck type can be chosen from the plate I-girder or box girder. The deck in the designs is constructed making use of the plates. The plate structure resembles the plate I-girder type, moreover, the deck is a modular piece. Therefore, its structure cannot be modified. The stay cables are reproduced in the designs using the diagonals that are also modular elements. As the cables are always covered with a protection, under which there are numerous parallel wires. The cables are presumed to be the mono strand cable. As the diagonals behaviour is the most like the mono strand cable.

The study developed three designs of a physical model. Only three designs were created as such number exploited the maximum differences between the bridge components. It provided the differences between the designs. If more designs were created, the model structures would have more similarities. As the model share numerous identical components. The focus was placed on increasing the distinguishability between them.

Summing up, all the designs have the arrangement of the cable stays as the radial type and the position of the cables along the deck is the two-vertical planes system. The tower type is the H-type, while the deck is constructed of the plate I-girder. The cables are mono strand cables.

The models share numerous elements which are identical. It is because such application of effective Mola pieces affects the stability in the best possible way. The stability of the models is crucial factor for the acceleration response test and shaking table test. The designs must be stable enough that these tests can be performed. If any external way of supporting stability is provided, it does not record the real model response. Thus, the results are not reliable.

First of all, the tower types are identical in the three models: they are H-type with diagonals D6x6. The internal diagonals D6x6 limit the displacement in y-axis increasing the stiffness.

The pylons and the deck are supported using the rigid connection 90°, such solution provides extra stability in X-axis and minimizes the deck deflection. The X-axis will be named in the research as the transversal direction. The models have also rigid connections 90° around the lowest column at the base. This is decided because of applying this element on the pylon column reduces bending in both directions. The columns have shorter bending length; thus, they are more stable in their bending length.

The models differ instead on other elements, such as the deck and the number of the stays. The precise description of each model is presented in the following subchapters.

1st Model Design

This model is characterized by the fewer number of stays. This is possible because the internal part of the deck is represented by the plate 6x12, that provides stability to the model due to its weight. This design uses more bars 12, affecting positively the model stability. The eternal deck parts are supported by the diagonals D6x12 that they are lighter and do not cause the much deck deflection. The pylons have been described at the beginning of this chapter.

The model design views are presented in figures below. Figure 2-21 presented the front view, Figure 2-22 includes the top view, and Figure 2-23 demonstrates the side view.

The model is composed of:

- 4x ground connection
- 16x bars 6
- 6x bars 12
- 16x connections
- 8x diagonals D6x12
- 12x diagonals D6x6
- 2x plates 6x6
- 1x plate 6x12

The total weight of the model is 599,4 grams.

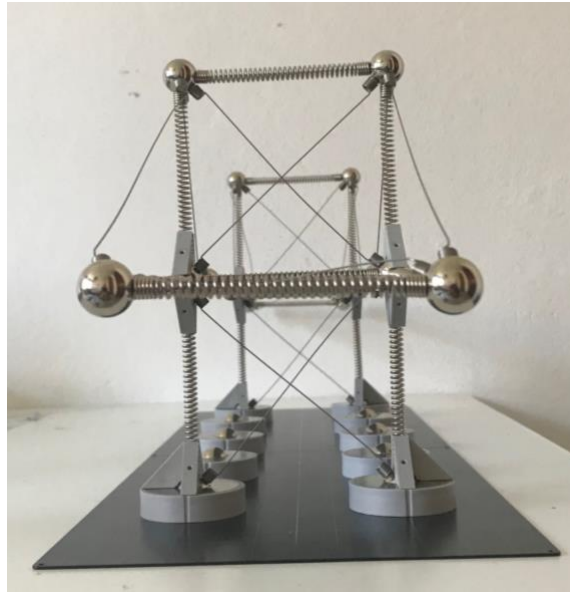


Figure 2-21 The front view of the 1st Model Design

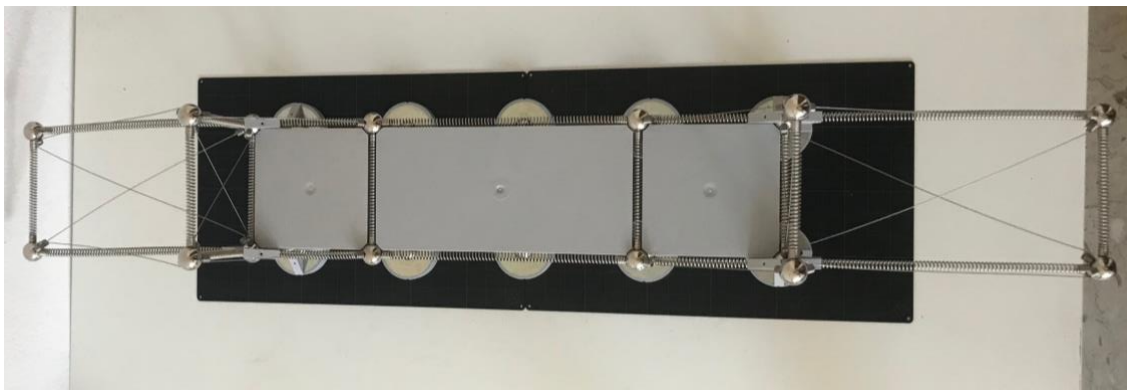


Figure 2-22 The top view of the 1st Model Design



Figure 2-23 The side view of the 1st Model Design

The advantages and disadvantages of the 1st Model Design are listed in Table 2-5.

Advantages	Disadvantages
Very stable the internal part of the deck	Too flexible the external parts of the deck
Little deck deflection	Little support of the deck
Fast to build and convenient to test	More difficult to testing than the 2 nd Design due to side spans being supported by the diagonals what makes it difficult to place the counterbalancing weight
Relatively flexible in comparing to other deigns, less stiffness decreases the natural frequency	Relatively low weight comparing to other models, lower weight increases the natural frequency

Table 2-5 Advantages and Disadvantages of 1st Model Design

2nd Model Design

This design has an unequal distribution of the stays. The external part of the deck is supported by the short and long cables. The short cable is done using the diagonal D6x6 and the long cable is made of the diagonal D6x12. The internal part of the deck is supported only by the long stay that uses the diagonal D6x12. Moreover, the internal part of the deck is constructed of the bars 12, and the external part uses the bars 6. The deck is filled with the plates 6x12 between the pylons. Outside the pylons, the deck is filled with the diagonals D6x6 positioned closer to the tower, and further from the tower there is the plate 6x6. The plate 6x6 at the edges counterbalances the plates 6x12 in the middle. However, the deck is deflected due to the weight of the plates 6x6 at the edges. The middle deck is stiff enough, although its transition point is in the middle, what increases the deck deflection.

The model design views are presented in figures below. Figure 2-24 presented the front view, Figure 2-25 includes the top view, and Figure 2-26 demonstrates the side view.

The model is composed of:

- 4x ground connection
- 18 bars 6
- 4x bars 12
- 18x connections
- 14x diagonals D6x12
- 8x diagonals D6x6
- 2x plates 6x6
- 8x plate 6x12

The total weight of the model 667 grams.

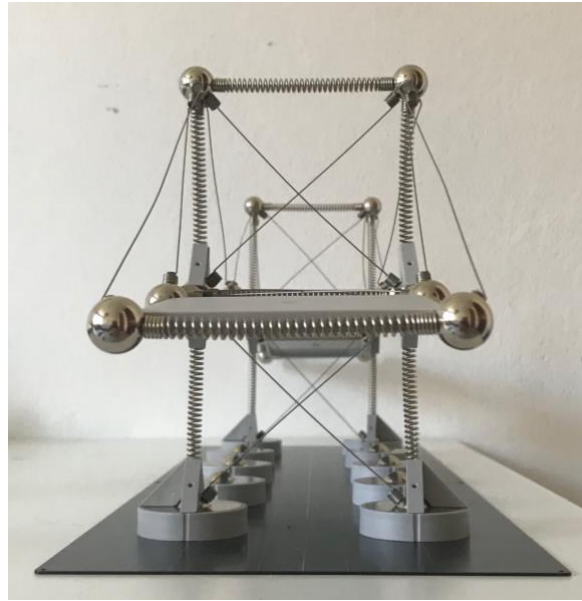


Figure 2-24 The front view of the 2nd Model Design



Figure 2-25 The top view of the 2nd Model Design



Figure 2-26 The side view of the 2nd Model Design

The advantages and disadvantages of the 2nd Model Design are listed in table 2-6.

Advantages	Disadvantages
A stiff internal part of the deck	Too heavy external parts of the deck cause more instability comparing to other designs
Low displacement in Y-axis	Too much deck deflection
Flexible in X-axis	Unequal cable distribution causes the base column bending
Easy to build as the model is constructed of bigger pieces such as the plate 6x12 and bars 12	Too strong load impact and the model loses stability
	The middle of the deck is its weak point; thus, it is sensitive to testing with possibility of collapsing

Table 2-6 Advantages and Disadvantages of 2nd Model Design

3rd Model Design

This design has the most equal distribution of the stays. The external and internal parts of the deck are supported by the short and long cables. The short is done using the diagonal D6x6 and the long is made of the diagonal D6x12. Moreover, the internal and external parts of the deck is constructed of the bars 6. The internal part desk is filled with the plates 6x12. Outside the pylons, the deck is filled with the plates 6x6 positioned closer to the tower, and further from the pylon there is the diagonals D6x6. The plate 6x6 right close to the tower keeps the deck stiff, moreover, the mass distribution is equal.

The model design views are presented in figures below. Figure 2-27 presented the front view, Figure 2-28 includes the top view, and Figure 2-29 demonstrates the side view.

The model is composed of:

- 4x ground connection
- 34 bars 6
- 22 connections
- 18 diagonals D6x12
- 8x diagonals D6x6
- 2x plates 6x6
- 3x plate 6x12

The total weight of the model 814.1 grams.

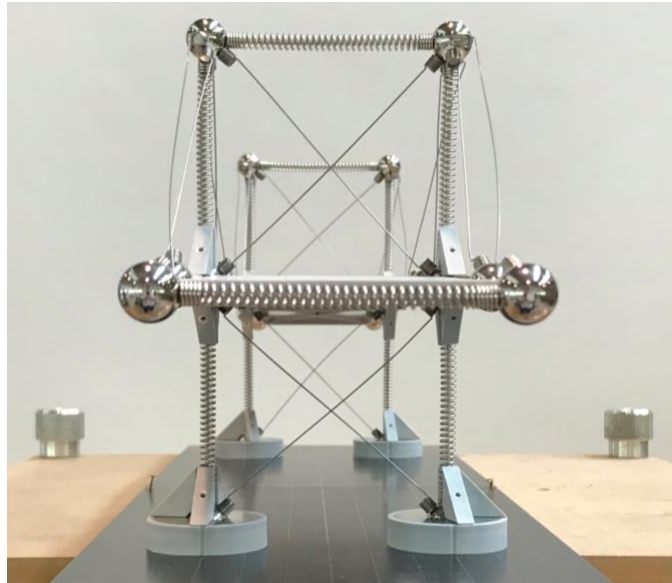


Figure 2-27 The front view of the 3rd Model Design

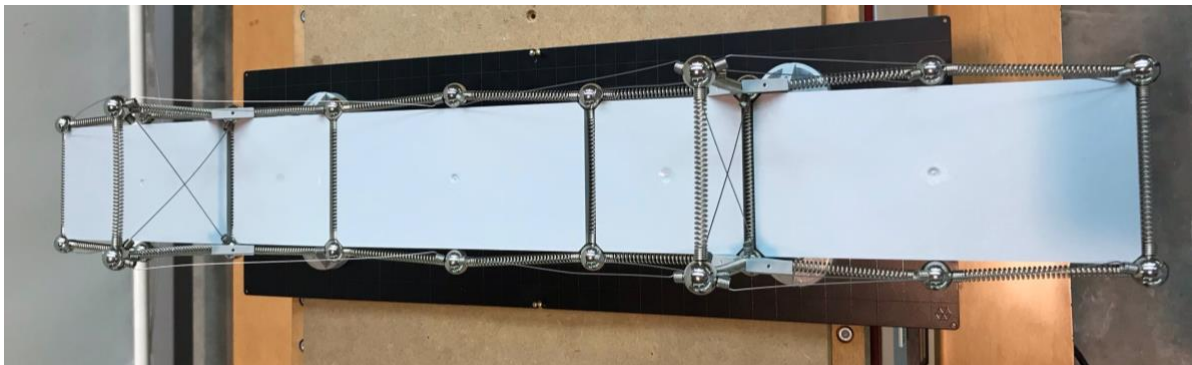


Figure 2-28 The top view of the 3rd Model Design



Figure 2-29 The side view of the 3rd Model Design

The advantages and disadvantages of the 3rd Model Design are listed in table 2-7.

Advantages	Disadvantages
The cables are equally distributed	More time-consuming construction process comparing to other designs
Continuous deck stiffness	
The most stable model out of all designs	
The weightiest model, higher mass lowers the natural frequency	

Table 2-7 Advantages and Disadvantages of 3rd Model Design

2.3 Structural Analysis

A structure is a system of interconnected members constructed as a stable configuration, and its purpose is to support a load or a combination of loads. The load effect can be distributed vertically or laterally along the structural components (Cruz, 2010).

The loads acting on a structural system must be defined to ensure that this system will meet its function. The way to secure that a structure does not collapse is to conduct a structural analysis.

Structural analysis is a detailed examination of structure behaviour investigating the influence of different loads. It comprises the set of mechanics theories that follow physical laws essential to study and calculate the behaviour of structures. Mechanics theories are Newtonian mechanics, the theory of motion, which is known as kinematics, and forces, acknowledged as dynamics. The focus of structural analysis is placed on the ability of a structure to withstand loads. These actions (known as loads) have a classification, which is lied in the table below based on Formichi (2004).

Action Type	Description	Variation in time	Classification (direct/indirect)	Nature (static/dynamic)	Source
Self-weight	It is the intrinsic weight of a structure that remains relatively constant over time.	Permament	Direct	Static	EN 1991-1-1
Soil movement & Earth pressure	It is the load caused by soil exerting in horizontal direction.	Permament / variable	Direct / indirect	Static	EN 1997

Prestressing	It is the introduction of a compressive force to the concrete to counteract the stresses that will result from an applied load.	Permanent / variable	Direct	Static	EN 1990 EN 1992 to EN 1999
Snow loads	The load that comes from snow which is calculated as thickness multiplied by density.	Variable / accidental	Direct	Static / dynamic	EN 1991-1-3
Seismic	It is the inertia force on a structure and its magnitude and distribution on a structure changing in time.	Variable / accidental	Direct	Dynamic	EN 1990 (4.1) EN 1998
Temperature	It is caused by any change in in temperature of material.	Variable	Indirect	Static	EN 1991-1-5
Pre-deformations	It is when an element is deformed before there is an applied load	Permanent / variable	Indirect	Static	EN 1990
Shrinkage	It is when the volume decreases with time causes strain.	Permanent / variable	Indirect	Static	EN 1992 EN 1993 EN 1994
Wind action	It is the force acting on a structure due to wind	Variable / accidental	Direct	Static / dynamic	EN 1991-1-4
Actions due to water	It is the gravity load of a fluid.	Permanent / variable / accidental	Direct	Static / dynamic	EN 1990

Atmospheric ice loads	It is the gravity load of an ice	Variable	Direct	Static / dynamic	ISO 12494
Accidental	It is a result of special circumstances such as collision or explosion	Accidental	Direct / indirect	Static / dynamic	EN 1990 EN 1991-1-7
Personnel and hand tools	It is the load of people and relatively small objects	Variable	Direct	Static	EN 1991
Storage moveable items	It is the load caused by remaining elements that will be removed, such as container	Variable	Direct	Static / dynamic	EN 1991-1-1
Moveable equipment	It is the load caused by the machinery which is used during activities, such as cleaning machinery	Variable	Direct	Static / dynamic	EN 1991-2 EN 1991-3

Table 2-8 Classification of loads

Below, the sources are explained as the table of Eurocodes (table 2-9).

EN 1990	Eurocode :	Basis of Structural Design
EN 1991	Eurocode 1:	Actions on structures
EN 1992	Eurocode 2:	Design of concrete structures
EN 1993	Eurocode 3:	Design of steel structures
EN 1994	Eurocode 4:	Design of composite steel and concrete structures
EN 1995	Eurocode 5:	Design of timber structures
EN 1996	Eurocode 6:	Design of masonry structures
EN 1997	Eurocode 7:	Geotechnical design
EN 1998	Eurocode 8:	Design of structures for earthquake resistance
EN 1999	Eurocode 9:	Design of aluminium structures

Table 2-9 Eurocode Standards

Structural analysis is the method that enables to calculate and determine the effects of loads and internal forces on structures. The significance of structural analysis is crucial for structural engineers. It ensures understating of the load paths and load impacts on the structure design. It guarantees that an element of structure can fulfil its requirements, such as withstanding the estimated loads. It allows engineers or designers to ensure a piece of equipment or

structure is safe for use under the estimated loads it is expected to withstand (Connor & Faraji, 2009).

The objective of structural analysis is to obtain the structure deformation, internal forces and stresses. Practically, structural analysis exposes the structural performance of the engineering design ensuring the reliability of structural design (Chang, 2015).

In civil engineering, it provides a following advantage; it reveals a minimum of material for a structure, which affects reducing cost.

Before the structural analysis can take place, information such as structural load, geometry, support conditions and material properties have to be known. The result of the structural analysis provides values of support reactions, stresses bending moments, displacement and deflection. Consequently, these values must be compared to safety criteria that indicate the failure conditions. The approach of structural analysis is based on the 3 fundamentals relations: equilibrium, constitutive and compatibility (Sarkar, Prasad, & Menon, 2010).

The Eurocode standards integrate numerous principles during designing a structure. The principles described below are of the limit state design based on EN 1990:1999 (E).

The first step is to choose the relevant design situation. The design situation refers to the condition of use.

Below classification of the design situations (Gulvanessian, Calgaro, & Holický, 2002):

- persistent design situations referring to the conditions of normal use
- transient design situations referring to the temporary conditions applicable during circumstances such as execution or repair
- accidental design situations referring to the exceptional conditions such as fire, explosion or consequence of failure
- seismic design situations referring to the conditions when a structure is subjected to seismic events

The next step is to verify the Ultimate limit state concerning:

- the safety of people
- the safety of structure

This state is verified considering the structural loss of equilibrium, the failure by the excessive deformation of a structure and the failure of structural elements caused by fatigue or time-dependent effects.

The following element is to confirm the Serviceability limit state regarding:

- the normal functioning of a structure and its members
- the comfort of people
- the appearance of the construction work

The SLS is confirmed based on 3 main criteria; deformation, vibration and damage. The deformation affects the structural appearance, functioning and users comfort. The vibrations

that cause the discomfort to users and reduce the functionality of a structure. While, the damage influences on the appearance, durability and structure functioning.

The last element, which needs verification during a design phase, is to check the limit state design. It is based on the use of structural and load models for applicable limit states. The limit states are verified by checking if the relevant design values such as action, material properties, product properties and geometrical data do not exceed the limit state.

2.2.3 Seismic Analysis

Seismic analysis is a subcategory of structural analysis. It is a tool which focuses on the response of a structural system to ground motions. It is used to estimate how a structure will react to an earthquake and it is a part of the designing process that calculates earthquake resistant structure (El-Reedy, 2015).

The objective of seismic analysis is to develop a time function that enables to convert ground motions at structure base to loading. The ground motions expressed as a loading time function provide enough measurable data that allows to elaborate more precise information regarding the dynamic behaviour of a structure.

If loading is defined, it provides input for a reliable assessment of a structural system (Costa & Luís, 2003).

In the range of seismic analyses, four types can be distinguished. The type of seismic analysis is chosen based on an external action and the behaviour of structure or structural materials (Kakpure & Mundhada, 2016):

- Linear Static Analysis
- Non-linear Static Analysis
- Linear Dynamic Analysis
- Non-linear Dynamic Analysis

The type of seismic analysis is chosen based on an external action and the behaviour of structure or structural materials, however, before the characteristics of these analyses are described in the following chapter, several concepts must be introduced to provide full understanding.

Degree-of-Freedom

The definition of degrees of freedom is the number of coordinates that it takes to uniquely specify the position or motion of a system.

A structural system can be treated as single-degree-of-freedom system (S-DOF) and multi-degree-of-freedom system (M-DOF). Single-Degree-of-Freedom is when a single coordinate is sufficient to define the position or geometry of the mass of the system at any instant of time. Multi-Degree-of-Freedom is if more than one independent coordinate is required to completely specify the position or geometry of different masses of the system at any instant time. In MDOF system masses move independently with each element displacement (Damodarasamy, 2009) ; (Rubenzer, 2012). Visual representation of different DOF is presented in Figure 2-30.

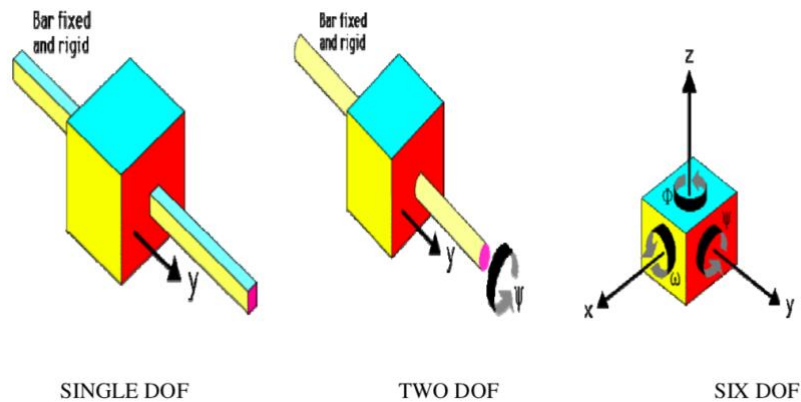


Figure 2-30 Various Degree of Freedom

Elastic & Plastic Region

A tension test, which investigates the material behaviour to controlled tension, provides the result as Stress-Strain curve (figure 2-31). Strain is the response of a system to an applied stress, while the stress is produced during material loading with force. Stress causes material deformation.

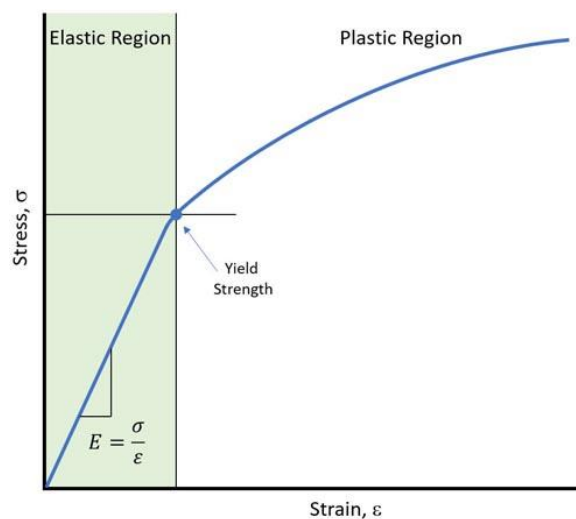


Figure 2-31 Stress-Strain Curve

It presents the linear area in the Elastic Region and the nonlinear behind the Yield Strength.

The stress-strain curve can be divided into two deformation regions, which are the elastic and the plastic region. In the elastic region, material deforms temporarily and fully recovers when the load is removed. In the plastic region, material deforms permanently and does not fully recover when the load is removed, because only a small portion of elastic part in the deformation is recovered.

Explanation of elastic and plastic region provides information about the dynamic behaviour indicating in which region a structure is. Moreover, it explains the crucial assumptions, for example, stiffness and dumping are linear and do not vary in time.

Seismic Loading

Seismic loading is ground motion expressed as time function. During seismic analysis, different types of loading can be investigated. The loading classification relevant for seismic activity is presented in the Figure below (Bai & Xu, 2019).

Harmonic loading is when the applied load varies with time harmonically. It can be expressed as a sine or a cosine function. The example of harmonic load is presented in Figure 2-32.

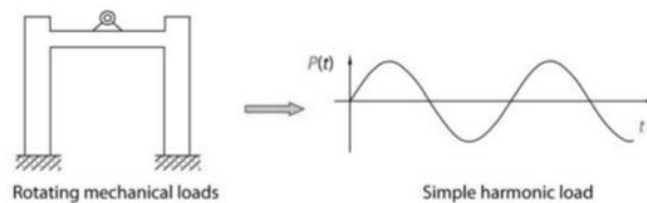


Figure 2-32 Simple Harmonic Load

Random loads are difficult to be expressed due to its complexity or arbitrariness of its magnitude and direction. The example of random load is presented in Figure 2-33.

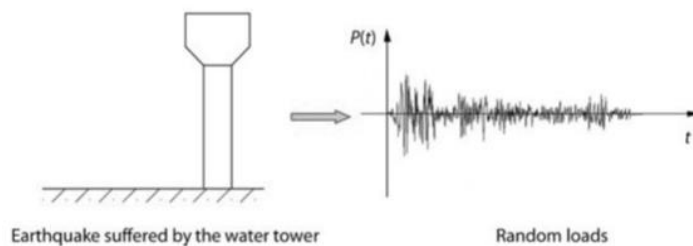


Figure 2-33 Random load

$P(t)$ is an external dynamic force, while t is time.

Free Vibrations

When a structure is subjected to loading, it vibrates. An initial force must act on the structure and then the force is withdrawn to generate free vibrations of the structure. The structure starts vibrating, and continues the motion according to its vibration frequency. In free vibrations, time does not vary to external forces acting on the system (Brower, 2020).

Frequency

The frequency is a motion that repeats itself after an interval of time, for example, a second.

Natural Frequency

The natural frequency is the frequency at which the system resonates. It is the frequency of free vibration of a system. Defining the vibration frequency allows to calculate stiffness. The higher the model stiffness is, the more resistant the model becomes to dynamic loading. Because with higher stiffness, the model is able to resist higher acceleration of loading.

The undamped natural frequency equation for a single-degree-of-freedom system is presented below.

$$f_n = \frac{1}{2\pi} \sqrt{\frac{k}{m}}$$

Equation 2-1 The Undamped Natural Frequency Equation

f_n is the natural frequency, k is stiffness and m is mass

Defining the natural frequency allows to check if the structural system can withstand loading. The natural frequency can be read from observing a system subjected to ground motions, such as these generated during a shaking table test.

Vibration mode

The vibration mode of a system is the mode having the lowest vibration frequency. Vibration modes are independent on external applied loads; they depend only on structural properties. Vibration modes relate to degrees-of-freedom, as the number of DOF defines the number of the vibration modes.

Damping

Free vibration can be damped (figure 2-34). It means that the amplitude of a vibration reduces over time because of energy being drained from the system to overcome the resistive forces (Steidel, 1989).

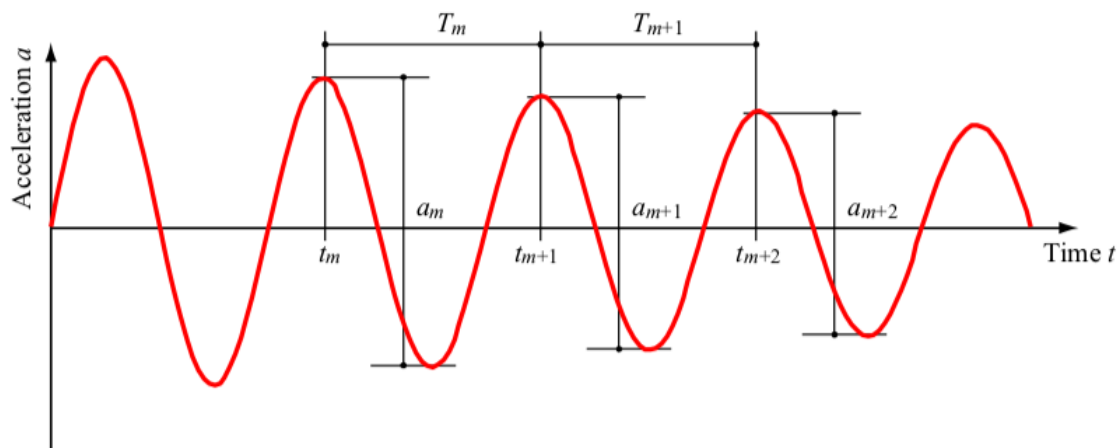


Figure 2-34 Damped Free Vibration

a_m is the peak-to-peak amplitude in acceleration, T_m is the peak-to-peak amplitude in time, +1,2 indicates the number of the cycle.

Dynamic Resonance

Dynamic resonance is a phenomenon when an applied force cause the vibrations of a structural system. The occurred vibrations have the frequency of its natural frequency. When

a structural system is in resonance, subjected the structural system to small force produces a large vibration response (D'Evelyn & Taniguchi, 1999).

2.2.4 Static vs Dynamic Analysis

In the previous chapter four seismic analyses were mentioned:

- Linear Static Analysis
- Non-linear Static Analysis
- Linear Dynamic Analysis
- Non-linear Dynamic Analysis

This chapter focuses on explaining the major difference between these analyses, presenting how they are conducted and their characteristics.

Linear Static Analysis

Linear Static Analysis integrates numerous assumptions, such as the rigidity and corresponding stiffness value of the materials that are assumed constant. A crucial condition that must be fulfilled is that the relationship between load and deformation occurs in proportion to the material stiffness. The loads are static and constant in direction while an analysis is performed. In a linear static analysis, the structure returns to its prior shape after removing the load (Liu, Y., Y., Luan, & Xue, 2006).

Linear static seismic analysis takes a set of forces acting on a structure that represents the effect of seismic ground motions. The first step is to calculate the base shear that the structure must withstand; the base shear is further distributed along the structure height. From the base shear, it is possible to obtain the lateral loads at each level, which can be spread along the width and breadth of the structure. The lateral load is then a horizontal live load that represents ground motion (figure 2-35).

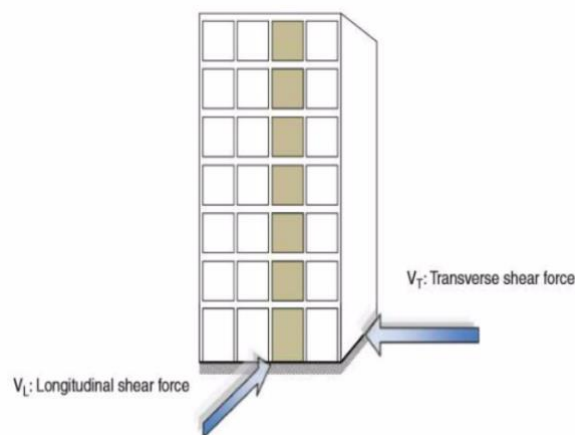


Figure 2-35 Lateral shear forces along two orthogonal axes

This method presumes that a structure responds in one vibration mode, because of treating the structure as a SDOF system. In seismic engineering, the application of static linear analysis is limited to the structure height and can be performed on buildings that are classified as low-rise (Zaidi, Jaffer, Khan, & Maher, 2020). A structure subjected to this analysis must have a

regular mass and stiffness distribution along the structure height (Bhaduri & Krishnagr, 2016).

Non-linear Static Analysis

Contrary to linear static analysis, non-linear static analysis integrates diverse assumptions, so for example the relation between applied forces and displacement is non-linear. The non-linearity comes from analysing the material in the elasto-plastic region of the stress-strain diagram (Dodds Jr i Lopez, 1980). The objective of this analysis is to estimate the strength and drift capacity of a structure, known as seismic capacity. Before it can be determined, it is necessary to define the seismic demand. The seismic demand for the structure is based on selected ground motions. The seismic demand is given as a form of Response Spectrum where you can find pairs of design acceleration with its corresponding natural period (Fajfar, Vidic, & Fischinger, 1989). This analysis checks the non-linear deformation of single elements or the whole structural system by applying lateral loads, which represent the inertia forces during an earthquake. The lateral load application continues until the target displacement is obtained. The final deformation before the collapse of a structure is called the target displacement. The non-linear static approach treats a structure as a SDOF system. The calculation process begins from applying a set of forces along the structure, moreover, the load distribution changes with the displacement of floor levels to induce the non-linear properties.

The non-linear static analysis can be used for higher buildings; hence, it is not only restricted to low-rise buildings. It provides more certainty in the case of calculations as the whole structure behaviour is presented (Bhaduri & Krishnagr, 2016).

Linear Dynamic Analysis

Linear dynamic analysis is used to assess the dynamic response of a structural system when loads are applied relatively quickly. These loads are expressed as time functions. However, the elements of the motion equation, such as the mass, stiffness, and damping do not vary in time. The material deformation is linear; thus, it returns to its primary shape. In this type of analysis, a structural system can be treated as single or multi DOF, providing a finite number of vibration modes as the objective of this analysis method (Dodds Jr & Lopez, 1980). The dynamic analysis may be defined by formulating a mathematical problem, which further leads to differential equations. These equations describe the behaviour of the motion of a physical system as a function of time. The equations of motion consist of inertial force, damping energy and elastic force (Bellos & Inman, 1990). The type of loading does not change the way in which the dynamic response is obtained. Below the equation of motion to give an insight in the dynamic response of a structure (equation 2-2).

Inertia Force – generated by accelerated mass.

Damping Force – an energy dissipation mechanism which induces a force that is a function of a dissipation constant and velocity.

Restoring Force - is due to the elastic resistance in the system and is a function of the displacement and stiffness of the system.

Applied Load – is defined as a function of time, moreover, is independent of the structure to which is applied.

$$m\ddot{u}(t) + c\dot{u}(t) + ku(t) = p(t)$$

INERTIA FORCE

DAMPING FORCE

RESTORING FORCE

APPLIED FORCE

Equation 2-2 Equation of Motion for Single Degree of Freedom

m – mass	u(t)– mass displacement
c – damping coefficient	$\dot{u}(t)$ – mass velocity
k – stiffness coefficient	$\ddot{u}(t)$ – mass acceleration
p(t) – applied force	

This analysis has restrictions regarding the structure irregularities; mainly, the plan or vertical surfaces of a structure cannot be assessed using linear dynamic analysis because a material must remain linear, thus, the mass and stiffness of a structural system must be continuous (Željana, Smoljanović, & Zivaljić, 2015).

Non-linear Dynamic Analysis

The nonlinear dynamic analysis investigates the response of a structural system to an earthquake. Thus, the loading can be random, causing the non-linearity in the material behaviour. As well, while performing non-linear analysis, the stiffness, mass and damping of a structural system or response may vary in time. This is also the main difference comparing to linear dynamic analysis. The material enters the plastic region, while the analysis provides the whole outline of a structural behaviour during loading (Oller, 2014).

Non-linear dynamic analysis can be used to analyse all types of structures, including these which cannot be assessed using the previously described analyses. A structure can have irregularities and discontinuity in its plan and vertical surfaces. It is the most complex way of obtaining a structure response as it integrates all aspects, such as non-linearity and dynamic effects (Chambers & Kelly, 2004).

This analysis is elaborated using the equation of motion at the joints of a structural system presented in Equation 2-3 (Wilson, Farhoomand, & Bethe, 1973).

$$\mathbf{M}_t \Delta \ddot{\mathbf{u}}_t + \mathbf{C}_t \Delta \dot{\mathbf{u}}_t + \mathbf{K}_t \Delta \mathbf{u}_t = \mathbf{R}_{t+\Delta t}^*$$

Equation 2-3 Equation of Motion for Non-linear System

\mathbf{M}_t – Mass at time

\mathbf{C}_t – Damping at time

\mathbf{K}_t – Stiffness at time

$\Delta\ddot{u}_t$, $\Delta\dot{u}_t$, and Δu_t - changes in the accelerations, velocities and displacements during the time increment

This research will use linear dynamic analysis in which ground motions will be generated by a shaking table. The ground motions will have a type of a harmonic loading with the vibration frequency of 4,8 Hz. The design of a scaled physical model will be constructed in such way to obtain the frequency below the frequency of the shaking table. Thus, the material will be only in the elastic range and its behaviour will be linear.

2.3.3 Preliminary Test

This research makes use of the linear dynamic analysis, in which ground motions will be generated by a shaking table. The ground motions will follow harmonic loading with the vibration frequency of 4,8 Hz. The design of a scaled physical model will be constructed in such way to obtain the frequency below the frequency of the shaking table. Thus, the material will be only in the elastic range and its behaviour will be linear.

In order to perform a linear dynamic analysis with harmonic loading, it is fundamental to perform a preliminary test which measures the acceleration response. An acceleration response test of a ground motion can be defined as the ratio between the natural vibration period of a SODF and the maximum acceleration that affects a system due to the ground motion. The natural vibration period can be defined as the time required for one cycle of free vibration, from the moment when a loading is withdrawn till the vibrations become completely damped (Wang, Liu, Liu, & He, 2018).

To measure acceleration response, a system must be subjected to an axial shock load. An axial load is a force that is directed along the lines of an axis, while a shock load is a rapid and impulsive force with a high amplitude. An acceleration sensor must be placed on a system to measure values obtained during testing. The acceleration response is always presented against time. The acquired data can be transformed to obtain the natural frequency. Hence, the acceleration vector must be transformed using Fast Fourier Transformation (FFT). More information about FFT are described in the following chapter (Hanly, 2016).

The acceleration response is a commonly used tool, for example, Lopez-Caballero, Modaresi-Farahmand-Razavi, Clouteau and Pitilakis (2005) investigated the effect of mitigation of clay on retrofitting of foundations using the acceleration response to obtain the vibration frequency. The seismic response of bridges was investigated focusing on the interaction between soil and structure. The ground motions were simulated studying the effect of pounding on the response of the scaled bridge system. The research was performed by recording the acceleration response of the bridge system with and without the effect of pounding (Kun & Chouw, 2015). The acceleration response test was performed to obtain the differences in the linear and non-linear response of a build-up structure. A three-legged test specimen was subjected to a series of axial shock loads, and the acceleration response was recorded (Segalman & Holzmann, 2005).

Acceleration response tests can be used for monitoring the health of a structure. Sarlo (2019) performed a test in which a Mola model of a truss bridge was subjected to a ground motion. The system that had all components in its place was called the healthy system, while the damaged system had a reduced number of rigid connections at the base columns. The

acceleration response of both systems was recorded, and further compared to indicate the differences (figure 2-35 & 2-36).

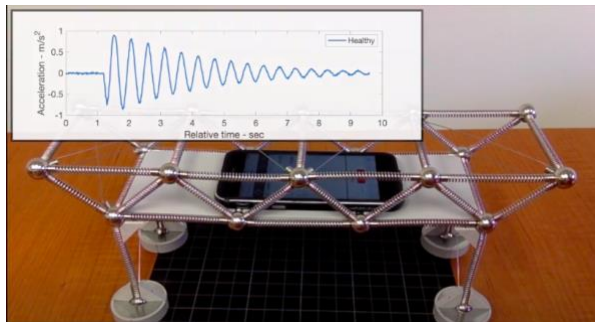


Figure 2-36 Acceleration Response of healthy Mola Model of a truss bridge

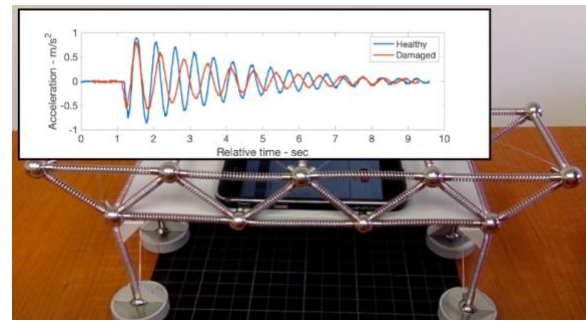


Figure 2-37 Acceleration Response of damaged Mola Model of a truss bridge

In figure 2-35 and 2-36, the blue line represents the healthy system, the red line represents the damaged one.

The acceleration signal obtained due to acceleration response can be then transformed using a fast Fourier transform to find the natural frequency

of the system. This transform translated the signal from the time domain into the frequency domain to obtain the natural frequency (Mercer, 2016), as further explained in the next chapter.

2.3.4 Fast Fourier Transformation in MATLAB

A fast Fourier transform (FFT) was primarily started in the development as a fast algorithm for a DFT in 1805 by Carl Friedrich Gauss. Throughout the 19th and 20th century, the algorithms were developed and numerous versions of FFT were published. In 1965 James Cooley and John Tukey a universal version of FFT. When Cooley and Turkey published the research paper, the FFT patent went into the public domain and become essential algorithm in digital signal processing (Cooley, Garwin, Rader, Bogert, i Stockham, 1969).

In literature, fast Fourier transform has been used to perform an analysis of earthquake records. The chosen earthquake records were transformed using FFT to determine the peaks of the amplitude in the frequency to identify the different seismic phases, the intensity of ground motions and the magnitude of the investigated earthquakes (Huerta-Lopez, Shin, Powers, & Roesset, 2000). A FFT was applied to differentiate ground motions between earthquakes and mining explosions. The research integrated reading the Fourier spectrum results to identify estimated amplitudes for specific frequencies. It allowed to identify the cause of the ground motions in Arizona (Mariani, Gonzalez-Huizar, Bhuiyan, & Tweneboah, 2017).

In principle, this is possible because Fourier analysis allows to deconstruct a signal into its individual frequency components.

A fast Fourier transform can be used to convert a signal from its domain, such as time, to a representation in the frequency domain. It can express the acceleration amplitude as a frequency function, providing the vibration frequency of a system.

In MATLAB, the command of a fast Fourier transform is performed writing a command `fft(x)` (MathWorks, 2020). In MATLAB, `x` represents a wave signal, that can be the amplitude of an acceleration or displacement expressed in the time domain (figure 2-38). The command transforms the wave signal into the amplitude expressed in frequency domain (figure 2-39).

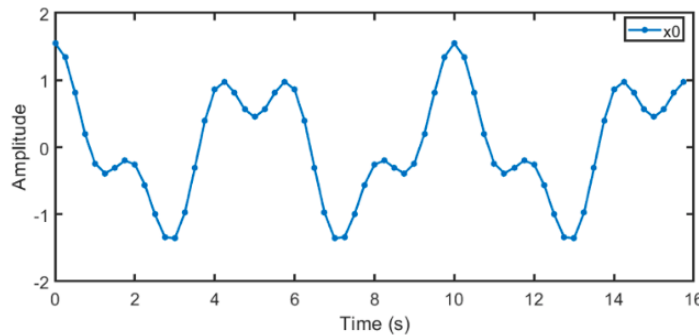


Figure 2-38 The acceleration amplitude expressed against time

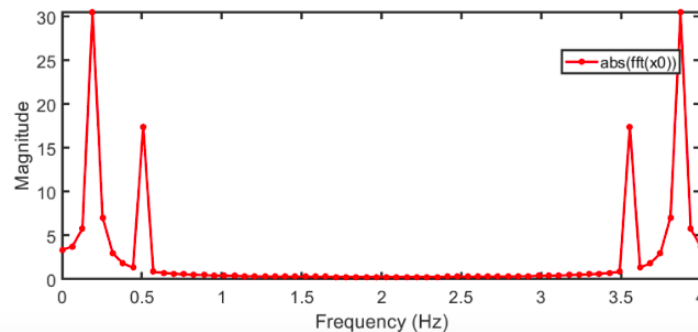


Figure 2-39 The acceleration amplitude presented against the frequency called the Fourier Spectrum

This research utilizes MATLAB due to its suitability for engineers and scientist. MATLAB allows to apply the theory to real life examples. It is possible to directly express the acceleration signal as a matrix or array; such advantage affects the fluency of processing or computing information. MATLAB is characterized by a wide-ranging plotting capabilities that enable to precisely visualize the data. Consequently, MATLAB is required in this research to be used as an analytical tool to conduct the linear analysis (MathWorks, 2020).

2.3.5 Shaking Table Test

The first shaking table was constructed in c.1890 in Japan (Wood, 1988). Again in 1906, the Californian earthquake caused that the Site Investigation Commission founded F. J. Rogers at the Stanford University to build a shaking table. After the 1930 Tokyo earthquake, D. S. Jacobsen started to develop shaking table at Stanford. The table ran on rails being powered by a pendulum strike or by rotating an unbalanced wheel attached to the table. The pendulum generated an initial impulse continued by a weakening vibration, while the unbalanced wheel provided a harmonic motion (Jacobsen, 1930). In 1936, at M.I.T., Ruge built a shaking table that was suspended by wires and controlled by wires attached to the ground. It was powered by an oil-fitted actuator. Moreover, the shaking table input was controlled by applying a defined motion to a specimen on the shaking table. In Japan in 1962, Muto created a 1-DOF

shaking table driven by the release of compressed springs at one side and counteracted by other springs at the other. It produced 2g acceleration and tested a scaled model of the core of the proposed power station at Tokai Mura (Muto, Bailey, & Mitchell, 1962). In 1972, MTS System corporation collaborated with the University of California, Berkley to construct 6x6m shaking table. It was equipped with 3 horizontal actuators acting in the same direction to generate resistance and 4 vertical actuators to produce vertical motion (Rekoske, i inni, 2020). By the end of 1970s, the Public Works Institute in Tsukuba City produced a 6x8m table with a maximum capacity of 100 tons. Moreover, it created a shaking table which consisted of four 2x2m linked tables which nowadays is referred as “multiple-support excitation” (Sawada, 1970). By 1980, a 6-DOF shaking table was constructed although it did not have very reliable control method. The goal of seismic engineers was to create a fully controllable 6-DOF shaking table.

The most significant example of shaking tables was constructed at E-Defence in Japan with dimensions of 20x15m with 3 directions having the frequency range from 0 to 30 Hz. The maximum payload is 12 000 kN. The number of actuators reaches 24 with 10 in the horizontal direction and 14 in the vertical direction (figure 2-40). This facility can test a full-scale 5-storey building, reinforced concrete structures, wooden houses, soil foundations and steel skeleton buildings (Nakashima, Nagae, Enokida, & Kajiwara, 2018).

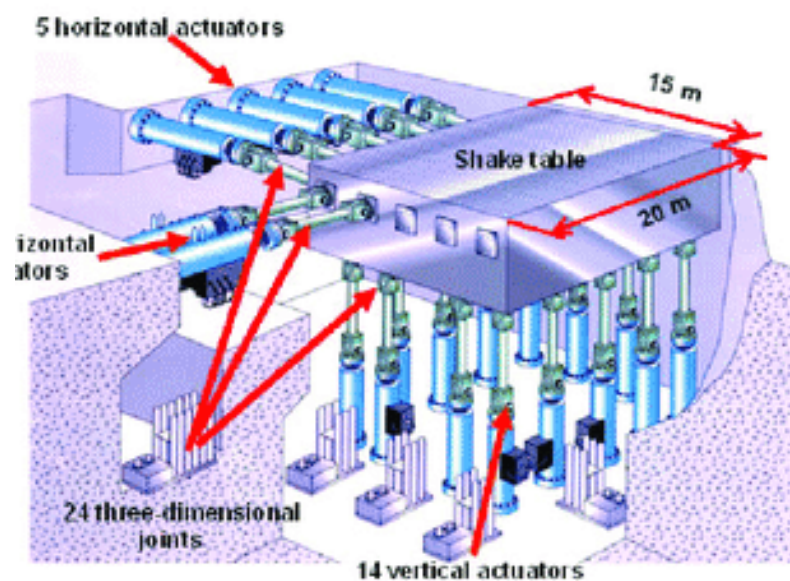


Figure 2-40 E-Defense shaking table

A shaking table is a device that simulates ground motions allowing to test the response of a structure to a dynamic load. Testing with a shaking table delivers the structural response of a structure, moreover, it reproduces realistically the process of seismic activity by modifying the frequencies of vibrations over time. Indeed, a shaking table can generate diverse type of external force, differentiating from 1-D to 6-D, harmonic or random wave.

The main components of shaking table are (Gao & Yuan, 2019)

- Actuator

- Simulator Platform
- Instrument for Measurement
- Controller

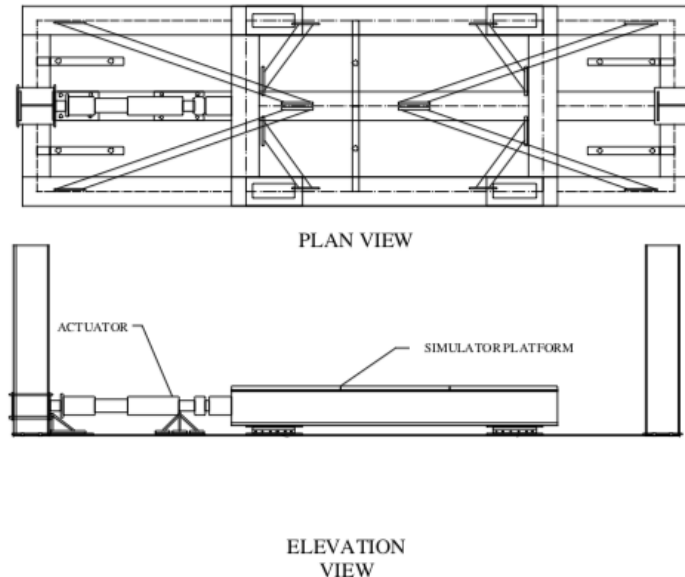


Figure 2-41 The plan and elevation view of a shaking table

An actuator is made of a cylinder containing a piston and a load cell transducer measuring force. The actuator piston movement is executed by putting high pressure hydraulic fluid to one side of the actuator piston. The fluid returns by the opened other side. The force of an actuator equals the effective piston area times the actuating pressure. Moreover, the maximum flow rate determines the maximum simulator base velocity (UPRM, 2019).

A simulator platform gives the surface for placing model. It is fixed to the system and its motion is controlled by the actuator (UPRM, 2019).

An instrument for measurements is usually done by applying accelerometers that are attached with screws to a platform. They are used to measure the displacement of the piston and platform (Tsai, Chen, Chiang, & Chen, 2006)

Finally, a controller can be attached to shaking table, such as a control panel or a computer that is connected to the system. Using a controller, the frequency and type of loading can be modified (Tsai, Chen, Chiang, & Chen, 2006)

The shaking table that has been used in this research has a platform with dimensions of 35x35cm, and its frequency range is from 0 to 4,8 Hz. Moreover, it can generate harmonic and random wave in 1-D.

A shaking table test is a method to investigate the dynamic properties of a structure. Testing on a shaking table allows to apply external forces from small amplitude to large, for instance from 0 to 50 Hz (Guo, Shao, Li, Long, & Mao, 2019). Thus, such method measures the response of a structure to external force. Analysing the response, it is possible to obtain the dynamic properties which are represented by natural frequency, damping ratio and vibration mode. A

shaking table test results in the elastic resonance curve and the time history of elastic or elastic-plastic response (Bairrao & Tvaz, 2000).

The test is executed by placing a physical model on the shaking table base; then the actuators begin to generate the chosen vibration frequencies. The shaking table can generate random wave to obtain the behaviour in the elastic-plastic range (Lu, Fu, Shi, & Lu, 2008) but for a physical model to remain in the elastic range, the amplitudes of the input harmonic waves must be low.

The frequency of the harmonic wave may be modified, then the accelerations at the base and at the top will be taken on the recording paper (figure 2-42).

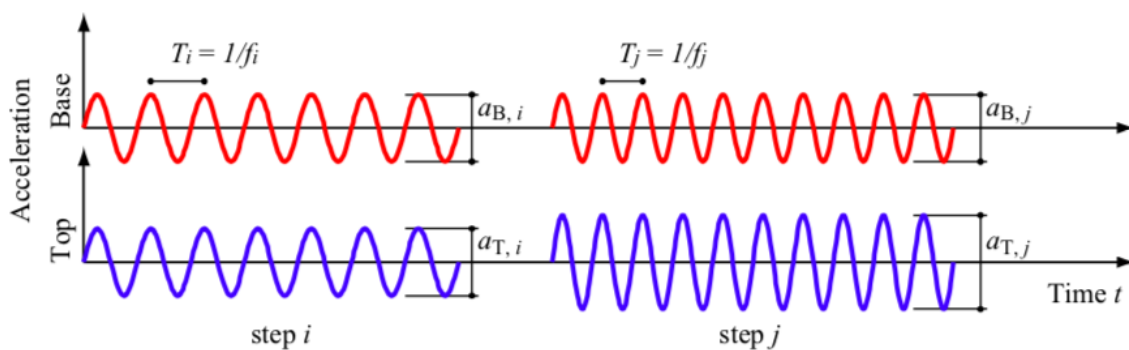


Figure 2-42 Acceleration record from a shaking table test

i & j indicate the used frequency, T_i & T_j is undamped natural period, a_B is the peak-to-peak amplitude of acceleration at the bottom, a_T is the peak-to-peak amplitude of acceleration at the top (Okamoto, Kitagawa, & Motoda, 1994).

3 Methodology

3.1 Construction of a physical model

A complete description of creating the physical models is provided. The designs of a physical model of a cable-stayed bridge were created for the comparison purpose.

The construction of a physical model began with an investigation of the possibilities of Mola Kit 1&2. A cable-stayed bridge is made of a tower, deck and cable stays. All types of the cable-stayed bridge components were studied and tried to be reconstructed. The phase of the model construction concluded that only few types of the bridge component could be reproduced. Mola Kit could recreate a physical model of a cable-stayed bridge whose components were:

- arrangement of the stay cables – radial system
- position of the cables along the deck – double-plane vertical system
- tower type – H-type
- deck type – open type
- cable type – mono strand type

The rest of the components was unable to reproduce maintained the physical model stability and equilibrium between the cable-stayed bridge components.

The physical models share majority of the identical bridge components, the differences between model are expressed using different number of stay cables and different deck.

All the materials used for the physical model construction are described in the following sub-chapter.

The first step of each physical model construction was placing the ground and ground connection (figure 3-1). The crucial aspect was to place the plates equally. The irregularities in the plates must have been eliminated to ensure the precision in the model construction. The ground connections are equipped with 4 axis markings to ensure its position on the ground plate. The 4 axis markings were positioned along the lines on the ground plates to keep the model straight.

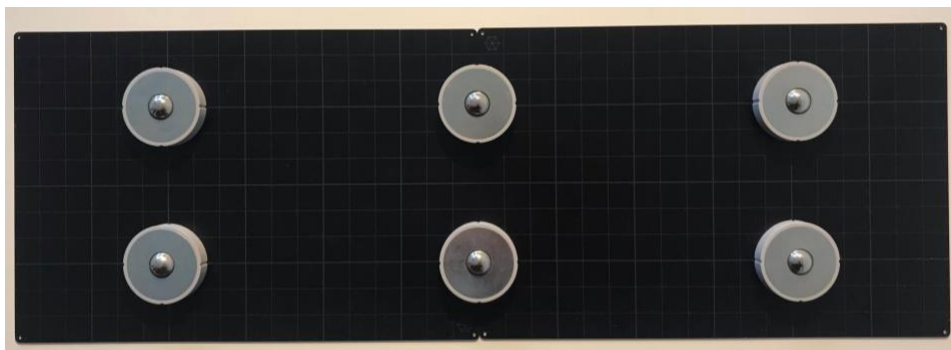


Figure 3-1 The ground and ground connections.

The next step of the physical model construction was to attach the bars 6 and diagonals D6x6 to the ground connections in the external parts of the ground plates (figure 3-2). The bars 6

were supported by using the rigid connection 90° that decreases the buckling length increasing the model stiffness.

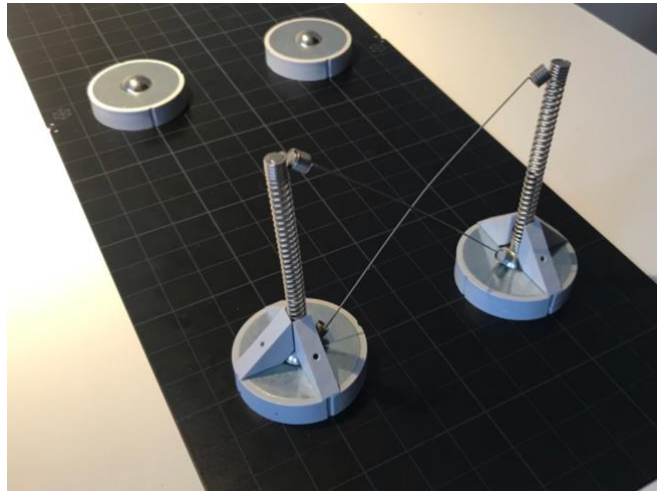


Figure 3-2 The bar 6, diagonal D6x6 and rigid connection 90° attached to the ground connection.

Two previous steps were identical for each design, because these elements do not change between three designs.

The following step was to divide the deck into two parts. Such approach eased to assemble the physical model. Two deck parts were different, the first part had more elements attached (figure 3-3). It had the tower top and eight cables attached to it. The deck was filled with the plate or diagonals. The tower was supported by the diagonals D6x6 in the transversal direction.

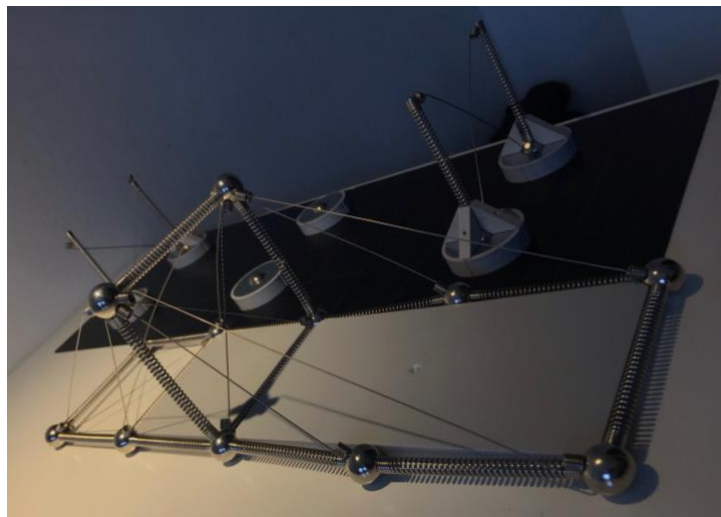


Figure 3-3 The first part of the deck

Consequently, the first deck part could be attached to the bottom part of the tower. The middle joints of the deck part were placed on the bars top and it was stabilized using the diagonals D6x6 that were attached to the deck joints. The middle part of the deck was supported by the bars 6 (figure 3-4). The bars 6 placed in the middle of the deck were placed temporally to provide the stability for a single part of the deck. The joint between deck and

tower was supported by the rigid connection 90° in the longitudinal direction to decrease the deck deflection and provide more stability (figure 3-5).



Figure 3-4 The first part of the deck attached to the bottom part of the tower



Figure 3-5 The rigid connections attached to the joint between the tower and deck

The second part of the deck was assembled, although its composition was different than the first part of the deck. The diagonals D6x12, bar 6 and two connections were not attached. The connections and bar 6 were already fixed to the part one of the deck. The diagonals D6x12 were not attached because, there was not any point of attachment for them as the connections were missing (figure 3-6).

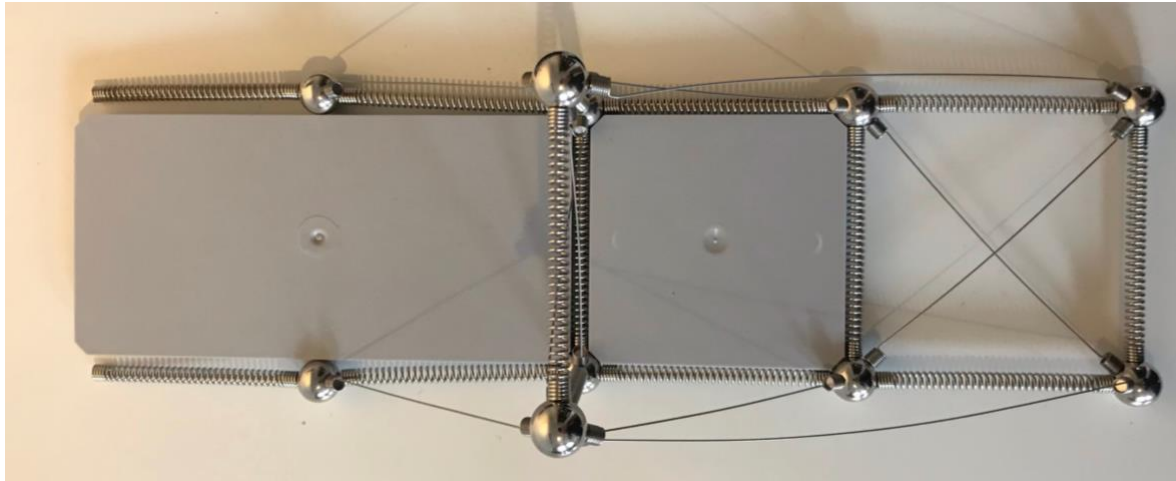


Figure 3-6 The second part of the deck

The second part of the deck was attached to the bottom part of the tower and the existing part of the physical model. The missing diagonals D6x12 were attached to the physical model. The rigid connections 90° were added to the physical model to support the deck around the tower (figure 3-7).

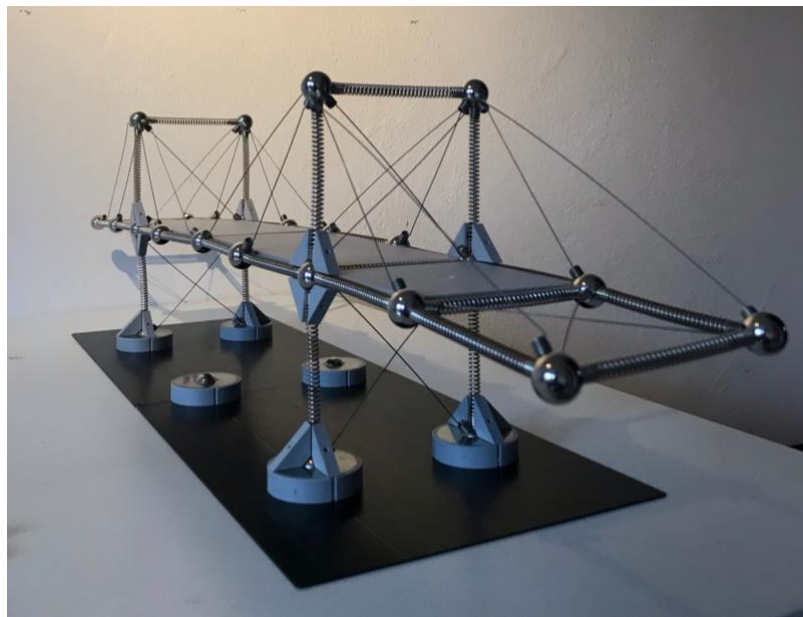


Figure 3-7 The finished physical model

It is the whole description of a construction process of a physical model of a cable-stayed bridge. The same procedure was applied to construct the whole three models. The designs of the physical models are described in the chapter 2.2.3 Preliminary design of the variants

3.1.1 Materials used

As mentioned in the previous sub-chapter, here the materials used for the physical model constructions are described. The materials were already provided by Mola Kit 1&2, each element used to assemble the physical model will be described specified its characteristics, dimensions and weight.

The ground plate used to represent the soil of a structure (figure 3-8). It was made of a single piece of metal, steel; the top part of a ground plate was painted with the checked lines. There are two kinds of lines, thinner and thicker. The thicker lines create 24 squares, 4 in a transversal direction and 6 in a longitudinal direction. Each square is divided into smaller squares, 3 in a transversal direction and 3 in a longitudinal direction. The dimension of the small square is $1.5 \times 1.5 \text{ cm}^2$. The dimensions of a ground plate were 18 cm in width and 27 cm in length. The weight of a ground plate is not important as it is not counted for a physical model weight.

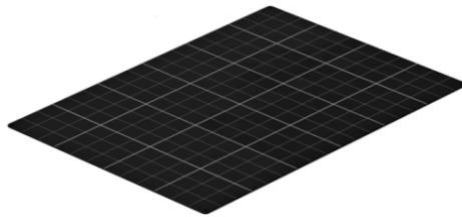


Figure 3-8 The ground plate

The ground connection was created of a composition of materials, a metal ball that was surrounded by a circular plastic elements. Its circuit had 4 axis markings (figure 3-9). The ball inside is called a connection according to Mola (2020). The connection was made of an alloy whose composition is unknown. It is a magnetised element and its weight was 32 grams. Its diameter was 4.5 cm and the height of plastic cover was 1 cm and the remaining part of a connection was 0.5 cm. The top of a ground connection was covered with a metal.



Figure 3-9 The ground connection

The bar 6 used as a column and beam for a physical model. It used an alloy to create an element that had a form a spring (figure 3-10). The endings of a spring were filled with a magnet that allowed to attach the springs to a connection. The bar diameter was 0.5 cm and its length was 7.5 cm. The weight of a bar 6 was 4.8 grams.



Figure 3-10 The bar 6

The diagonals were used in creating a physical model. They were used to recreate the stay cables of a cable-stayed bridge and the bracing in a bridge tower. Two kinds of the diagonals were used D6x6 and D6x12 (figure 3-11). The D6x6 represent the dimensions that could be placed in the frame made of the bars 6, while the diagonal 6x12 could be used in a frame made of the bars 6 and bars 12 (all Mola Kit components are described in the chapter 2.2.1

Mola Kit application to realize physical model in simple structure analysis). The diagonals had a magnet attached to each end that allowed to fix them in a physical model. The diagonal D6x6 had the weight of 1.5 grams, length of 11 cm and the diameter of the attachment point had 0.5 cm. The diagonal D6x12 had the weight of 1.7 grams, length of 19 cm and the diameter of the attachment point had 0.5 cm. The diagonals were made of an alloy.



Figure 3-11 The diagonals D6x6 and D6x12

The rigid connection 90° was made of solid plastic. The rigid connection had a shape of a triangle with one tip that was flat (figure 3-12). Three magnets were attached to it, at the tip and on the sides adjoined to the tip. The length of the adjoining side had 1.7 cm and the base side had 2.4 cm. The weight was 2.2 grams.



Figure 3-12 The rigid connection 90°

The connection used for a physical model was a steel ball (figure 3-13). It had a diameter of 1.5 cm and its weight was 14 grams.



Figure 3-13 The connection

The desk was constructed using a plate. Two kinds of plate were used 6x6 and 6x12 (figure 3-14 & 3-15). The plates were made of a rigid plastic. The plate 6x6 had dimensions of 8.5x8.5 cm², the plate thickness was 0.5 cm, and its weight was 20 grams. It was equipped with magnets at the external part of the corners which were flattened to enable the connection with other elements. The plate 6x12 had dimensions of 8.5x20.5 cm², the plate thickness was 0.5 cm, and its weight was 45 grams. The plate corners were flattened and equipped with magnets.

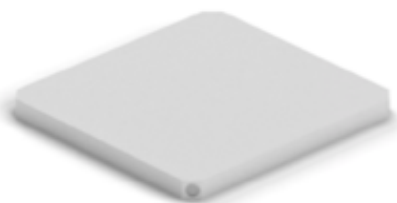


Figure 3-14 The plate 6x6



Figure 3-15 The plate 6x12

3.2 Preselection Test of Acceleration Response

The comprehensive description of the preselection test is provided in this chapter. The preselection test measured the acceleration response of each model.

Process of logging an acceleration signal

The acceleration signal obtained by applying an initial shock wave is registered by a sensor placed in the middle of a physical model deck. An application that was used to register the acceleration signal was MATLAB mobile version 8.1.

1. The sensor activation was performed from the menu interface of MATLAB mobile. The interface is screenshotted as Figure 3-16.
2. From the MATLAB menu interface, “Sensors” tab was selected to choose a sensor and its specification. Presented in Figure 3-17.
3. The place where the data was streamed was specified. The data could be streamed to “Log” or “MATLAB”. The “Log” means that it was logged on a device, while “MATLAB” means that it was streamed to MATLAB Drive. The “Stream to” tab is presented in Figure 3-18.
4. As the place of storing the data was selected. It was possible to choose the “Sample rate”. Opening the “Sample rate” tab, the sample rate could be specified choosing from the range of 0.5 to 100 Hz (Figure 3-19). The sample rate of 100 Hz was chosen, because the higher sample rate is, the more precise the acceleration signal is as it contains more values per a unit of time.
5. The acceleration sensor is activated by pressing the switch button. Green means it is activated (Figure 3-20).
6. The “START” button must be pressed to start recording the signal (Figure 3-21)

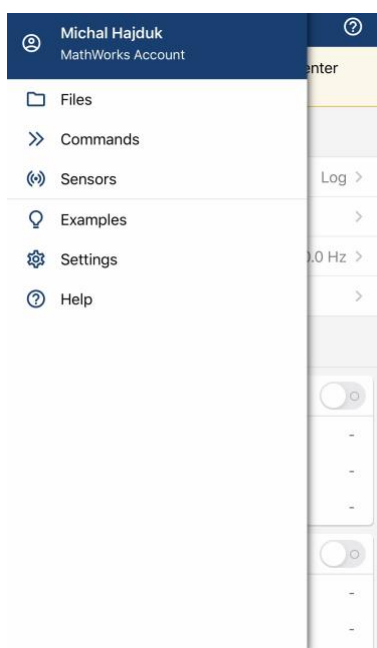


Figure 3-16 MATLAB mobile menu interface

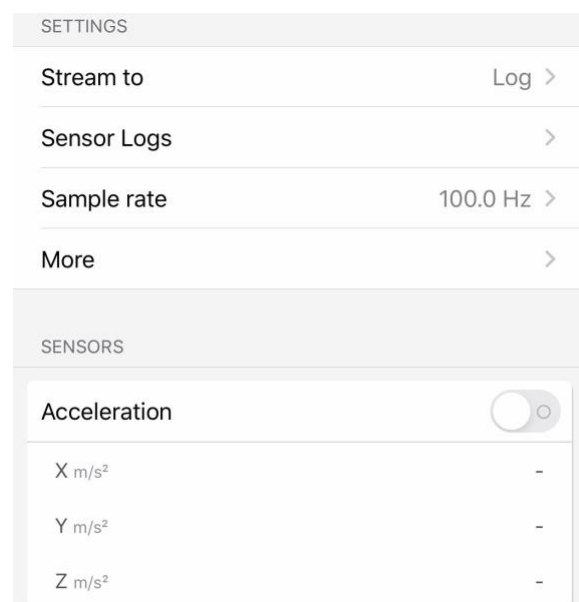


Figure 3-17 Sensors Tab in MATLAB mobile

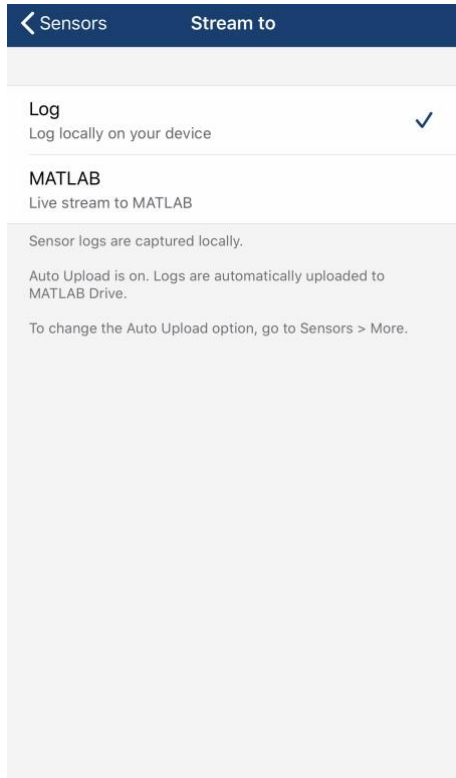


Figure 3-18 MATLAB mobile, “Stream to” tab

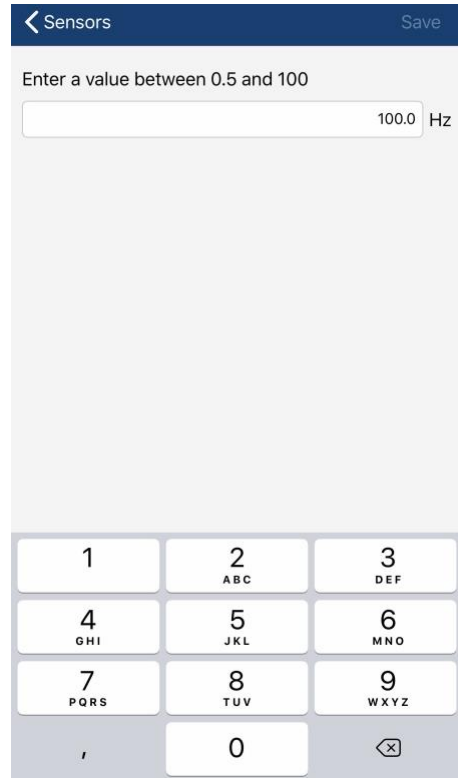


Figure 3-19 MATLAB mobile, “Sample rate” tab

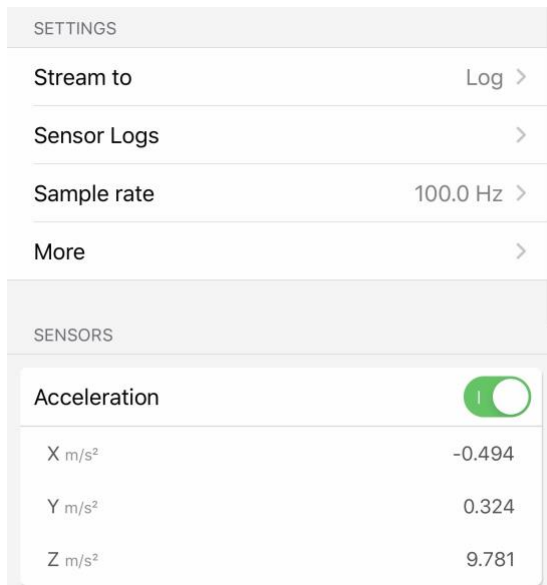


Figure 3-20 MATLAB mobile Acceleration sensor activation

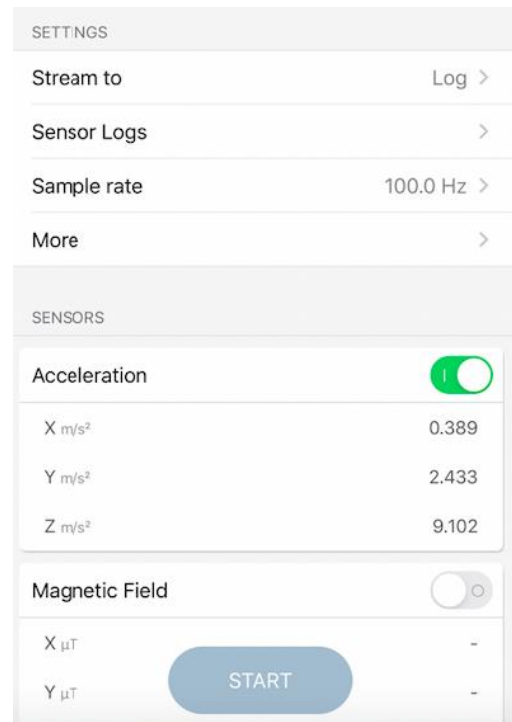


Figure 3-21 MATLAB mobile recording start

7. When the recording contains satisfactory amount of information. It can be stopped by pressing the red button “STOP”. The time of the recording is also presented (Figure 3-22).
8. The recording is saved by entering log name, this research integrated the model that saved the recording specifying the design and its number and the loading axis (Figure 3-23).
9. The recordings are automatically saved in the MATLAB Drive. The MATLAB Drive is accessible from the MATLAB mobile and computer version (Figure 3-24 & 3-25).
10. In the MATLAB Drive, a folder named “MobileSensorData” can be found where all acceleration signals are stored (Figure 3-26).



Figure 3-22 MATLAB mobile “STOP” button

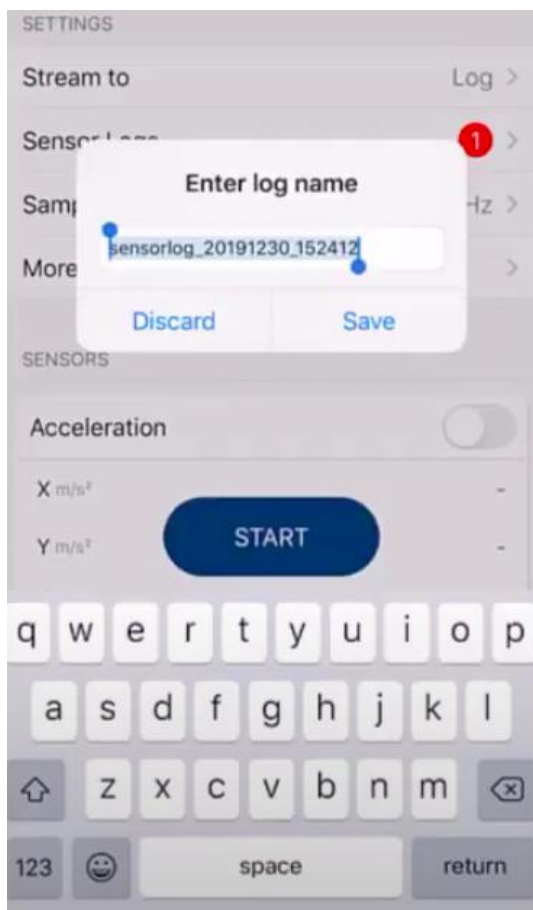


Figure 3-23 MATLAB mobile entering log name

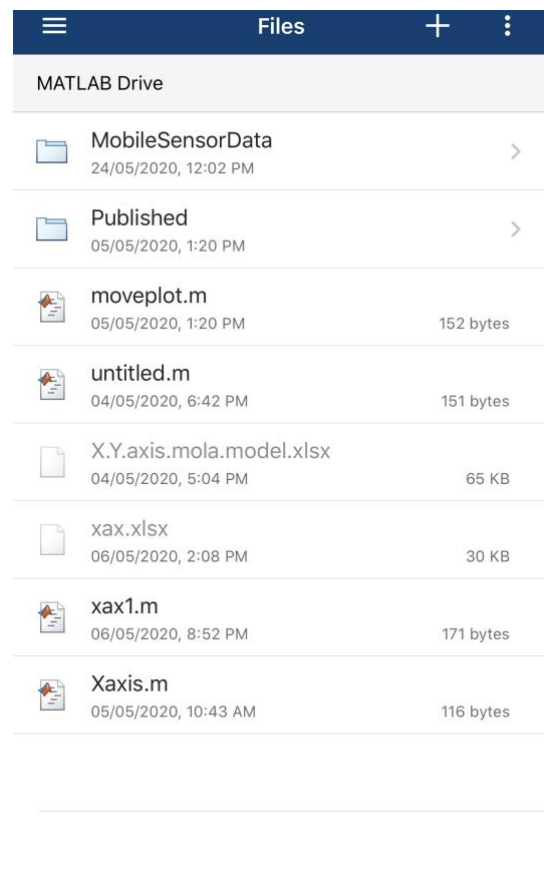


Figure 3-24 MATLAB Drive & its folder

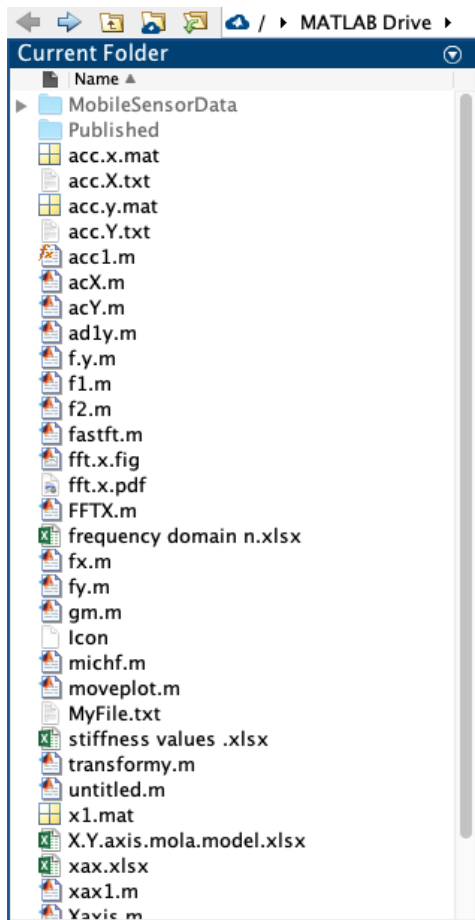


Figure 3-25 MATLAB Drive from computer interface

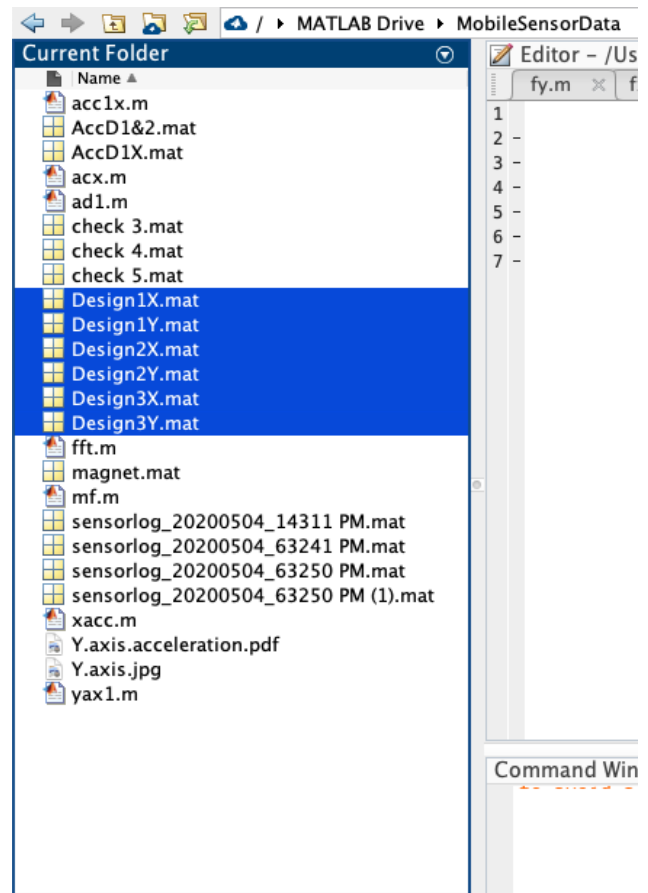


Figure 3-26 Opened folder of "MobileSensorData" with the logged acceleration recordings

The preselection test began from positioning the physical model on a stable surface. The physical model must have been checked if the model components were placed at its place. The model could not be damaged as it would provide unreliable results. The damaged model would not be able to explore as such high acceleration as the fully constructed physical model.

Details of the acceleration sensor

A sensor used for this test was obtained by downloading an app on a mobile. The mobile used in the test was an iPhone 7 Plus. The serial number of the mobile was F2LSDU8WHG04. Its dimensions were 15.82 x 7.79 x 0.73 cm (height x width x depth), the weight was 188 grams. The downloaded app was MATLAB mobile version 8.1 that enables to use sensors. The acceleration sensor was selected measuring the acceleration in X, Y and Z direction. The unit of measurement was m/s^2 , and the sampling rate could be set up from a range of 0.5 to 100 Hz. The sampling rate expresses the number of samples per second (Weik, 1996). The sampling rate chosen for the test was 100 Hz.

Setting up the preliminary test

The preliminary test was performed according to the steps mentioned below.

1. Construction of a physical model on a stable flat surface.
2. Turn on the acceleration sensor.

3. Place the counterweight on the deck sides and the acceleration sensor (mobile) in the middle of the deck.
4. Leave the physical model for accustoming to the added load as it becomes stable.
5. Subject the physical model to an axial shock load in one of the axes to obtain the free vibration of a physical model.
6. Wait until the free vibrations become dumped and the physical model does not vibrate.
7. Take the acceleration sensor off the physical model.
8. Save the acceleration recording naming it by the design number and the loading axis.

As the sensor was set up for a test, it could be placed on a physical model. The weight of a sensor was big enough to cause the physical model instability causing the excessive deck deflection. Thus, the physical model had to be counterbalanced placing two weights of 64 grams each on the external parts of the physical model deck. The weights used for the test were the ground connections two units of it were placed.

As the model was stable enough to perform the preliminary test, the sensor was activated to record the acceleration of a physical model. An initial shock load was applied to the physical model to obtain an acceleration response. A challenging element of this test was to generate the same shock load for all the three models, to acquire comparable results. To do so, each model was tilted 1cm from its position in the longitudinal direction and then released free to vibrate. Before the load was applied, the sensor placed on the deck was activated. As the physical model was in free vibration the acceleration signal was recorded. The acceleration signal was plotted in MATLAB to see whether it was not disturbed and could be used for the research purpose.

The next step was to measure the acceleration response applying an initial shock wave in the transversal direction. Hence, the physical model was tilted by 0.5 cm in the transversal direction. The difference between the tilts in the longitudinal and transversal direction was caused by the model stiffness, which is higher in transversal direction. The acceleration signal was plotted in MATLAB to see whether it was not disturbed and could be used for the research purpose.

When the model stopped vibrating, the recording of the acceleration system was stopped. The sensor was taken off the physical model and the data was logged locally at the mobile in MATLAB drive. The data was stored in the MATLAB drive in a folder MobileSensorData; hence, it was accessible from the MATLAB account after logging into MATLAB account on a laptop.

The acceleration signal was transformed using the fast Fourier transform and the transformation process is explained in the following chapter.

3.3 Transforming Acceleration using Fast Fourier Transform

The data acquired during the preliminary test was stored in the MATLAB cloud. Thus, it was accessible from the MATLAB interface. MATLAB version used for this research phase was MATLAB_R2020a Update 1 (9.8.0.1359463). The whole process of transforming the acceleration signal of each physical model is described.

1. The data was stored in MATLAB Drive in a folder MobileSensorData.

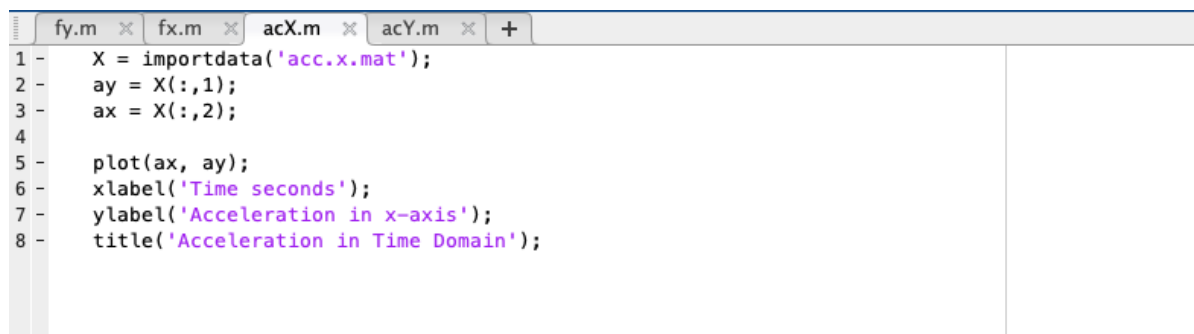
2. The acceleration signal and the test time were vectorised.
3. The acceleration signal was trimmed from the beginning of the increased acceleration values till the constant values of the acceleration.
4. The vectors of acceleration in X and Y axis were plotted versus the time vector to obtain the acceleration signal in the time domain.
5. The acceleration signal in the time domain was transformed using the Fast Fourier Transform to acquire the acceleration signal in the frequency domain.

To achieve the values of acceleration signal in the frequency domain, it was necessary to write a code in MATLAB. The code plots the acceleration signal versus the frequency vector, and it is further explained in the next paragraph.

MATLAB code for plotting the acceleration in the time domain

Acceleration in X-axis

1. Plotting the acceleration vector of X-axis begins from importing the measurement data of the X-axis acceleration of a physical model.
2. The data is imported; thus, it is available in the workspace and the folder with data is named "X".
3. The x and y values of the plot had to be specified, the "ay" represented the acceleration values, and the "ax" represented the time domain.
4. Writing the code of x and y values are taken from the table "X". The code for the x-axis values is named "ax". "X" identifies the name of the file from which the data is taken, ":" identifies the rows of the table. If a colon is written in the row space, it means that all rows are imported. "2" identifies the number of column. The code for the y-axis values is named "ay". "X" identifies the name of the file from which the data is taken, ":" identifies the rows of the table. If a colon is written in the row space, it means that all rows are imported. "1" identifies the number of column. As the x and y axis values were established, it was possible to plot them to obtain the graph.
5. Adding the x-label by writing a command "xlabel()". In the brackets, the x-label name is specified, the label characters must be enclosed in apostrophes to be visible for MATLAB.
6. Adding the y-label in the same way as the x-label, which was described in step 5. Including the one-letter difference in a command as "ylabel()".
7. Adding the title of the plotted data is realised by typing a command "title()". The title name is written enclosed in apostrophes in brackets of a command.



```

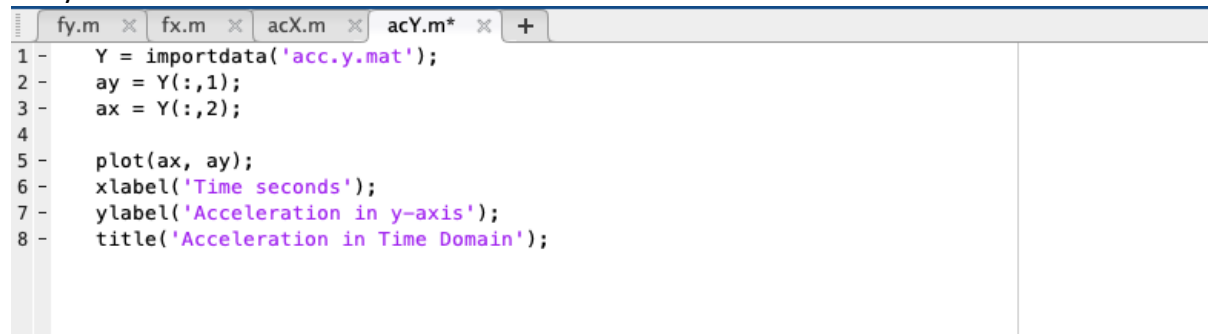
1 - X = importdata('acc.x.mat');
2 - ay = X(:,1);
3 - ax = X(:,2);
4
5 - plot(ax, ay);
6 - xlabel('Time seconds');
7 - ylabel('Acceleration in x-axis');
8 - title('Acceleration in Time Domain');

```

Figure 3-27 MATLAB code for plotting the acceleration in X-axis into the time domain

Acceleration in Y-axis

Obtaining the chart of Y-axis acceleration in time domain was obtained in the same way as described above. The difference is the file from which the data is imported and the name of the y label.



```
fy.m x fx.m x acX.m x acY.m* x +
1 - Y = importdata('acc.y.mat');
2 - ay = Y(:,1);
3 - ax = Y(:,2);
4
5 - plot(ax, ay);
6 - xlabel('Time seconds');
7 - ylabel('Acceleration in y-axis');
8 - title('Acceleration in Time Domain');
```

Figure 3-28 MATLAB code for plotting the acceleration in Y-axis into the time domain

MATLAB Code of FFT

The code written in MATLAB is performed for values in the X and Y-axis. The code allows to compute the FFT.

The code for the X-axis presented in Figure 3-29.

1. Computing the FFT of the acceleration values in X-axis begins from importing the measurement data of the X-axis acceleration of a physical model. The data is imported; thus, it is available in the workspace and the folder with data is named “xeas”.
2. The time vector is created, it is named “t” and it takes the data from the table “xeas”. The code integrates all rows of the table by putting “:” in the command and “2” identifies the number of a column.
3. The acceleration vector is called “ax”. The values are taken from the table “xeas” using all rows by writing “:” in the row space and writing “1” in the column space means that the data is taken from the column called 1.
4. The “ax” acceleration vector was built to be a zero-mean vector by putting the “ax-mean(ax)” command. Building a zero-mean vector helps to downstream the method and variance of the data. It eases to find the relationships between the values.
5. The sampling frequency was named “ns” and it uses code of 1 over the time. The vector length must have been updated, otherwise, it would be impossible to plot the values as they would have different lengths.
6. Adding zeros to the “ay” vector makes it equal with the next power of 2. This code it written because it makes the FFT more efficient.
7. The frequency vector is created “n” by writing the code that integrates the sampling frequency multiplied by the frequency range.
8. The code of the FFT computation is named “FTx” and written under where the %calculate the fft.
9. The values of the acceleration in X-axis are plotted versus the frequency vector. Using a command of “plot()”. In the brackets, the first values specify the x-axis data; thus, it is the frequency vector. In the brackets after a comma, the y-axis values are specified.

8. The command of “xlabel()” is used to add the x-label to the plotted data. The label name is specified, the label characters must be enclosed in apostrophes to be visible for MATLAB.
9. The command of “ylabel()” is used to add the x-label to the plotted data. The label name is specified, the label characters must be enclosed in apostrophes to be visible for MATLAB, too.
10. The title of the plotted data is added by writing the command of “title()” specifying the title name putting in in brackets and enclosed in apostrophes.
11. To finalize the code and obtain the plotted data, the system is run by pressing the “Run” button in the “Editor” tab, presented in Figure 3-30.

```

1 - xeas = importdata('acc.x.mat'); %import measurement data
2 - t = xeas(:,2); %time vector
3 - ax = xeas(:,1); %acceleration vector
4 - ax = ax-mean(ax); %build a zero-mean acceleration vector
5
6 - ns = 1/t(2); %sampling frequency
7 - Nt = nextpow2(length(ax)); %updated vector length
8 - ax = [ax; zeros((2^Nt-length(ax)),1)]; %add zeros to ay to make vector
9 %length equal to the next power of 2
10 - n = ns*(0:(Nt-1))/Nt; %frequency vector
11 - FTx=abs(fft(ax)); %calculate the fft
12
13 - figure()
14 - plot(n1(1:end/2),FTx(1:end/2)) %plot the fft versus frequency up to ns/2
15 - xlabel('Frequency Hz');
16 - ylabel('Acceleration in x-axis');
17 - title('Fast Fourier Transformation');|

```

Figure 3-29 MATLAB code of FFT for the X-axis

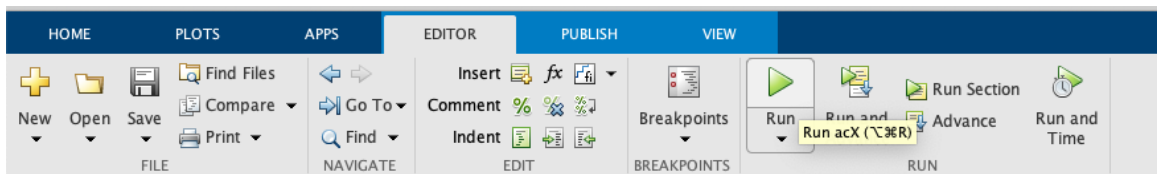


Figure 3-30 The “Run” button in MATLAB Editor tab

The code for the Y-axis presented in figure 3-31.

The same was repeated for computing the FFT of Y-axis acceleration values. The whole process is described above for the code for the X-axis. The difference is in the file that is imported into MATLAB, its name is “meas”. The acceleration values are named “ay” due to the Y-axis. The y label is different as it is for the Y-axis. All the commands that include the “x” are replaced with the letter “y”, as the axis indicator. The rest is identical as for the X-axis.

```

1 - meas = importdata('acc.y.mat'); %import measurement data
2 - t = meas(:,2); %time vector
3 - ay = meas(:,1); %acceleration vector
4 - ay = ay-mean(ay); %build a zero-mean acceleration vector
5
6 - ns = 1/t(2); %sampling frequency
7 - Nt = nextpow2(length(ay)); %updated vector length
8 - ay = [ay; zeros((2^Nt-length(ay)),1)]; %add zeros to ay to make vector
9 %length equal to the next power of 2
10 - n = ns*(0:(Nt-1))/Nt; %frequency vector
11 - FT=abs(fft(ay)); %calculate the fft
12
13 - figure()
14 - plot(n(1:end/2),FT(1:end/2)) %plot the fft versus frequency up to ns/2
15 - xlabel('Frequency Hz');
16 - ylabel('Acceleration in y-axis');
17 - title('Fast Fourier Transformation');

```

Figure 3-31 MATLAB code of FFT for the Y-axis

The codes were written for each acceleration signal. The plotted data was stored and is presented in chapter 4.1 Results of Fast Fourier Transform. The charts were used to find the design of a physical model of a cable-stayed bridge that was used to a shaking table test. The criteria for assessing the designs are described in the following chapter.

3.4 Multi-criteria analysis for selecting the design of a physical model

The design selection is based on the deciding factors:

- **Natural Frequency**
The natural frequency defines the frequency when a structural system starts resonating. The lower the natural frequency is, the earlier the structural system starts resonating. Thus, it is able to withstand higher frequencies. The properties such as a higher mass and softer beam decrease the natural frequency (Newport, 2020).
- **Physical Model Mass**
The model mass influences the natural frequency. The lower mass increases the natural frequency; hence, the design that weights more than other designs may have a lower natural frequency. The natural frequency is decisive to the stability of a structural system subjected to dynamic loading.
- **Continuous Deck Stiffness**
The continuous deck stiffness is key for the physical model stability. It provides the continuity in the physical model decreasing the number of weak points. The weak points constitute the transition zones where the physical properties differentiate. Thus, these points create the weak areas that may cause a failure during an external loading. Moreover, in the linear behaviour, the stiffness of a physical model must remain constant. Otherwise, the structure response may not be linear.
- **Construction Ease**
The physical model will be tested on a shaking table. The tests will be performed in the transversal and longitudinal direction with modifications in the structure or an added uniform load. The frequency of the ground motions applied by the shaking table may damage the physical model structure. Therefore, the physical model will have to be rebuilt numerous times, as the time spent on reassembling the model affects the testing efficiency.

The criteria weight is described below. It provides the importance of each factor and how influential it is for the design of a physical model of a cable-stayed bridge. The criteria sum is 100%. Below in Table 3-1.

Criterion	Weight	Description
Natural Frequency	25%	The natural frequency is crucial for the physical model stability during a dynamic loading. The designs with the lower natural frequency can withstand more the ground motions.
Physical Model Mass	30%	The mass affects the natural frequency. The higher mass is, the lower the natural frequency is. The mass of a physical mode affects the stability during a dynamic loading.
Continuous Deck Stiffness	30%	The continuous deck stiffness is responsible for reducing the number of weak points in the model structure. Thus, it influences on the overall model resistance while the ground motions are applied.
Construction Ease	15%	The frequency of the ground motions applied by the shaking table may damage the physical model structure. Therefore, the physical model will have to be rebuilt numerous times, as the time spent on reassembling the model affects the testing efficiency.

Table 3-1 The weight of criteria for the design selection

Three alternative models are considered to select the final design. Thus, a three-point system is used to perform the comparative analysis. The alternative models can be rated with value 0, 1 or 2. The higher the number, the more adequately the design fulfils such criterion.

Finally, the points assigned to each design are multiplied by the weight factor and positioned in Table 4-1 in Chapter 4.3 Design Selection. The values are summed up. The highest sum identifies the design of a physical model of a cable-stayed bridge that was used for a shaking table test.

3.5 Shaking Table Test

Test Regulations

The shaking table test was performed at the Engineering Laboratory of the University of Ferrara. Performing the test must be realized according to the laboratory regulations.

- Know the location of all exits, evacuation route, first aid kit, eyewash, fire extinguisher, and a safety shower.
- Wear approved eye protection (safety glasses, or goggles) always in the laboratory.
- Shoes must completely cover the foot. No sandals or crocs are allowed.
- Long hair must be tied back, and all loose clothing or dangling jewellery must be secured or removed while in the laboratory.
- No food or drink of any kind in the laboratory.
- No equipment may be without proper training or demonstrated competency.
- All aisles and workspace must be kept clear of clutter. All exits, fire extinguishers, electrical disconnects, eyewashes and safety showers must remain accessible always.
- All equipment guards must remain in place. You may not modify equipment without approval of the PI who must do a hazard assessment associated with proposed changes.
- All chemical storage rules must be observed always. All chemicals must remain closed until used, and all chemicals must be marked with substance name, hazard information, concentration, date of creation, and the person responsible.
- All waste chemicals must be put in approved and labelled containers. There is to be no hazardous waste into sinks or garbage cans.
- Any unsafe or dangerous behaviour must be reported to the PI.
- Any electrical work must be reviewed by an electrician prior to energization.
- Always wear a face mask and gloves in the laboratory due to the current circumstances of Covid-19.

Shaking Table Test Procedure

The shaking table test procedure was used to verify the natural frequency of the selected design of a physical model of a cable-stayed bridge.

- a. Check the shaking table and its area if the setup is in operation state.
- b. Remove the table platform from the shaking table by unscrewing the bolt cap.
- c. Attach the Mola ground plates to the table platform.
- d. Place the table platform on the shaking table in the transversal or longitudinal direction.
- e. Screw the bolt caps to secure the table platform.
- f. Construct the physical model.
- g. Secure the physical model checking whether all model components are interconnected.
- h. Plug in the power cable and turn on the shaking table.
- i. Attach a camera to a tripod in front of the shaking table, secure the camera by fixing the bolt from the tripod into the camera.

- j. Start increasing the frequency of the shaking table and increase gradually until the physical model starts resonating.
- k. Lessen the speed of increasing the frequency, when the physical model starts resonating.
- l. Continue increasing the frequency until the maximum frequency generated by the shaking table or the model collapse.
 - i. If the physical model is able to withstand the maximum frequency of ground motions, after reaching the maximum frequency, gradually decrease the frequency to zero.
 - ii. If the physical model collapses while the frequency is being increased. Decrease the frequency to zero.
- m. Turn off the camera.
- n. Pull-out the power cable and place it in a secure place away from walking aisle.
- o. Dismantle the physical model pieces and hide the pieces to a box.
- p. Leave the shaking table in a state as it was before the testing began.

Shaking Table Test (20th May 2020)

The shaking table test started with securing the working area. The shaking table were checked to detect any possible damage. As the area was secured, the first steps could be realised.

All shaking table tests were realised using a physical model that was constructed in accordance with the selected design. The design that was chosen for the shaking table test was the 3rd design. More information about the design selection can be found in previous chapter.

The first step was to decide which directions would be investigated first, whether transversal or longitudinal. It was decided that the transversal would be studied as the first.

The table platform was removed from the shaking table and placed on a table. This enabled to place the Mola ground plates on which the physical model would be built. The ground plates were secured by placing them at the table platform. The ground plates had tap holes that facilitated the connection to the table platform using metal nails. The ground plates were attached and checked, especially to verify whether the lines on the ground plates were equally placed. The table platform was placed back on the shaking table. The bolt nuts were screwed to the bolt threads. The shaking table was prepared for the testing. At this moment, it was time to construct the physical model. The construction process of the shaking table is described in the chapter, 3.1 Construction of a physical model.

A camera was placed on a tripod in front of the shaking table to record the testing. The recordings were reviewed after the testing to identify the natural frequency of the physical mode.

Details of the shaking table

The shaking table used in this research is single-degree-of-freedom table manufactured by Bonfiglioli. The table platform is 35 x 35 cm square. In the platform, the corners have tapped holes to fasten the top platform. The holes are dedicated to the bolt threads that protruded through them after a precise positioning of the table platform. On the bolt threads, a special type of bolt nut is attached to stabilize the table platform (figure 3-32). The table is driven by

a single actuator generating the frequency from 0 to 4.8 Hz. The motion generated by the shaking table was harmonic. The maximum weight of a physical model placed on the table was 5 kg.

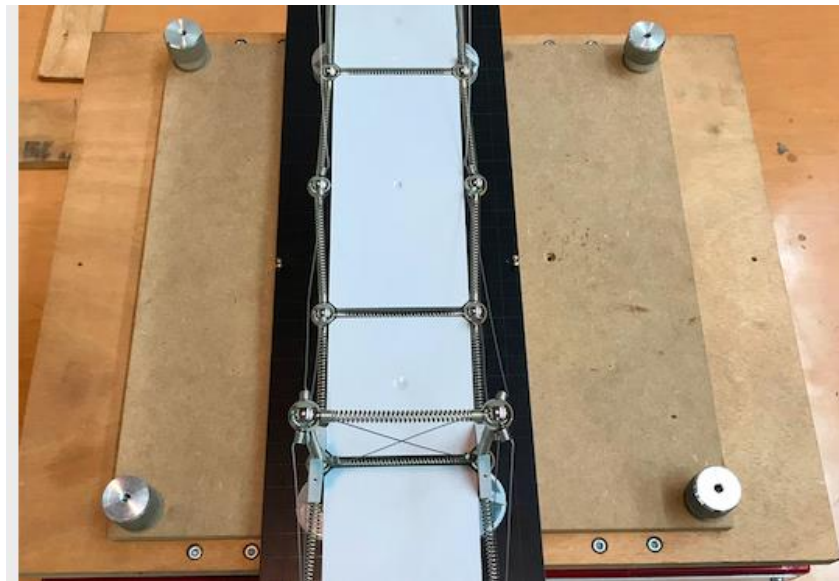


Figure 3-32 The table platform with the attached bolt nuts

The motions generated by the table were controlled by a knob placed at the back of the table. The knob operated from 0 to 10. The higher the number at the knob, the higher the generated frequency. The black knob is responsible for choosing a gear of motion: 0 is sinusoidal motion, and 1 is a random motion. The red button is the emergency button (figure 3-33). The shaking table was powered by the electrical voltage of 220 V using a square socket with three bolts connected to an extension. The power cable is attached to the table on the left side (figure 3-34). The front plane of the table has a meter that presents the generated frequency



Figure 3-33 The emergency button, gear knob and frequency knob



Figure 3-34 The shaking table with the 3rd Design of a physical model

The shaking table was positioned on a table to provide convenient using conditions. In this way, it was accessible at a comfortable height to a standing person. The table beneath is stable enough. It does not create any vibrations while the shaking table is operating.

Testing in the transversal direction

The testing began, the shaking table was activated starting from 0 to 4.8 Hz. The frequency was gradually increased to obtain the natural frequency.

The first testing in the transversal direction was performed on a physical model, which had diagonals between the bridge tower (figure 3-35).

The second testing in the transversal direction was conducted on a physical model, which had the diagonals replaced with the rigid connection 90° (figure 3-36). The test was conducted and recorded.

The physical model composition was changed during testing in the transversal direction. The bracing was replaced with the rigid connections. This approach allowed to identify the element that was providing considerable stiffness into the design of a physical model.

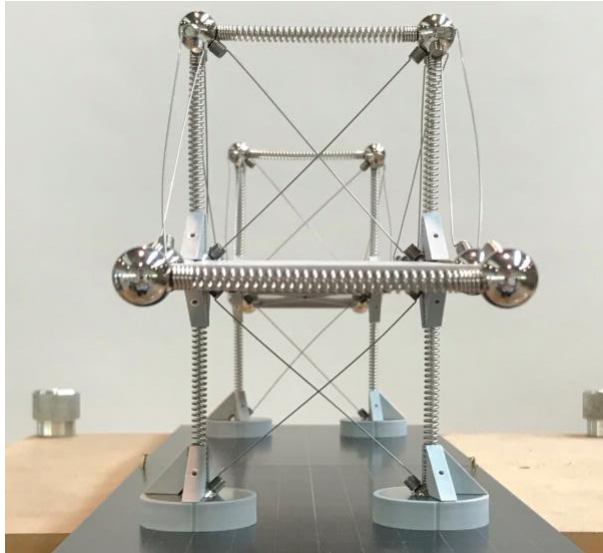


Figure 3-35 Testing the 3rd Design of the physical model in transversal direction; the bridge tower with the bracing

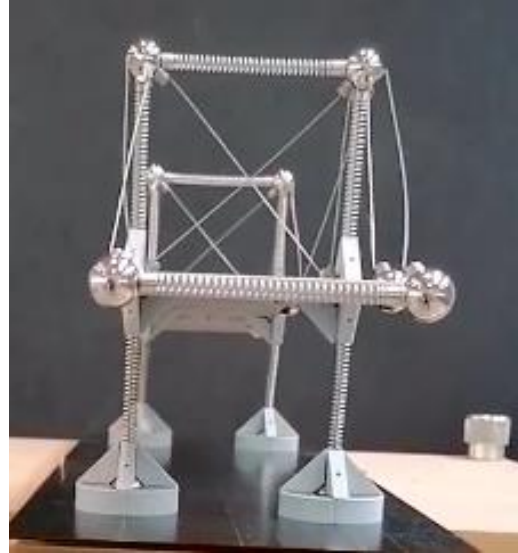


Figure 3-36 Testing the 3rd Design of the physical model in transversal direction; the bridge tower with the rigid connection 90°

Testing in the longitudinal direction

The next step was to test the dynamic response of a physical model in the longitudinal direction. The model was removed from the table platform. The bolt nuts were unscrewed and the table platform was rotated by 90 degrees. The platform was rotated to expose a physical model to the ground motions in the longitudinal direction. A physical model was built on the shaking table. The final check of a model was performed, whether the physical model was properly assembled that all model components were interconnected. After the check, the shaking table test could begin. The ground motions started being applied with the frequency from 0 till the physical model became damaged. The first test of a physical model in the longitudinal direction was performed (figure 3-37).

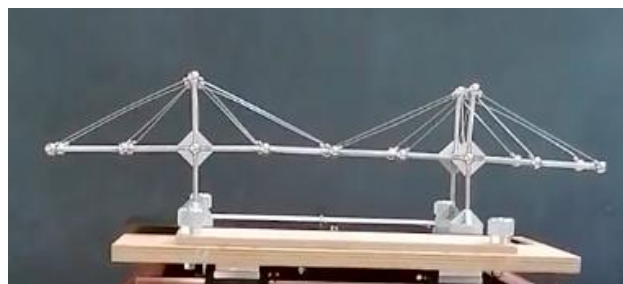


Figure 3-37 The 3rd Design of the physical model on the shaking table

The testing continued increasing the frequency until the moment in which the system became damaged. One of the longer stay cables disconnected from the system (figure 3-33). The ground motions were brought to 0 that the physical model could be rebuilt.

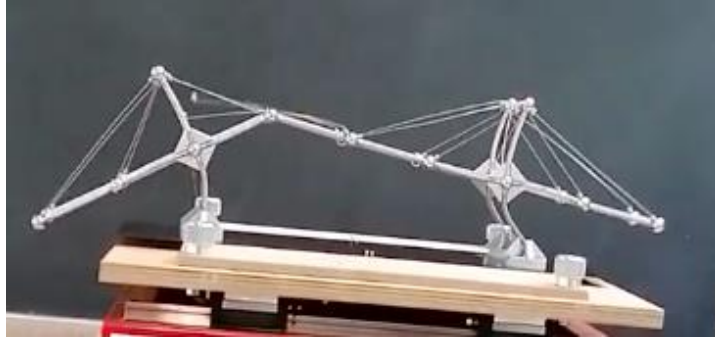


Figure 3-38 Collapse of the 3rd Design of the physical model during testing

The next test was performed, but the model mass was increased by adding distributed load along the model deck (figure 3-39). The plan was to observe the physical model and identify the natural frequency. The increased mass of the physical model affects the model stiffness. The physical model was tested with the centric load. The model was tested until the system became damaged.

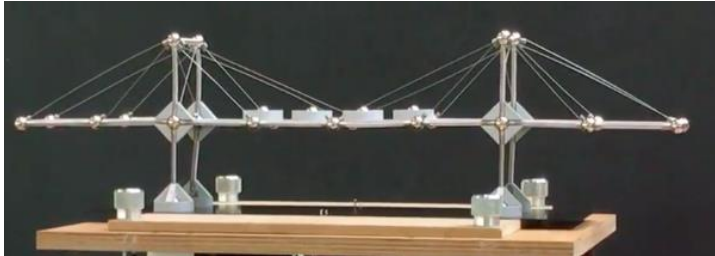


Figure 3-39 Testing the 3rd Design of the physical model with the centric load

The system was reconstructed and another test was performed. This time the system was tested with the eccentric load (figure 3-40). The same procedure as with the previous trails was repeated. the frequency of the ground motions was gradually increased until the system collapses. However, the process of increasing the frequency was lessened straightaway the system started vibrating. Placing the eccentric load was to check whether the deck torsion would appear.

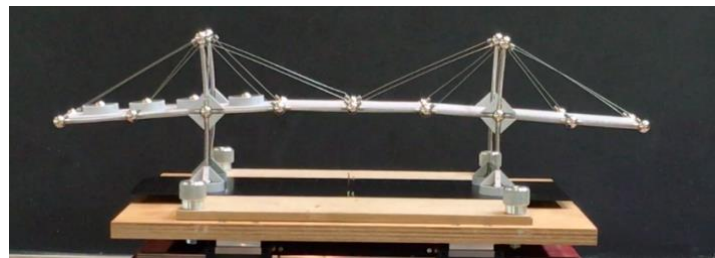


Figure 3-40 Testing the 3rd Design of the physical model with the eccentric load

Physical Model Stiffness & Mass Determination

The model stiffness was determined using Equation 3-1 for the undamped natural frequency. The process of determining the mass and stiffness of the physical model is precisely described.

Acquiring the physical model mass was realized by weighting every kind of component. The weight of all components and their quantity was summed. The total weight of all components provided the model mass.

The pieces were weighted using a digital kitchen scale manufactured by Soehnle. The model of the kitchen scale was Compact with a product number 65122. The maximum load capacity was 5 kg, and the kitchen scale was equipped with an LCD digital screen. The scale had the weighting precision to 1 gram increment.

To obtain more precise mass values, the pieces were weighted in a quantity of 10 units. Then, the average mass was concluded. As the weight of pieces was known. The physical model components were identified in its quantity, and the total mass of the physical model was calculated.

The model stiffness was determined by identifying the natural frequency of the physical model. The natural frequency was obtained from the recordings of the shaking table tests. The moment in which the physical model started vibrating indicated the natural frequency of a system. The natural frequency (f_n) was implemented into the formula of the undamped natural frequency (formula 1). The model components were weighted; thus, the mass could be implemented into the formula. The solved equation delivered the value for the stiffness of the selected physical model.

$$k = f_n^2 * (2\pi)^2 * m$$

Equation 3-1 Stiffness vs Frequency and Mass Equation

4 Results

4.1 Introduction

The results of the preliminary test, multi-criteria analysis for the design selection and shaking table tests are presented in this chapter. The acceleration signals were transformed using FFT and its results are provided. The FFT of the designs is used for the multi-criteria analysis to select the design of a physical model.

The selected design was used to perform a shaking table test as it fulfils one of the research objectives. The results of the shaking table test are presented in Chapter 4.4 Shaking Table Test Results. The results present obtained values of:

- The natural frequency of the selected design verified by a shaking table test
- The stiffness of the physical model

4.2 Results of Preliminary Test

The results of the preliminary test are divided into two parts. The first presents the acceleration response of the designs subjected to an axial load. The second presents the fast Fourier transform on the design acceleration signals.

The graphs present the acceleration signals of each model in the X and Y-axis. The acceleration signals were transformed and the FFT graphs are presented in the following chapter. The x-axis is the transversal direction, while the Y-axis is the longitudinal direction.

Acceleration Response of the 1st Model Design

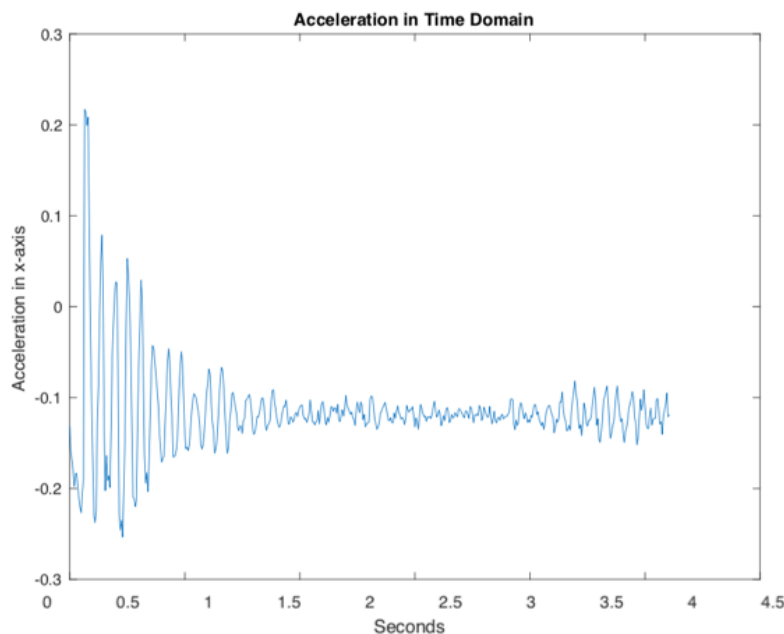


Figure 4-1 Acceleration signal of the 1st model design in X-axis

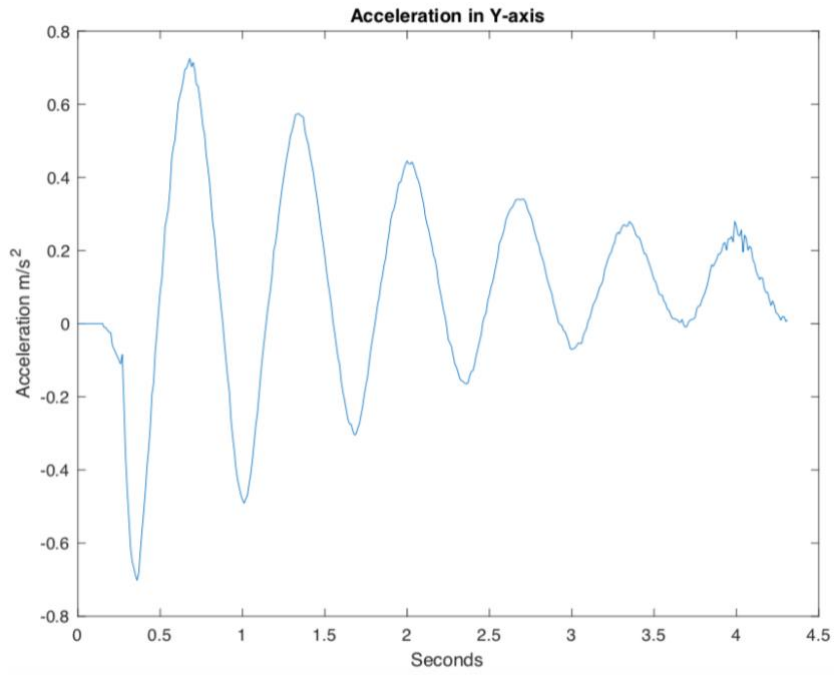


Figure 4-2 Acceleration signal of the 1st model design of the physical model in Y-ax

Acceleration Response of the 2nd Model Design

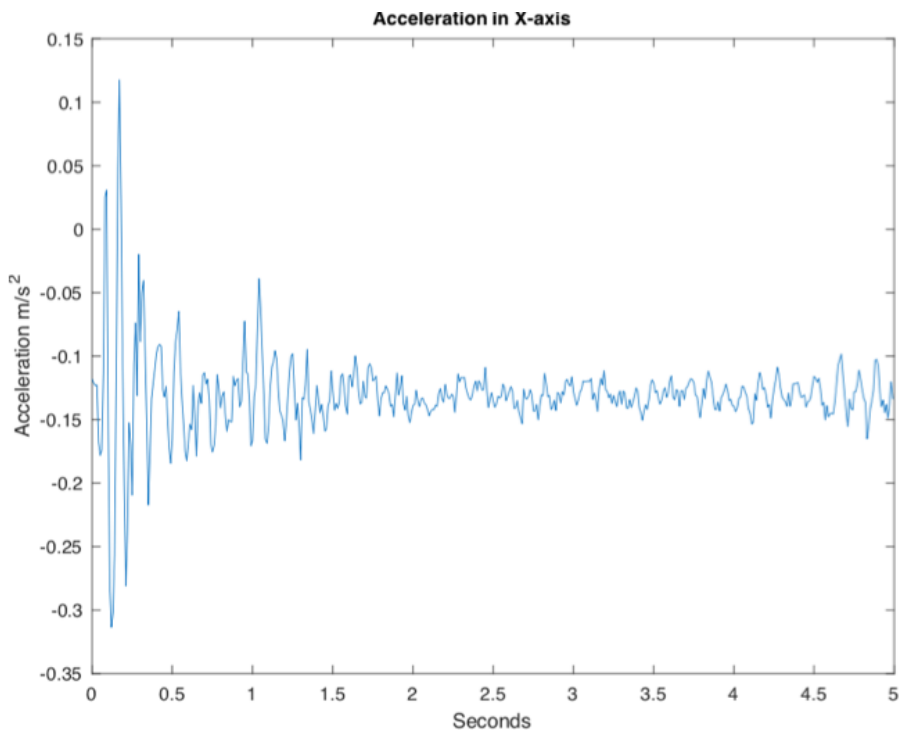


Figure 4-3 Acceleration signal of the 2nd model design in X-axis

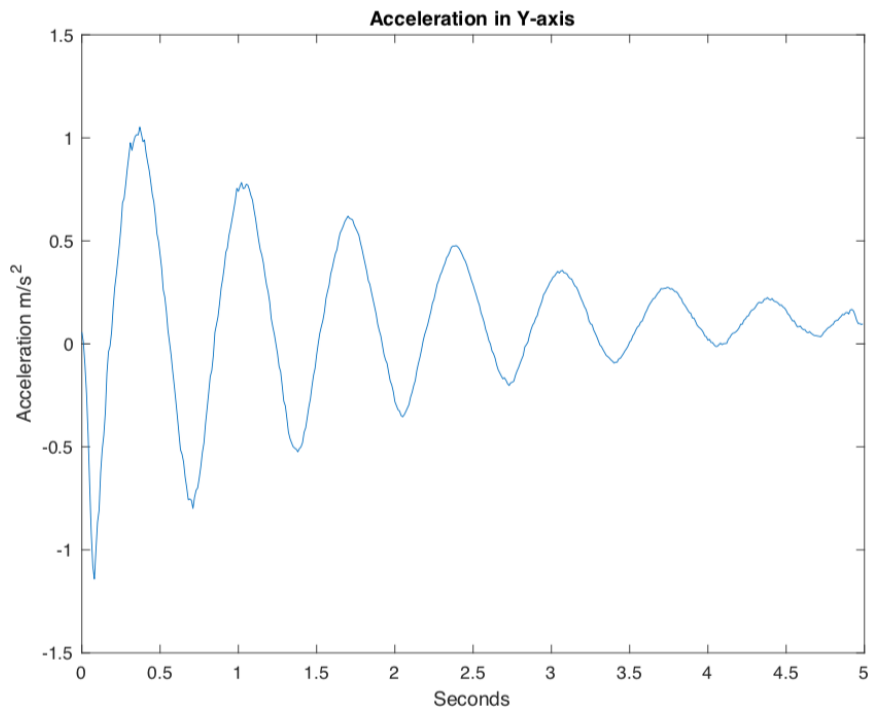


Figure 4-4 Acceleration signal of the 2nd model design in Y-axis

Acceleration Response of the 3rd Model Design

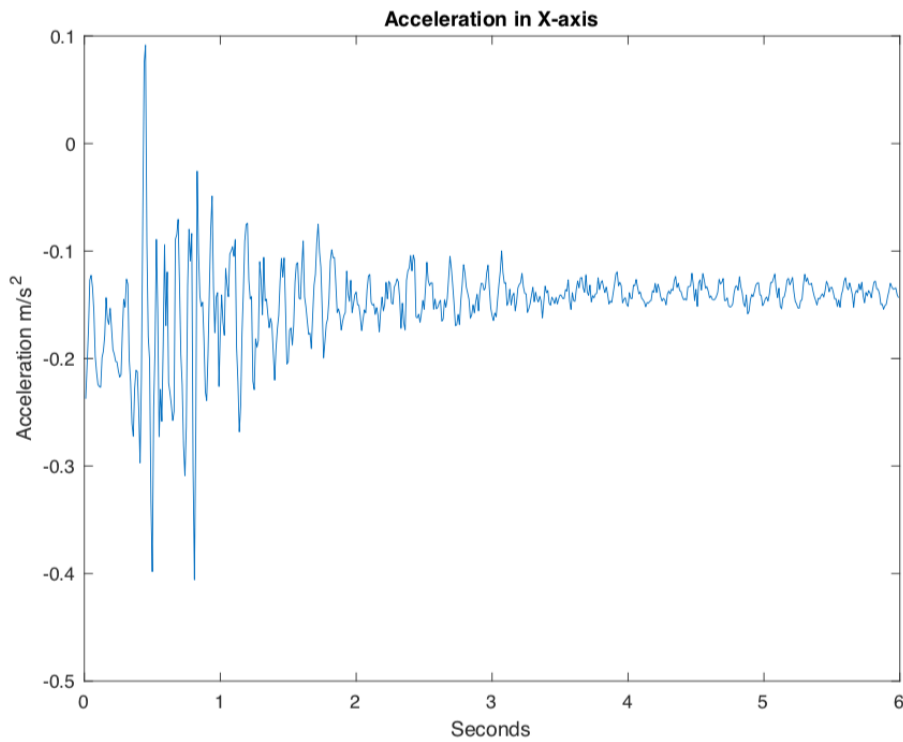


Figure 4-5 Acceleration signal of the 3rd model design in X-axis

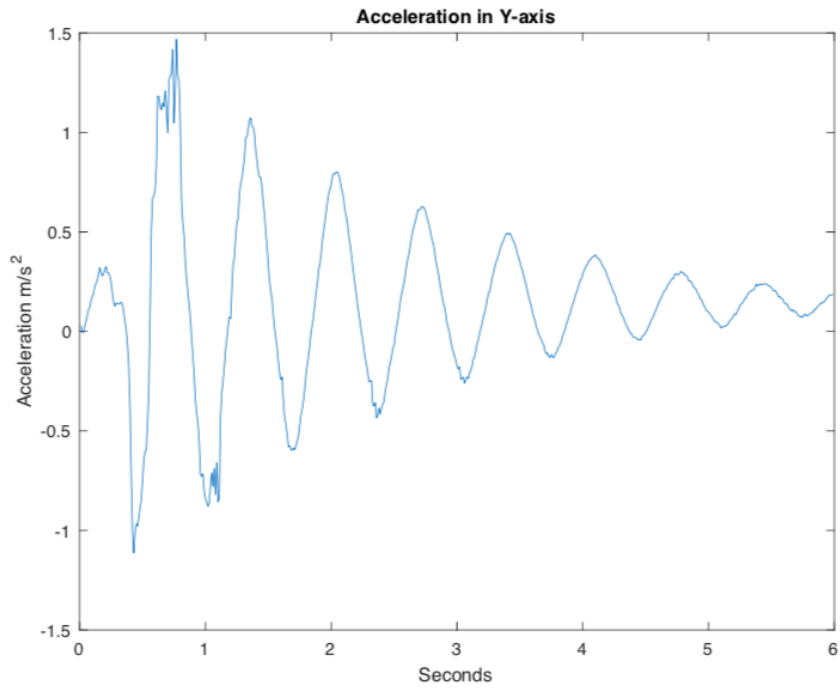


Figure 4-6 Acceleration signal of the 3rd model design in Y-axis

Fast Fourier Transform of the 1st Model Design

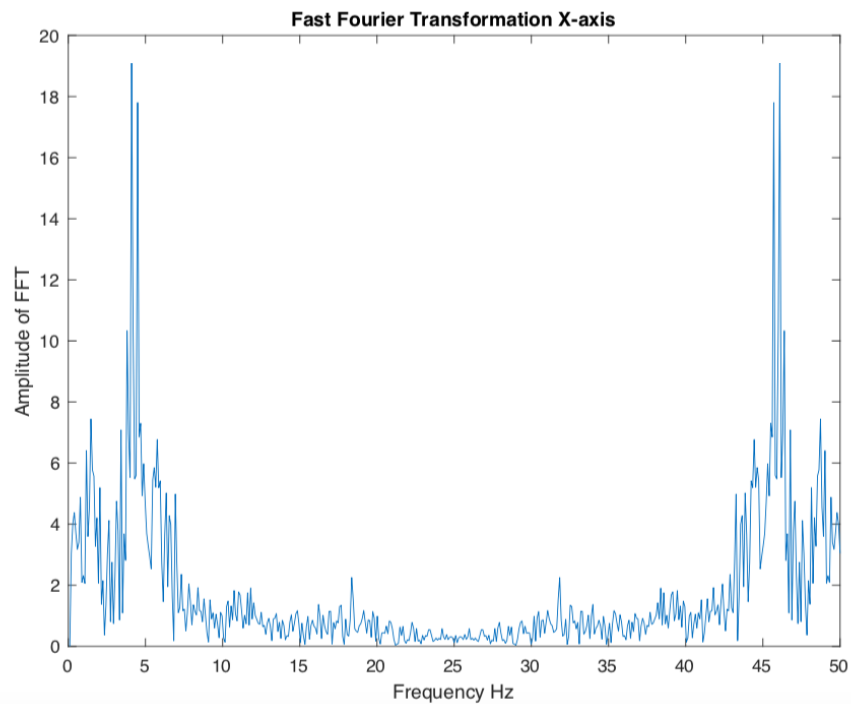


Figure 4-7 Fast Fourier Transform of the 1st model design in X-axis

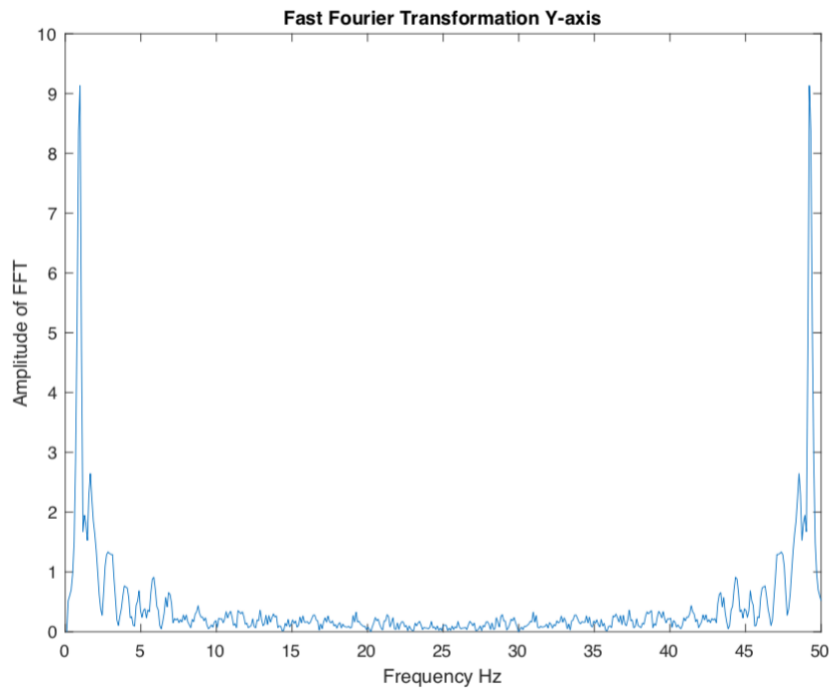


Figure 4-8 Fast Fourier Transform of the 1st model design in Y-axis

Fast Fourier Transform of the 2nd Model Design

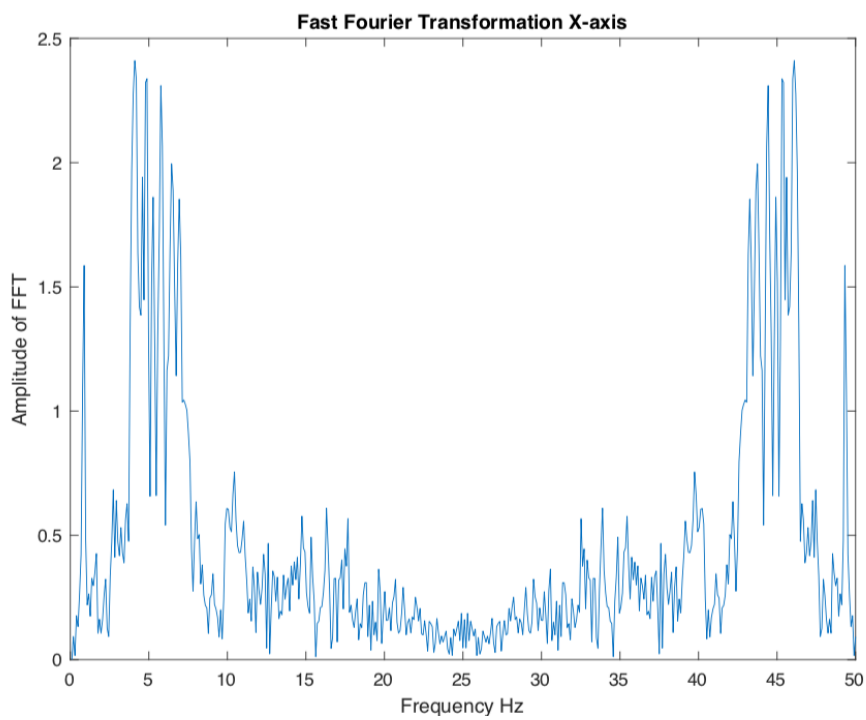


Figure 4-9 Fast Fourier Transform of the 2nd model design in X-axis

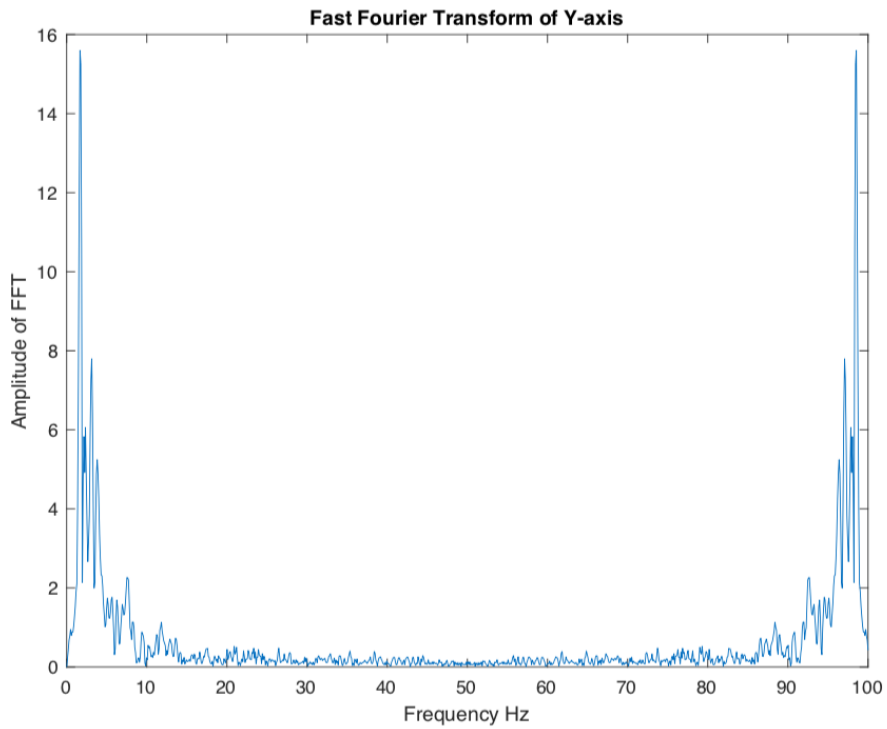


Figure 4-10 Fast Fourier Transform of the 2nd model design in Y-axis

Fast Fourier Transform of the 3rd Model Design

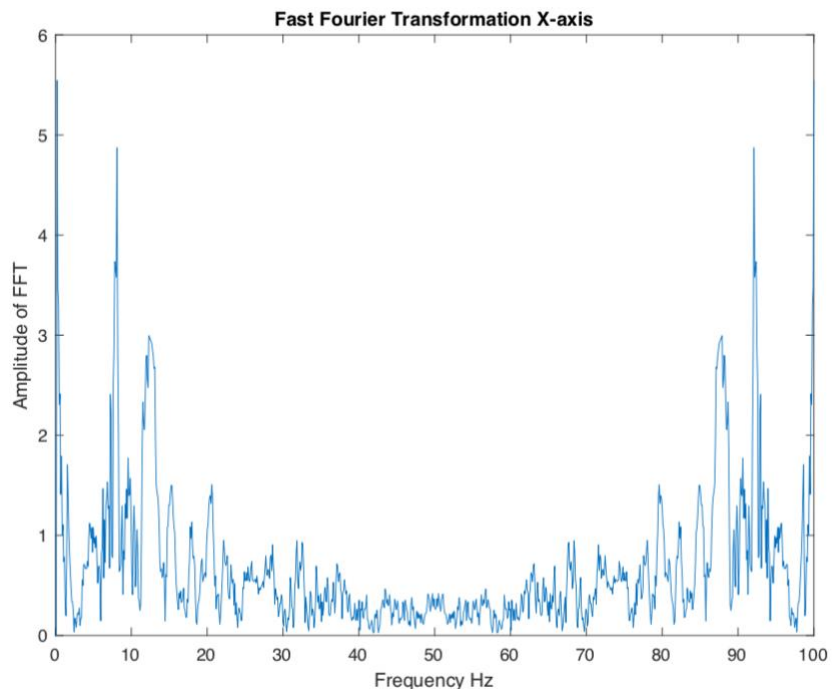


Figure 4-11 Fast Fourier Transform of the 3rd model design in X-axis

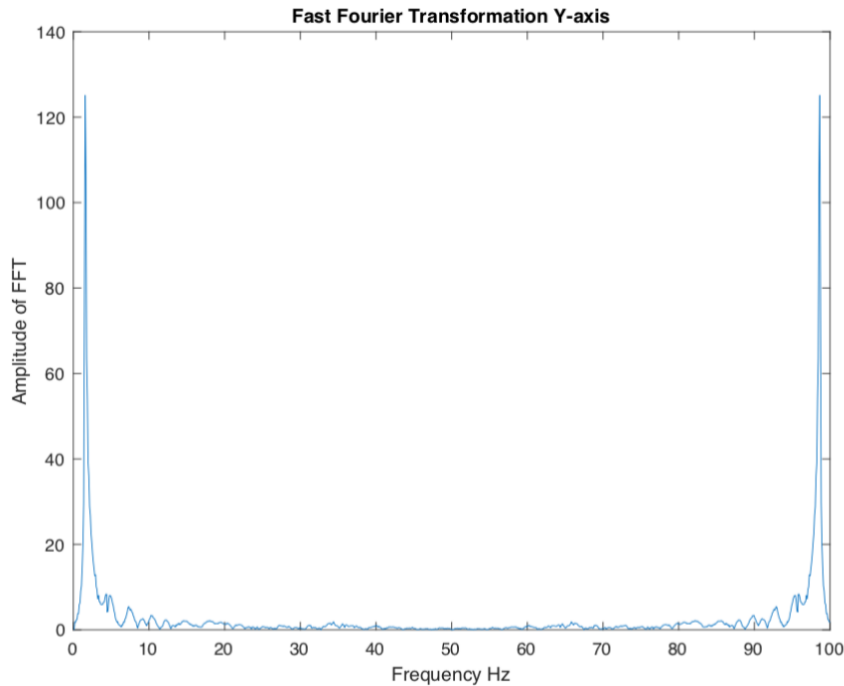


Figure 4-12 Fast Fourier Transform of the 3rd model design in Y-axis

The preliminary test delivered two kinds of results, the acceleration response of each design and the Fast Fourier Transform performed on an acceleration signal.

The acceleration maximum response of the 1st design in X-axis, given by the maximum between the peak and bottom acceleration values, indicates an acceleration value of about of 0.44 m/s^2 . The maximum acceleration amplitude of the 2nd model design, similarly to the previous one, 0.44 m/s^2 . While the 3rd model design has an acceleration maximum response of 0.48 m/s^2 . The acceleration response of the 1st design does not vibrate as quickly as the 2nd or 3rd design. It may be observed by looking at the x-axis and seeing that the number of peak or bottoms per second. The 1st and 2nd designs present more peaks or bottoms per second. It means that their period is smaller. A smaller period is responsible for the faster vibrating back and forth. The time of vibrations is different between models, the 1st and 2nd designs took around 5 seconds to dumped the vibrations, while the 3rd design spent around 6 seconds to stop vibrating. Such difference in the time of free vibration was due to the mass of a physical model. The higher mass increases the amplitude of resonance extending the time of free vibrations (CSUN, 2015).

The acceleration maximum response in Y-axis of all three designs had different amplitudes. The 1st design has $1,6 \text{ m/s}^2$, the 2nd design presented the amplitude of 2.2 m/s^2 , and the 3rd design had an amplitude of 2.6 m/s^2 . The period of these acceleration responses is characterized by small differences, in fact, these periods are almost identical being different by the second fractions.

To summarize the fast Fourier transformations, it is necessary to focus on the frequency peaks as they can be treated as the frequency indicators. The natural frequency of the model is presented, and the natural frequency is the first vibration mode. As the systems are treated as an SDOF system, these designs have one vibration mode in one axis. The FFT graphs of X axes have peaks at different frequencies. The 1st model design has its first peak at around 5

Hz. The peaks are positioned in relation to the FFT Amplitude that is understood as the peak value of the acceleration response in the time domain. The 2nd model design in X-axis has a frequency of around 5 Hz. While the 3rd design has the frequency of around 8.5 Hz, which means that the system starts resonating at this frequency. The FFT in Y-axes have the natural frequency at more less the same level, their natural frequencies are smaller than 2 Hz. The 1st model design has around 1.41 Hz, the 2nd model design has at 1.43 Hz. The 3rd design has 1.46 Hz.

4.3 Selected Design Model

The multi-criteria for selecting the design of a physical model of a cable-stayed bridge is presented in Table 4-1. The design with the highest number is selected to be used for a shaking table test.

The model designs were analysed considering all criteria, which are described in Chapter 3.5. A weight is assigned to each criterion, it displays the importance for the study objectives. The final model design was selected based on those criteria, the results of these analysis are presented below. The scores are translated in the following way; the models are assigned with values 0, 1 or 2. The higher the number is, the better the model performance is in indicated criterion. Subsequently, the assigned score is multiplied by the criterion weight, it is used to select the most reliable model design.

Criterion	Physical Model Design		
	1 st Design	2 nd Design	3 rd Design
Natural Frequency	0.5	0.25	0
Physical Model Mass	0	0.3	0.6
Continuous Deck Stiffness	0.3	0	0.6
Construction Ease	0.3	0.15	0
Total	1.1	0.7	1.2

Table 4-1 The final design selection

The 3rd design was selected to be used in the shaking table test.

The scores are precisely explained in this chapter. The 1st design model scored the maximum in the natural frequency criteria. This design presented the lowest natural frequency in X and Y-axis, the natural frequency was read from the x-axis of each graph. The second place was given to the 2nd design as its natural frequencies were higher than the 3rd design and smaller than the 1st design. The 1st design had the lowest mass; thus, it is placed with the lowest score. The mass of the 2nd design was higher, while the mass of the 3rd design was the highest. The 3rd design had the continuous deck stiffness, while the 1st design had two stiffness discrepancies. The 2nd design had five stiffness discrepancies and was granted with

the lowest score. The construction ease was the lowest for the 3rd design as it had the biggest number of pieces, while the 2nd design had more pieces. The winner of this criterion was the 1st designs as it was the easiest to construct.

The table 4-2 presents the values that were used for the design assessment.

Criterion	Physical Model Design		
	1 st Design	2 nd Design	3 rd Design
Natural Frequency (X & Y-axis in Hz)	5 & 1.41	5 & 1.42	8.5 & 1.46
Physical Model Mass (in grams)	599,4	667	814.1
Continuous Deck Stiffness (yes/no)	NO	NO	YES
Construction Ease (time spent on construction in minutes)	< 1:30	< 2:10	< 2:40

Table 4-2 The final design selection including values

4.4 Shaking Table Test Results

The shaking table tests were performed on the selected 3rd design. The shaking table test allowed to identify the natural frequency. As the moment when the physical model starts resonating. The natural frequency is used to determine the model stiffness. The stiffness values are presented in this chapter.

4.4.1 Natural Frequency of Selected Design

The natural frequency will be presented in the screen on the shaking table test. The visual representation of the performed shaking table test is presented in this chapter. The screenshots are taken at the moment when the physical model presents its natural frequency.

Transversal Direction (X-axis)

Physical Model with the braced towers had the natural frequency of 4.28 Hz. The obtained frequency presented the effect of the physical model stiffness on the natural frequency. The model tower created with bracing demonstrated very high stiffness in the transversal direction. It was because the bracing decreased the effect of load from the columns by transferring the force in the bracing and it limited the displacement of the tower columns.

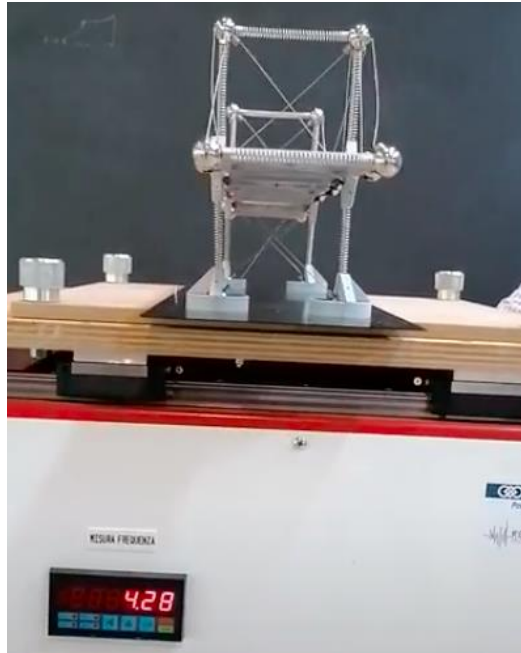


Figure 4-13 The physical model (3rd Design) with bracing and its natural frequency in the transversal direction on a shaking table test

Physical Model with the rigid connection 90° used for the towers has the natural frequency of 1.84 Hz. After replacing the bracing with the rigid connection in the tower structure, the model became less stiff. It was due to the lack of bracing. The rigid connection decreased the bending length. However, they did not affect the column displacement. The significant column displacement can be seen in Figure 4-15 comparing to the lack of column displacement included in Figure 4-14.



Figure 4-14 The physical model (3rd Design) without bracing and its natural frequency in the transversal direction on a shaking table test

Longitudinal Direction (Y-axis)

Physical Model without the additional load has the natural frequency of 2.30 Hz. The natural frequency in the longitudinal direction is smaller than in the transversal direction. The physical model started resonating at the frequency of 2.30. The physical model in the longitudinal direction is less rigid. The physical model columns were displaced due to the deck mass.

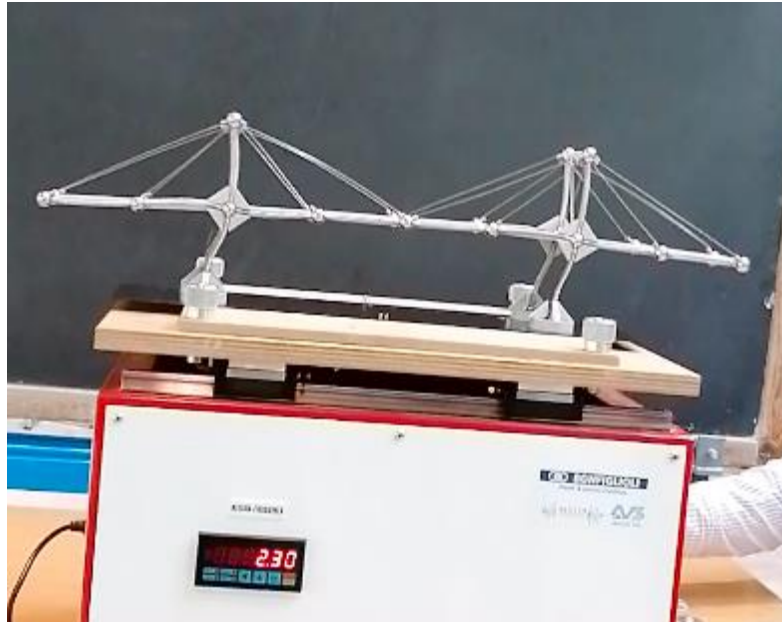


Figure 4-15 The physical model (3rd Design) and its natural frequency in the longitudinal direction on a shaking table test

Physical Model with the centric load has the natural frequency of 1.80 Hz. The increased mass affected lowering the natural frequency. If the mass was increased and the natural frequency decreased, it is possible that the physical model stiffness was also lowered. The exact stiffness value are found in the following chapter.

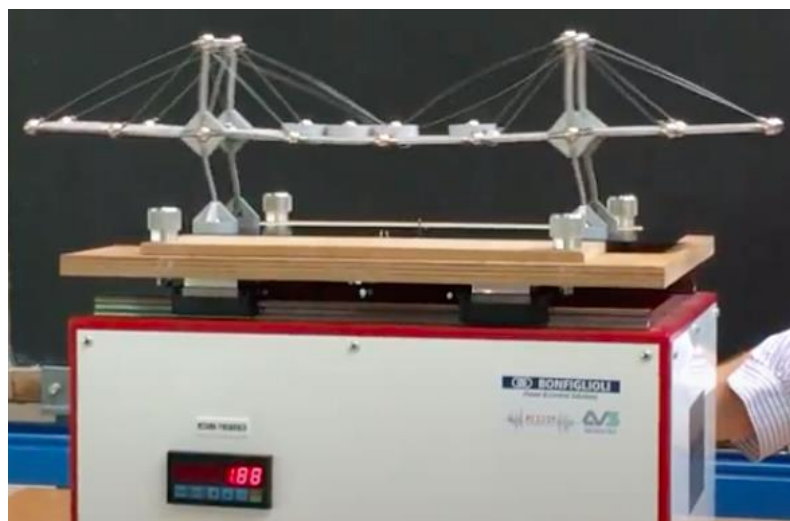


Figure 4-16 The physical model (3rd Design) with a centric load and its natural frequency in the longitudinal direction on a shaking table test

Physical Model with the eccentric load has the natural frequency of 1.64 Hz. The increased mass that is located around the one tower may decrease the physical model stiffness. It is proven by the natural frequency that was lower comparing to the physical model with the centric load.

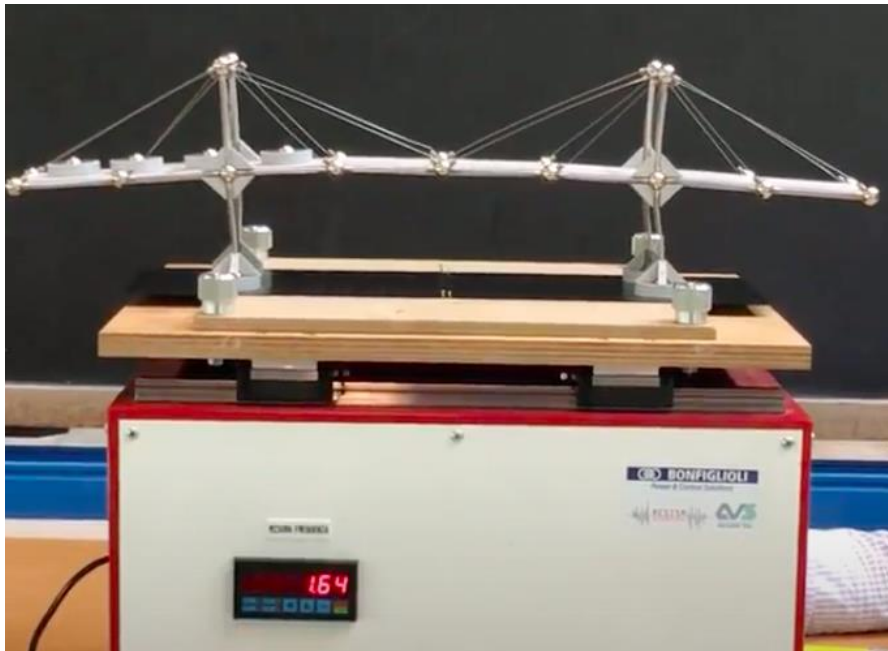


Figure 4-17 The physical model (3rd Design) with an eccentric load and its natural frequency in the longitudinal direction on a shaking table test

The results of shaking table test delivered the natural frequency of the physical model. The shaking table test was used to verify the natural frequency determined by the preliminary test. The natural frequency found during shaking table testing showed different values than those obtained from the preliminary test.

The physical model with bracing tested in the transversal direction presented a much higher frequency. Thus, its stiffness was much higher, in fact, the physical model was extremely stiff in the transversal direction. The physical model started resonating at the frequency of 4.28 Hz. To extend the study of the physical model in the transversal direction, the model composition was modified. The modification details are described in Chapter 3.6. The composition change affected the model stiffness, hence, the natural frequency was lowered to 1.84. The difference in the model stiffness is considerable. The physical model tested in the longitudinal direction was studied in three variants, without a load, with a centric and eccentric load. The details of the testing in the longitudinal direction are described in Chapter 3.6. The physical model tested without an additional load demonstrated the natural frequency of 2.30 Hz. The centric and eccentric loading influenced on the natural frequency demonstrating 1.80 Hz (centric load) and 1.64 Hz (eccentric load). The explanation of these frequencies is based on the natural frequency property, such as an increased mass decreases the natural frequency.

The natural frequencies obtained from the preliminary test and shaking table test are more less similar. The shaking table test was applied to verify the values obtained from the

preliminary test. The method of determining the natural frequency of the designs was comprehensively explained in Chapter 3.3.

The frequencies of 3rd Design of a physical model are compared, because only the 3rd design was tested on a shaking table. The comparison of these natural frequencies is presented in Table 4-3. The frequencies that are compared were generated while the physical model had the same composition and were without an additional load.

Natural Frequency (Hz)			
Preliminary Test		Shaking Table Test	
X-axis	Y-axis	X-axis	Y-axis
5	8.5	2.3	4.28

Table 4-3 Comparison of Natural Frequencies

The natural frequencies of the physical model (3rd Design) in X and Y-axis are slightly different.

The natural frequencies generated during the shaking table test and those frequencies obtained from the fast Fourier transform present different values. The reason why these differences occurred is explained in Chapter 5.3.

4.4.2 Stiffness of Selected Design

The value of natural frequency was implemented in the formula of the undamped natural frequency. The stiffness values are presented in Table 4-4.

	Physical model				
	Transversal direction		Longitudinal direction		
	with bracing	with rigid connection 90	without load	with centric load	with eccentric load
Natural Frequency fn (Hz)	4,28	1,84	2,3	1,88	1,64
Stiffness k (N/m)	588,7420144	110,37	170,02	132,29	100,67
Mass m (kg)	0,8141	0,8258	0,8141	0,9481	0,9481

Table 4-4 The stiffness values for all the tested design modifications

The model stiffness was obtained based on the natural frequencies determined to make use of the shaking table test.

The stiffness values differ between the model compositions and loads. The physical model with bracing has the stiffness of 4764.37 N/mm. When the bracing was replaced with the rigid connection 90o, its stiffness was 1133.12 N/mm. The stiffness has considerable changed. It was expected to reckon from the natural frequency. The stiffness values in the longitudinal direction were less differing. The physical model without an external load had the stiffness of 1745.39 N/mm. The models with applied centric and eccentric loads reached the values of 1358.0.9 N/mm and 1033.48 N/mm. The increased mass affected the stiffness. Moreover, the load distribution had an effect, too. The eccentric load affected more one of the towers, thus, its stiffness was lowered.

5 Discussion & Conclusion

The research focus was to design a physical model which subjected to ground motions presents the natural frequency below 4.8 Hz. The determination of the physical model natural frequency allowed to obtain its physical properties such as stiffness and mass. Stiffness and mass are two main criteria that affect the natural frequency. Therefore, they must be known to fully understand the dynamic behaviour of a physical model.

The study has concluded the following:

The design of a physical model was found fulfilling the main requirement such as the natural frequency below 4.8 Hz. The natural frequency of a design of a physical model was 2.3 Hz in the longitudinal direction and 4.28 Hz in transversal direction.

Setting design criteria enabled to select the final design. The criteria were inserted in the multi-criteria analysis to pick the final model design. The criteria were the following: natural frequency, physical model mass, continuous deck stiffness and construction ease.

It was necessary to establish the functional and technical requirements of a model design. The design model applicability increased due to the elaborated requirements. It narrowed the research activities to focus more on the research objectives. The functional requirements concentrated on the utility of a physical model, while the technical requirements described the preset design aspects.

The creation of alternative designs enabled to obtain the most relevant design that could fulfil the research objectives. A shaking table test utilized the selected design model. The designs were different, altering its composition, such as the number of cable stays or deck type. The designs assessment used a preliminary test and other factors put in the multi-criteria analysis. Combining these steps provided the most relevant design in case of the study applicability.

The shaking table test delivered the elastic linear response of the selected model design. The model testing was performed in both directions, transversal and longitudinal. The shaking table test was repeated numerous times to investigate the model response under various circumstances. During the tests, modifying the physical model composition provided more insights into the model response. It allowed to conclude which model components were crucial for the elastic linear response. For instance, testing in the transversal direction identified the side bracing as the component the most increasing the model stiffness.

The study activities determined the physical model stiffness and mass. The model mass was obtained by weighting the pieces and summing the values. The model stiffness was acquired by performing mathematical operations. The process applied the natural frequency formula to find the stiffness. The value was found by being derived from the mentioned formula and put the known values in it. The result of this mathematical operation was the physical model stiffness.

The results obtained were expected to be as they are. The objective was to create the design of a physical model of a cable-stayed bridge whose natural frequency is below 4.8 Hz. Researches that studied the dynamic behaviour of physical models obtained the natural frequencies approximately 2 Hz.

For instance, de Alcântara Segundinho, Alves Dias and Carreira (2011) in the study evaluated the vibration of a small-scale model of a footbridge. The study conclusion was the natural frequency of the bridge, which was 2.626 Hz in the longitudinal direction. While Cunha & Caetano (1999) probe the dynamic measurements on cable-stay bridges, and their conclusion was the natural frequency that reached maximum 1.15 Hz. Thus, it was expected that the natural frequency of this bridge would be around this value. However, the unexpected results were obtained from the preliminary test. The natural frequencies of three model designs determined using the preliminary test were around 5 Hz in the transversal and 8.5 Hz in the longitudinal direction. There can be a reasonable explanation of such, an outcome this topic is further elaborated in Chapter 5.3.

5.2 Limitations of Results

There are two major limitations in this research that should be mentioned. First, the study focused only on physical models of a cable-stayed bridge made of Mola Kit. Second, the preliminary test was performed outside a laboratory. Moreover, the equipment used for this testing was not certified, and the sensor was not calibrated due to technical reasons.

The first limitations are of the values obtained through the research are specific for the physical models constructed of Mola Kit and having a form of a cable-stayed bridge. The limitation regarding constructing a physical model using Mola Kit. Mola pieces were designed to perform a qualitative analysis, while this research is focused on quantitative analysis. Thus, the found values are only applicable to the physical models of a cable-stayed bridge constructed of Mola Kit. The physical model stiffness values of the selected designs can be applied to any other calculations of different models constructed of Mola Kit. The values were obtained performing the shaking table test, thus, the values obtained differently could be different. This assumption narrows the applicability of these results. The second limitation is regarding the acceleration response. It was registered by the sensor that could record results with a dose of imperfection. The sensor was a feature of a software MATLAB mobile. The sensor could not be calibrated before the preliminary test. Hence, it must be assumed that the obtained values were a bit imprecise. It provided a contour that could be used for the approximated outline of the acceleration response. It explains the differences in the obtained natural frequencies why the results from the preliminary test were not similar to the shaking table test. Therefore, the preliminary test did deliver less precise values. However, it was used to estimate the frequencies and as a factor for the multi-criteria analysis. While the precision of results was not the most crucial, because it enabled to estimate the values.

The possible alternative to decrease the limitations of the values obtained from working on Mola Kit, it is to find a single stiffness value of each piece. The stiffness of a single element would deliver the reliable information and could be used for prospective studies. It would provide the calibration feature to increase the precision and reliability of the obtained values.

5.3 Results Complication

The obtained results became problematic, as the validity of the results of the preliminary test should be distinguished. The preliminary test integrated an axial load which was described in Chapter 3.3. The load strength could have differences between the three designs. The amount of force applied was equated as much as possible. However, the preliminary test did not

include any certified equipment. Therefore, the differences in the axial load must have occurred. As this issue was known, it was not used as the only factor. But it was supported by more factors that instructed the design selection and enriched the criteria variety.

5.4 Implication of Results

The found results presented in Chapter 4 can be used for the prospective studies. They answer the research questions. These results may have significant implications for the researches working on Mola Kits. It delivers a method of dealing with physical models constructed of Mola Kits. They are relatively new in the field of physical models; thus, their application might increase in the following years. While this study might be used to clarify the basic question of performing shaking table tests on physical models made of Mola Kits. Divergence from the traditional physical models made of specific elements towards the Mola models that are made of modular pieces. The modular pieces may decrease the cost of testing and the time spent on pre-test preparation. Such an approach does not need to construct specific pieces, but to use already constructed pieces. It is suggested to adjust these pieces for research objectives to provide more precise results. Furthermore, the way of using the Mola Kit for a shaking table test eases its application, broadening the range of users. As the knowledge, necessary to construct a physical model out of Mola Kit demands smaller expertise in comparison with the traditional physical models. Thereby, the research results present that the Mola Kit can be applied for specific studies integrating the use of a shaking table.

5.5 Recommendations

The list of recommendations is provided in this chapter. These suggestions were outside the research scope. Thus, the critical way of looking at the work allowed to create this recommendation list. It provides more comprehensible approach to superficially mentioned aspects.

Physical Model

The diversity in the design of a cable-stayed bridge made of Mola model can be higher. Such an approach enhances the variety between Mola pieces. It enables to assemble models characterised by different type of cable-stayed bridge components. More various pieces can provide that each bridge components is different than other alternatives. The designs can be more diverse. They can be modified by creating various tower types, arrangement of cable stays or positions of cables along the deck. They can be modified by creating various tower types, arrangement of cable stays or positions of cables along the deck.

Preliminary Test

The preliminary test results can be more precise. It is recommended to use a professional acceleration sensor to obtain higher precision of the preliminary test. A professional acceleration sensor is calibrated separately for each test, and it would gather more precise values. Applying an initial load to the physical model can be realised more measurably. The equally applied load provides equal results; thus, their relevance can be higher. Moreover, these results do not have to be supported by other criteria.

Further research on Mola Kit

Mola Kit can be a great tool for numerous scientific studies. However, its physical properties of Mola Kit have not been investigated yet. Determining the physical properties of Mola pieces may widen its applicability for scientific purposes. The ease of assembling numerous structural systems can have an enormous effect on encouraging people to study structural behaviour. Whereas Mola Kit was primarily created for the qualitative study. Therefore, its applicability can be extended to qualitative analysis. Especially, Mola models are used to represent numerous structural systems, and structural system hardly happens to be an object.

6 Bibliography

Anwar, N. (2016). *Structural Design of Bridges*.

Bai, Z., & Xu, Z. (2019). *Structural Dynamics*. Beverly: Wiley-Scrivener Publishing.

Bairrao, R., & Vaz, C. (2000, January). Shaking table testing of civil engineering structures—the LNEC 3D simulator experience. In *Proceedings 12th World Conference on Earthquake Engineering*. Auckland, New Zealand, Paper (Vol. 2129).

Balawi, S., Shahid, O., & Mulla, M. A. (2015). Similitude and scaling laws-static and dynamic behaviour beams and plates. *Procedia Eng*, 114, 330-337.

Baghani, M., Fattahi, M., & Amjadian, A. (2012). Application of the variational iteration method for nonlinear free vibration of conservative oscillators. *Scientia Iranica*, 19(3), 513-518.

Bellos, J., & Inman, D. J. (1990). Frequency response of nonproportionally damped, lumped parameter, linear dynamic systems.

Broo, H. (2008). *Shear and Torsion in Concrete Structures Non-linear Finte Element Analysis in Design and Assessment*. Chalmers University of Technology.

Bruneau, M. (1992). Evaluation of system-reliability methods for cable-stayed bridge design. *Journal of Structural Engineering*, 118(4), 1106-1120.

Candeias, P., Costa, A. C., & Coelho, E. (2004, August). Shaking table tests of 1: 3 reduced scale models of four story unreinforced masonry buildings. In *Proceedings of the 13th world conference on earthquake engineering*. Vancouver, Canada.

Casaburo, A., Petrone, G., Franco, F., & De Rosa, S. (2019). A review of similitude methods for structural engineering. *Applied Mechanics Reviews*, 71(3).

Chambers, J., & Kelly, T. (2004, August). Nonlinear dynamic analysis—the only option for irregular structures. In *13th World Conference on Earthquake Engineering*.

Chang, K. H. (2015). Chapter 14-Rapid Prototyping. *e-Design*.

Chen, W. F., & Duan, L. (Eds.). (2013). *Handbook of international bridge engineering*. CRC Press.

Chen, D. W., Au, F. T. K., Tham, L. G., & Lee, P. K. K. (2000). Determination of initial cable forces in prestressed concrete cable-stayed bridges for given design deck profiles using the force equilibrium method. *Computers & Structures*, 74(1), 1-9.

Chen, J., Wang, L., Racic, V., & Lou, J. (2016). Acceleration response spectrum for prediction of structural vibration due to individual bouncing. *Mechanical Systems and Signal Processing*, 76, 394-408.

Clough, R. W., & Penzien, J. (1995). *Dynamics of structures Third Edit.*, Berkeley, CA 94704 USA: Computers & Structures.

- Connor, J. J., & Faraji, S. (2016). *Fundamentals of structural engineering*. Springer.
- Cooley, J., Garwin, R., Rader, C., Bogert, B., & Stockham, T. (1969). The 1968 Arden House workshop on fast Fourier transform processing. *IEEE Transactions on Audio and Electroacoustics*, 17(2), 66-76.
- Costa, J. D. (2003). *Standard methods for seismic analyses*.
- Crewe, A. J., & Severn, R. T. (2001). The European collaborative programme on evaluating the performance of shaking tables. *Philosophical Transactions of the Royal Society of London. Series A: Mathematical, Physical and Engineering Sciences*, 359(1786), 1671-1696.
- Cunha, A., & Caetano, E. (1999). Dynamic measurements on stay cables of cable-stayed bridges using an interferometry laser system. *Experimental Techniques*, 23(3), 38-43.
- da Sousa Cruz, P. J. (2010). *Structures & Architecture*. CRC Press.
- Dalrymple, R. A. (2018, December). Introduction to physical models in coastal engineering. In *Physical modelling in coastal engineering: Proceedings of an international conference, Newark, Delaware, August 1981* (p. 3). Routledge.
- Dalrymple, R. A. (1989). Physical modelling of littoral processes. In *Recent advances in Hydraulic physical modelling* (pp. 567-588). Springer, Dordrecht.
- Damodarasamy, S. R. (2009). *Basics of structural dynamics and aseismic design*. PHI Learning Pvt. Ltd..
- Datta, T. K. (2010). *Seismic analysis of structures*. John Wiley & Sons.
- de Alcântara Segundinho, P. G., Alves Dias, A., & Carreira, M. R. (2011). Evaluating vibrations on a small-scale model of a timber footbridge. *Maderas. Ciencia y tecnología*, 13(2), 143-152.
- D'Evelyn, M. P., & Taniguchi, T. (1999). Elastic properties of translucent polycrystalline cubic boron nitride as characterized by the dynamic resonance method. *Diamond and Related Materials*, 8(8-9), 1522-1526.
- Dihoru, L., Dietz, M. S., Crewe, A. J., & Taylor, C. A. (2012). Performance Requirements of Actuation Systems for Dynamic Testing in the European Earthquake Engineering Laboratories. In *Role of Seismic Testing Facilities in Performance-Based Earthquake Engineering* (pp. 119-134). Springer, Dordrecht
- Dodds Jr, R. H., & Lopez, L. A. (1980). Substructuring in linear and nonlinear analysis. *International Journal for Numerical Methods in Engineering*, 15(4), 583-597.
- Del Corso, R., & Formichi, P. (2004, June). A proposal for a new normative snow load map for the Italian territory. In *Snow Engineering V: Proceedings of the Fifth International Conference on Snow Engineering*, 5-8 July 2004, Davos, Switzerland (p. 85). CRC Press.
- Ernst, M. D. (2003, May). Static and dynamic analysis: Synergy and duality. In *WODA 2003: ICSE Workshop on Dynamic Analysis* (pp. 24-27). New Mexico State University Portland, OR.

Gladwell, G. M. L., & Doyle, J. F. (1991). *Static and Dynamic Analysis of Structures: With An Emphasis on Mechanics and Computer Matrix Methods*. Springer Netherlands.

Gulvanessian, H., Calgaro, J. A., & Holický, M. (2002). *Designer's guide to EN 1990: eurocode: basis of structural design*. Thomas Telford.

El-Reedy, M. A. (2015). *Marine Structural Design Calculations-Book*.

Gawronski, W. (2004). *Advanced structural dynamics and active control of structures*. Springer Science & Business Media.

Fajfar, P., Vidic, T., & Fischinger, M. (1989). Seismic demand in medium-and long-period structures. *Earthquake Engineering & Structural Dynamics*, 18(8), 1133-1144.

Gao, C. H., & Yuan, X. B. (2019). Development of the Shaking Table and Array System Technology in China. *Advances in Civil Engineering*, 2019.

Gonçalves, C. A., Ferreira, R. F. C., Gonçalves Filho, C., & Dias, A. T. (2013). Componentes estruturais e conjuntos parcimoniosos na explicação do desempenho organizacional: um estudo nos setores da indústria e serviço. *Revista Ibero Americana de Estratégia*, 12(3), 66-92.

Gimsing, N. J., & Georgakis, C. T. (2011). *Cable supported bridges: Concept and design*. John Wiley & Sons.

Guo, W., Shao, P., Li, H. Y., Long, Y., & Mao, J. F. (2019). Accuracy Assessment of Shake Table Device on Strong Earthquake Output. *Advances in Civil Engineering*, 2019.

Hanly, S. (2016). *Vibration Analysis: FFT, PSD, and Spectrogram Basics*. Mide, <https://blog.mide.com/vibration-analysis-fft-psd-and-spectrogram>.

Hansen, J. B., & Svendsen, I. A. (1985). A theoretical and experimental study of undertow. In *Coastal Engineering 1984* (pp. 2246-2262).

Hongwei, W. (2009). *Fft basics and case study using multi-instrument*. Virtins Technology, Rev, 1.

Huerta-Lopez, C., Shin, Y. J., Powers, E., & Roesset, J. (2000). Time-Frequency Analysis of Earthquake Records. *Earthquake Spectra*, 23(1), 77-94.

Hughes, S. A. (1993). *Physical models and laboratory techniques in coastal engineering* (Vol. 7). World Scientific.

Jacobsen, L. S. (1930). Motion of a soil subjected to a simple harmonic ground vibration. *Bulletin of the seismological society of America*, 20(3), 160-195.

Kakpure, G. G., & Mundhada, A. R. (2016). Comparative Study of Static and Dynamic Seismic Analysis of Multistoried RCC Building by ETAB: A Review. *International Journal of Emerging Research in Management & Technology*, 5, 17-20.

Kamphuis, J. W. (1991). *Physical Modelling*. Handbook of Coastal and Ocean Engineering, ed. J. Herbich.

- Kun, C., & Chouw, N. (2015). Seismic Response of Bridges Including Effects of Pounding and Soil-Structure Interaction (SSI).
- Le Méhauté, B. (1990). *Similitude, The Sea, Part 2*. Edited by B. Le Méhauté, University of Miami, USA, John Wiley & Sons Inc, Printed in USA, ISBN: 0 471 63393 3.
- Li, S., Wu, C., & Kong, F. (2019). Shaking Table Model Test and Seismic Performance Analysis of a High-Rise RC Shear Wall Structure. *Shock and Vibration*, 2019.
- Lin, W., & Yoda, T. (2017). *Bridge Engineering: Classifications, Design Loading, and Analysis Methods*. Butterworth-Heinemann.
- Lirola, J. M., Castaneda, E., Lauret, B., & Khayet, M. (2017). A review on experimental research using scale models for buildings: Application and methodologies. *Energy and Buildings*, 142, 72-110.
- Liu, G. R., Li, Y., Dai, K. Y., Luan, M. T., & Xue, W. (2006). A linearly conforming radial point interpolation method for solid mechanics problems. *International Journal of Computational Methods*, 3(04), 401-428.
- Lu, X., Fu, G., Shi, W., & Lu, W. (2008). Shake table model testing and its application. *The Structural Design of Tall and Special Buildings*, 17(1), 181-201.
- Mariani, M. C., Gonzalez-Huizar, H., Bhuiyan, M. A. M., & Tweneboah, O. K. (2017). Using dynamic fourier analysis to discriminate between seismic signals from natural earthquakes and mining explosions. *AIMS Geosciences*, 3(3), 438-449.
- Mercer, C. (2006). Acceleration, velocity and displacement spectra omega arithmetic. *Prosig signal processing tutorials*, 1-8.
- Modares, M. (2014). Static Analysis of Structures Subjected to Interval Displacements. In *Vulnerability, Uncertainty, and Risk: Quantification, Mitigation, and Management* (pp. 2237-2243).
- Muto, K., Bailey, R., & Mitchell, K. (1962). Nominated lecture: Special requirements for the design of nuclear power stations to withstand earthquakes. *Proceedings of the Institution of Mechanical Engineers*, 177(1), 155-203.
- Naghizadeh, M., & Innanen, K. A. (2011). Seismic data interpolation using a fast generalized Fourier transform. *Geophysics*, 76(1), V1-V10.
- Nakashima, M., Nagae, T., Enokida, R., & Kajiwara, K. (2018). Experiences, accomplishments, lessons, and challenges of E-defense—Tests using world's largest shaking table. *Japan Architectural Review*, 1(1), 4-17.
- Nikolić, Ž., Krstevska, L., Marović, P., & Smoljanović, H. (2017). Shaking table test of scaled model of Protiron dry stone masonry structure. *Procedia engineering*, 199, 3386-3391.
- Nikolić, Ž., Smoljanović, H., & Zivaljić, N. (2015). Application of finite discrete element method in dynamic analysis of masonry structures. In *COMPLAS XIII: proceedings of the XIII International Conference on Computational Plasticity: fundamentals and applications* (pp. 1020-1030). CIMNE.

- Noble, D. W., Radersma, R., & Uller, T. (2019). Plastic responses to novel environments are biased towards phenotype dimensions with high additive genetic variation. *Proceedings of the National Academy of Sciences*, 116(27), 13452-13461.
- Okamoto, S., Kitagawa, Y., & Motoda, Y. (1994). International Institute of Seismology and Earthquake Engineering. *Structural Engineering International*, 4(1), 62-63.
- Oller, S. (2014). Convergence Analysis of the Dynamic Solution. In *Nonlinear Dynamics of Structures* (pp. 53-76). Springer, Cham.
- Price, W. A. (1978). Theme Speech: Models, Can We Learn from the Past and Some Thoughts on the Design of Breakwaters. In *Coastal Engineering 1978* (pp. 25-48).
- Quanser. (2019, September). Shake Table I-40 Meets the Mola Structural Model Kit [Video]. Youtube. <https://www.youtube.com/watch?v=MREd7qfPjFO>
- Rogers, F. J. (1930). Experiments with a shaking machine. *Bulletin of the seismological society of America*, 20(3), 147-159.
- Rekoske, J. M., Thompson, E. M., Moschetti, M. P., Hearne, M. G., Aagaard, B. T., & Parker, G. A. (2020). The 2019 Ridgecrest, California, earthquake sequence ground motions: Processed records and derived intensity metrics. *Seismological Research Letters*.
- Rouff, M. (1997). Analytical computation of differential equations involved in dynamical nonlinear optimal problems. *Computer methods in applied mechanics and engineering*, 142(1-2), 153-163.
- Saranik, M., Lenoir, D., & Jézéquel, L. (2012). Shaking table test and numerical damage behaviour analysis of a steel portal frame with bolted connections. *Computers & structures*, 112, 327-341.
- Sarlo, R. (2019, July). Civil Engineering - Structural Health Monitoring with Mola Kit and MATLAB Mobile [Video]. Youtube. <https://www.youtube.com/watch?v=54JbniK5Bd0&t=1s>
- Sawada, K. (1970). Strength and vibration characteristics of large type shaking table. *Technical Review*, 7(3).
- Sarkar, P., Prasad, A. M., & Menon, D. (2010). Vertical geometric irregularity in stepped building frames. *Engineering Structures*, 32(8), 2175-2182.
- Sáez, E., Lopez-Caballero, F., & Modaressi-Farahmand-Razavi, A. (2013). Inelastic dynamic soil-structure interaction effects on moment-resisting frame buildings. *Engineering structures*, 51, 166-177.
- Schweber, L. (2013). The effect of BREEAM on clients and construction professionals. *Building Research & Information*, 41(2), 129-145.
- Segalman, D. J., & Holzmann, W. (2005, February). Nonlinear response of a lap-type joint using a whole-interface model. In *23rd International Modal Analysis Conference (IMAC-XXIII)*, Orlando, Florida.

- Shi, W., Shan, J., & Lu, X. (2012). Modal identification of Shanghai World Financial Center both from free and ambient vibration response. *Engineering Structures*, 36, 14-26.
- Sirois, F., & Grilli, F. (2015). Potential and limits of numerical modelling for supporting the development of HTS devices. *Superconductor Science and Technology*, 28(4), 043002.
- Srilatha, N., Latha, G. M., & Puttappa, C. G. (2013). Effect of frequency on seismic response of reinforced soil slopes in shaking table tests. *Geotextiles and Geomembranes*, 36, 27-32.
- Steidel, R. (1989). *An introduction to mechanical vibrations* (No. BOOK).
- Stikeleather, L. F. (1976). Review of ride vibration standards and tolerance criteria. *SAE Transactions*, 1460-1467.
- Troitsky, M. S. (1988). *Cable-stayed bridges: an approach to modern bridge design*. Van Nostrand Reinhold.
- Tsai, C. S., Chen, W. S., Chiang, T. C., & Chen, B. J. (2006). Component and shaking table tests for full-scale multiple friction pendulum system. *Earthquake engineering & structural dynamics*, 35(13), 1653-1675.
- Wang, X., Liu, K., Liu, H., & He, Y. (2018). Damping identification with acceleration measurements based on sensitivity enhancement method. *Shock and Vibration*, 2018.
- Weik, M. H. (1996). Excerpts,“. *Communications Standard Dictionary, Third Edition.*” Chapman & Hall.
- Weisstein, E. W. (2002). *CRC concise encyclopedia of mathematics*. CRC press.
- Wood, R. M. (1988). Robert Mallet and John Milne—earthquakes incorporated in victorian britain. *Earthquake engineering & structural dynamics*, 17(1), 107-142.
- Wujek, J. B. (1999). *Applied Statics, Strength of Materials, and Building Structure Design*. Pearson College Division.
- Yalin, M. S. (1971). Principles of the Theory of Similarity. In *Theory of Hydraulic Models* (pp. 35-50). Palgrave, London.
- Yalin, M. S. (1989). Fundamentals of hydraulic physical modelling. In *Recent Advances in Hydraulic Physical Modelling* (pp. 1-37). Springer, Dordrecht.
- Zhang, C., & Jiang, N. (2017). A shaking table real-time substructure experiment of an equipment–structure–soil interaction system. *Advances in Mechanical Engineering*, 9(10), 1687814017724090.
- Zaidi, S. A., Jaffer, N., Khan, K., & Maher, A. (2020). Categorization of Buildings Based on the Relative Effect of Lateral & Vertical Forces with Change in Height. *American Journal of Civil Engineering and Architecture*, 8(1), 19-24.